Interrelationship of Hydrology, Microbial Colonisation and Hydrometallurgy in a Simulated Chalcopyrite Heap Leach

Nicholas Robert Louis Spurr

Full-thesis submitted for the fulfilment of the academic requirements for the degree of Masters of Science in Applied Science in the Department of Chemical Engineering

University of Cape Town

February 2008

Abstract

Chalcopyrite is the most abundant primary copper sulphide mineral found worldwide. As copper grades of ores available for extraction decrease, heap bioleaching is gaining interest as a potential operating alternative to traditional methods of roasting and smelting. The efficiency by which bacteria assist leaching chalcopyrite is governed by their interaction and association to the sulphide mineral in the ore. While both planktonic and mineral-associated micro-organisms contribute to the bioleaching of mineral sulphides through the oxidation of ferrous iron little information exists as to their ability to adhere and leach low grade chalcopyrite ore.

This study was undertaken to determine the association of defined and mixed microbial species on a chalcopyrite concentrate and a chalcopyrite ore. *At. ferrooxidans*, *At. caldus*, *At. thiooxidans* and *L. ferrooxidans* were grown in pure culture and used to investigate the mineral-microbe association within defined experimental parameters of two experimental operations.

Firstly, an attachment study was conducted to determine the association between a defined microbial species of *L. ferrooxidans* and a chalcopyrite concentrate. Secondly, to better improve and understand the colonisation and propagation of microorganisms within a heap leach context, in situ monitoring of a simulated heap leach was undertaken. This could assist in developing an understanding for optimising heap operations with the end goal being a reduction in heap leach times and a better operational understanding of the complex interactions between microorganisms and mineral in order to optimise the leaching process to improve leaching performance.

Results from the attachment study suggest that microbial association with chalcopyrite is rapid with a small population weakly adhered. Only with the repeated agitation by a detergent could the majority of the cell adhered population be dislodged. The in-situ study of the simulated heap leaches under varying conditions revealed a conical attachment of microorganisms from the entry point. The migration of microorganisms follows closely to that of liquid flow dynamics with the associated residence times influencing the leaching rate and copper elution. Under standard operating conditions of 5 L/m^2/hr, it was found was sufficient for reasonable microbial attachment and copper leaching when compared to a high flow rate of 15.5 L/m^2/hr

Acknowledgements

I would like to firstly thank my supervisors Prof. Sue Harrison and Dr. Rob van Hille for there time and patience with my thesis. Without them my thesis would not have been a success.

To each of the following individuals I would like to express a sincere word of appreciation:

Mrs. Fran Pocock, our lab manager for whom our student problems were always her first concern and priority.

Mrs. Sue Jobson for all the administration work and her ability to always find a solution.

Mrs. Helen Divey for her assistance with the acid digestions and sieving of the concentrates

Mr. Emmaneul Ngomo for his help when it came to agglomerating the ore and technical knowledge of setting up the simulated heap leaches

Charlie Nemugumoni for his knowledge of reactor maintenance and the use of his drawing.

To all my friends who have helped me through the write process: Carl, Dannie, Caryn and Fan-Jai I wish to say a very big thank you

I would also like to thank AMIRA International and the National Research Foundation for there financial support.

Finally, I would like to express my deepest gratitude to my parents and brother, Phillip Spurr, who have all been a huge support and been with me through the thick and thin of my MSc and write up.

Table of contents

Abstract ii
Acknowledgements iii
List of figures vii
List of tables x
Nomenclature xi
1. Introduction 1
2. Literature review 3
2.1 History of biomining 3
2.2 Introduction to biomining 4
2.2.1 Stirred tank bioleaching 4
2.2.2 Heap leaching 5
2.3 Potential for heap bioleaching 5
2.4 Mechanisms of leaching 6
2.4.1 The indirect and direct mechanism 6
2.4.2 Leaching pathways 8
2.5 Abiotic vs biotic heap leaching 10
2.6 Microorganisms involved in heap leaching 10
2.7 Bioleaching of chalcopyrite 11
2.8 Current heap leaching practices 14
2.8.1 Prevalence of copper heap bioleaching 14
2.8.2 Practices of setting up and operating bioheaps 14
2.9 Microbial attachment 17
2.9.1 Chemotaxis 17
2.9.2 Hydrophobicity 17
2.9.3 Electrostatic potential 18
2.9.4 Extracellular polymeric substance 19
2.9.5 Crystal boundaries 22
2.10 Studies around attachment and colonisation 22
2.10.1 Quantifying attached leaching microorganisms 22
2.10.2 Studies on the attachment to a chalcopyrite concentrate 24
2.10.3 Studies on a simulated heap environment 25
2.11 Study objectives 26
3. Materials and methods 28
3.1 Chalcopyrite concentrates 28
3.2 Chalcopyrite ore 28
3.3 Microbial cultures 29

3.5 Experimental protocol for microbial attachment 30
3.5.1 Attachment run 1 31
3.5.2 Attachment run 2 31
3.5.3 Attachment run 3 32
3.6 Simulated heap set-up 32
3.7 Experimental protocol for simulated heap leaches 33
3.7.1 Heap leach 1 34
3.7.2 Heap leach 2 34
3.7.3 Heap leach 3 34
3.7.4 Heap leach 4 35
3.8 Analytical methods 36
3.8.1 Volume 36
3.8.2 pH analysis 37
3.8.3 Redox potential 37
3.8.4 Ferrous iron determination 37
3.8.5 Copper, total iron and ferric iron determination 38
3.8.6 Cell counting 38
3.8.7 SEM 39
3.8.8 Cell separation from leached ore 39
3.8.9 Water and acid soluble precipitate from leached ore 40
3.8.10 Total acid digests of ore 40
4. Results and discussion 41
4.1 Analysis of column attachment studies 41
4.1.1 Attachment run 1 41
4.1.2 Attachment run 2 43
4.1.3 Attachment run 3 43
4.1.4 Discussion of mineral attachment studies 44
4.2 Analysis of simulated heap leaches 44
4.2 Analysis of simulated heap leach 4 45
4.2.1 Volume elution 45
4.2.2 Residence time 48
4.2.3 pH analysis 50
4.2.4 Mineralogical analysis 54
4.2.5 Microbial attachment 55
4.2.6 Redox potential 58
4.2.7 Iron elution 60
4.2.8 Copper elution 61
4.2.7 Post operational analysis 64
4.3 Analysis of simulated heap leach 3 70

4.3.1 Volume elution....71
4.3.2 Residence time....73
4.3.3 pH analysis....74
4.3.4 Microbial attachment....75
4.3.4 Redox potential....77
4.3.5 Iron elution....78
4.3.6 Copper elution....79
4.3.7 Post operational analysis....80
4.4 Analysis of simulated heap leach 2....84
4.4.1 Volume elution....85
4.4.2 Residence time....86
4.4.3 pH analysis....87
4.4.4 Microbial attachment....88
4.4.4 Redox potential....89
4.4.5 Iron elution....90
4.4.6 Copper elution....90
4.4.7 Post operational analysis....91
4.5 Analysis of simulated heap leach 1....92
4.5.1 Volume elution....92
4.5.2 Residence time....94
4.5.3 pH analysis....94
4.5.4 Microbial attachment....95
4.5.5 Redox potential....96
4.5.7 Copper elution....97
4.6 Analysis of scanning electron microscope....98
5. Conclusion....100
6. References....104
Appendix A....116
Appendix B....117
Appendix C....124
Appendix D:....125

List of figures

Figure 2.1: Woodcut from the book *de re metallica* written by Georgius Agricola (1494 – 1555) illustrating the recovery of copper from mine effluents which are collected in wooden basins and concentrated in the sun (Schiffner, 1977) 3

Figure 2.2: Schematic representation of microbial leaching of a metal sulphide (adapted from Petersen *et al*., 2004) 6

Figure 2.3 (a) and (b): Contact and cooperative leaching mechanisms (adapted from Rawlings *et al.*, 1999) 8

Figure 2.4: Cycle of oxidative pyrite by bacterial and/or chemical leaching (Schippers *et al.,* 1996) 9

Figure 3.2: Division of reactor into upper and lower layers with shade cloth being used to segregate the divisions (A – Outer region; B - Middle region; C - Inner region) 33

Figure 3.3: Numbered points for sample collection on underside of container 33

Figure 3.4: Simulated heap reactor set-up 33

Figure 4.1: Daily flow collected from inner (point 1), middle (points 2-5) and outer (points 6-9) region outlet points 46

Figure 4.2: Total volume eluted per day for the inner, middle and outer regions from Day 1 to 15 46

Figure 4.3: Middle (red) and outer (green) regional daily flow rates during the 58 day leach period 47

Figure 4.4: Percentage volume eluted from points within the inner, middle and outer regions 48

Figure 4.5: Residence times in each of the nine zones of the bed, estimated as a function of duration of experiment (b) and scaled to show high residence time 50

Figure 4.6: Daily eluted pH readings for outlet points 1 to 9 51

Figure 4.7: pH and residence time for point 5 from Day 1 to 18 52

Figure 4.8: The relationship between pH eluted and residence time for point 7 52

Figure 4.9: Cell elution profile for the duration of the experimental leach 58

Figure 4.10: Daily redox measurements of collected eluted volumes 60

Figure 4.11: Daily iron concentration collected from the feed and eluted volumes of the inner, middle and outer regions 61

Figure 4.12: Daily copper concentrations eluted from inner, middle and outer region points 62

Figure 4.13: Cumulative copper released daily per point for inner, middle and outer regions 62

Figure 4.14: Total copper leached for eluted volumes collected for the duration of the leach experiment 63

Figure 4.15: Daily copper leaching rate for eluted volumes collected 64

Figure 4.16: Number of attached cells per gram for the top level 65
Figure 4.17: Biofilm formation beneath dripper during post operational analysis of reactor 4 66
Figure 4.18: Attached cell number per gram of regional ore for the bottom layer 66
Figure 4.19: Microbial attachment per regional area of ore for the top and bottom layers of the reactor 67
Figure 4.20: Copper leached per regional ore with microbial attachment 68
Figure 4.21: Copper leaching efficiency per region ore including precipitate 69
Figure 4.23: Daily volume elution from inner (point 1), middle (points 2-5) and outer (points 6-9) region outlet points 71
Figure 4.24: Middle (red) and outer (green) regional flow rates 72
Figure 4.25: Total volume eluted for inner, middle and outer regions from Day 1 to 30 72
Figure 4.26: Percentage volume eluted from points within the inner, middle and outer regions 73
Figure 4.27: Residence times associated with elution points within the inner, middle and outer regions of the ore bed 74
Figure 4.28: Daily eluted pH readings for elution points 1 to 9 75
Figure 4.29: Daily cell elution profile for the duration of reactor 3 leach 76
Figure 4.30: Comparison of feed and inner region pH 77
Figure 4.31: Redox potential as a function of leach time for reactor 3 78
Figure 4.32: Daily iron collected from the eluted volumes of the inner, middle and outer regions 79
Figure 4.33: Copper leaching rate for eluted volumes collected 80
Figure 4.34: Comparison of copper leached across the radial regions 80
Figure 4.35: Attached cell number per gram of top layer regional ore 81
Figure 4.36: Attached cell number per gram of bottom layer region ore 81
Figure 4.37: Comparison of top and bottom layer cell attachment per g ore 82
Figure 4.38: Comparison of reactor 4 and reactor 3 residence times for all regions..83
Figure 4.39: Comparison of reactor 4 and reactor 3 cell attachment numbers for all regions 84
Figure 4.40: Comparison of copper elution from reactor 3 and reactor 4 84
Figure 4.41: Daily volume elution from inner (point 1), middle (points 2-5) and outer (points 6-9) region 85
Figure 4.42: Total volume eluted for inner, middle and outer regions from Day 1 to 5 86
Figure 4.43: Low residence times associated with reactor 2 87
Figure 4.44: High residence times associated with reactor 2 87

Figure 4.45: Daily eluted pH readings for elution points 1 to 9 88
Figure 4.46: Daily elution profile for reactor 2 89
Figure 4.47: Redox potential readings for reactor 2 89
Figure 4.48: Daily iron collected from the eluted volumes of the inner, middle and outer regions 90
Figure 4.49: Daily copper collected for total eluted volumes 91
Figure 4.50: Adhered cell per region sample of ore collected 92
Figure 4.51: Daily volume elution from inner (point 1), middle (points 2, 3, 5) and outer (points 6, 9) region outlet points 93
Figure 4.53: Residence times associated with elution points within the inner, middle and outer regions of reactor 1 94
Figure 4.54: Daily eluted pH readings for inner, middle and outer region points 95
Figure 4.55: Daily cell elution profile for the leach run of reactor 1 96
Figure 4.56: Daily redox readings for reactor 1 97
Figure 4.57: Daily copper concentrations eluted from the inner, middle and outer regions 97
Figure 4.58: Sample of *At. ferrooxidans* taken from bio - reactor 98
Figure 4.60: Magnification of bio-film from reactor 4 99

List of tables

Table 2.1: Oxidation rates of a biotic and abiotic system at 68° C (Nemati & Harrison, 2000) 10

Table 2.2: Commercial bioheap leach operations (Watling, 2006) 14

Table 2.3: Chemical composition of EPS from cells of At. ferrooxidans and L. ferrooxidans grown on pyrite (Gehrke et al., 1995) 20

Table 2.4: Size of mesophilic leaching bacteria (Rawlings, 2007) 23

Table 2.5: Saturation capacity of At. ferrooxidans on varying pieces of pyrite (Asai et al., 1992) 24

Table 3.1: Elemental and mineralogical analysis of Mintek chalcopyrite concentrate 28

Table 3.2: Growth media for microbial stock cultures 30

Table 3.4: 10 x 9 K basal salts medium 31

Table 3.7: Summary of the parameters and experimental analyses performed on the simulated heap leaches 1 - 4 36

Table 4.1: Cells released from packed column on elution basal salts 42

Table 4.2: Tween-20 treated concentrate prior to a basal salt wash 42

Table 4.3: Cells released with iron and sulphate media wash 43

Table 4.4: Cells released with a Triton–x wash 43

Table 4.5: Theoretical H^+ concentration and increase in H^+ ions during the replenishment of the recycle feed on Day 28 (Recycle bin 1) 53

Table 4.6: Theoretical H^+ concentration and increase in H^+ ions during the replenishment of the recycle feed on Day 29 (Recycle bin 2) 53

Table 4.7: Theoretical H^+ concentration and increase in H^+ ions during the replenishment of the recycle feed on Day 31 (Recycle bin 2) 53

Table 4.8: Theoretical H^+ concentration and increase in H^+ ions during the replenishment of the recycle feed on Day 34 (Recycle bin 1) 54

Table 4.9: Mineral dissolution rates and their reactivity to a low pH environment 54

Table 4.10: Cell elution and attachment over the initial 24 hour period of Day 1 56

Table 4.11: Specific growth rates for At. ferrooxidans and L. ferrooxidans 57

Table 4.12: Comparison of copper leached per mass region of ore 63

Table 4.13: Comparison of metal release by acid and water washing 69

Table 4.14: Average residence times for the inner, middle and outer regions for reactors 4 and 3 74

Table 4.15: Average residence times for reactors 1 to 4 94

Table 4.16: Comparison of daily eluted Copper (mg) elutions per total volume for reactors 1 to 4 98

Nomenclature

Abbreviations

EPS	Extracellular polymeric substance
FA	Fluorescent antibody
IEP	Iso – electric point
SE / EW	Solvent extraction / Electrowinning
UCT	University of Cape Town
CO_2	Carbon dioxide
O_2	Oxygen
Fe^{2+}	Ferrous ion
Fe^{3+}	Ferric ion
T	Residence time
Vp	Void volume
Q	Volumetric flow rate (L / Day)

1. Introduction

The world demand for copper has steadily increased in recent years, from 9 million tons to 16 million tons per annum over the period from 1984 to 2005 and is predicted by the Australian Bureau of Agriculture and Resource Economics to reach close to 18 million tons by 2006 (Watling, 2006). While the demand for copper is growing, the minerals industry is increasingly faced with the need to process low grade ores to meet the rising demand.

The processing of copper from low grade ores requires low-cost operating methods such as heap leaching. Bacterially assisted heap leaching has been successfully applied to the extraction of secondary sulphide minerals such as chalcocite. However, heap leaching of the refractory primary copper sulphide, chalcopyrite, has yet to be implemented at a commercial scale (Watling, 2006). Chalcopyrite is considered to be the most abundant copper bearing ore found worldwide (Lizama *et al*., 2003) and is a potential valuable source of copper to the mining industry with millions of tonnes of low grade ore awaiting the development of an efficient and economic bioleach process (Watling, 2006).

Heap bioleaching offers potential for low cost treatment of low grade mineral ores. In this process crushed, agglomerated ore is placed on permeable pads through which an acidic solution is passed. Microbes are introduced into the heap to facilitate the leaching process. As such the heap leaching process represents a non-ideal and extremely complex bioreactor environment (Petersen *et al*., 2004). This can be attributed to the interplay of a number of sub processes operating at different levels, from the micro scale of the individual grain to the macro scale of the entire heap.

At the level of a single mineral grain, leaching is governed by electrochemical interactions at the grain's surface. Sulphide minerals generally leach by the oxidative action of ferric ions in solution, with the reaction kinetics being a function primarily of temperature, the concentration of ferric ions and mineral availability.

Micro-organisms play a key role in mineral bioleaching through the regeneration of the ferric leach agent, sulphur oxidation and acid generation. The exact interaction between microbes and minerals in a heap bioleach is not well defined. There is a limited understanding of microbial colonisation tendencies i.e. the selection and cohabitation of various species, the interactions and symbioses between these, and

their propagation through the porous matrix and across the particle surface (Petersen *et al*. 2004).

At the level of the ore particle, topological effects create another degree of complexity. This refers to the way in which the mineral grains are disseminated through a particular ore particle, and how they are distributed across the different particle sizes. Mineral grains may occur as free grains, grain clusters on gangue particle surfaces and grains and vein-lets permeating a gangue matrix.

At the meso-scale or particle agglomerate level, three processes contribute to the overall rate of leaching: the gas (oxygen and CO_2) uptake; the bacterial growth, propagation and oxidation at this level and the intra and inter particle diffusion.

At the macro level, transport phenomena within a heap are taken into account which encompasses solution flow, heat flow and gas flow.

The scope of this study is to better understand the colonisation of a selected group of microorganisms, namely the mesophilic bioleaching microorganisms *Acidithiobacillus ferrooxidans*, *Acidithiobacillus thiooxidans*, *Acidithiobacillus caldus* and *Leptospirillum ferrooxidans* on chalcopyrite and low grade chalcopyrite ore. Following the study of the attachment of the micro-organisms to the sulphide mineral, a simulated heap leach was analysed with particular reference to microbial concentration in the liquid and solid phases as a function of location with regard to differing irrigation regimes.

In Chapter 2 the background of the project is set through a review of the literature that relates to the history of leaching processes, current understanding of leaching mechanisms and practices, as well as the role microorganisms play in a leach environment. Thereafter the state of knowledge of microbial colonisation in the heap bioleach environment is reviewed. Chapter 3 presents the materials and methods used in this study. In Chapter 4, the results of the mineral attachment experiments and the simulated heap leaches are reported and their significance discussed. Chapter 5 presents the conclusions of the research findings and makes recommendations with regards to future research and application.

2. Literature review

2.1 History of biomining

Microorganisms naturally assist in extracting metals from ores. Microbes have participated in the deposition and solubilisation of heavy metals in the earth's crust since geologically ancient times (Rawlings, 2002). The history of harnessing the natural capability of these microbes to decompose a variety of mineral deposits dates back to Roman times in the first century. These early miners used the microbial activity to leach minerals from ore without being aware that microbes were involved (Rawlings *et al.*, 2003). One of the first reports of leaching is described by the Roman writer Gaius Plinius Secundus (23 – 79 AD). In his report, he described how copper was obtained by the slow passage of water through a mine in winter and the evaporation of the leachate in summer leaving behind the copper (König, 1989).

A German physician and mineralogist, Georgius Agricola (1494 – 1555) described in his work *de re metallica* techniques for the recovery of copper based on the leaching of copper containing ores (Schiffner, 1977). An illustration from *de re metallica* (Figure 2.1) shows the manual transport of metal-containing leachates from mines and their evaporation in sunlight.

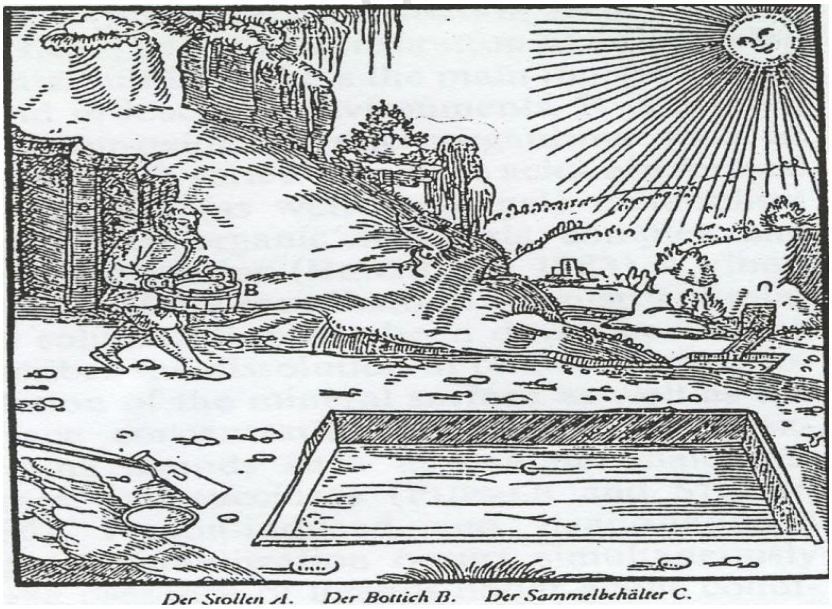

Figure 2.1: Woodcut from the book *de re metallica* written by Georgius Agricola (1494 – 1555) illustrating the recovery of copper from mine effluents which are collected in wooden basins and concentrated in the sun (Schiffner, 1977)

The Rio Tinto mines in south western Spain are considered to be the cradle for biohydrometallurgy. The first industrialised bioleaching operations were developed here in the early 1890s. The contribution of bacteria to metal leaching was confirmed only in 1961, when *Acidithiobacillus ferrooxidans*; then known as *Thiobacillus ferrooxidans*; was identified in the leachates from the Rio Tinto mines (Salkfield, 1987). The ability of microorganisms to solubilise metals from ores for commercial purposes has given rise to the biomining industry of today (Brierley, 1997).

2.2 Introduction to biomining

The term biomining refers to the bioleaching and bio-oxidation technologies used in the hydrometallurgy industry (Rawlings, 2002). The bioleaching process involves the dissolution of a specific metal, typically a base metal, from its mineral source with the aid of leaching microorganisms. The metal is then recovered from the solution (Rawlings, 1998). During the bio-oxidation process, a host-mineral is pre-treated using leaching microorganisms to make accessible the relevant metal in the solid phase prior to metal processing (Brierley, 1997).This approach is used in the biomining of gold from sulphidic ores. These processes can be classified into two categories, namely stirred tank bioleaching and heap bioleaching (Brierley, 1997).

2.2.1 Stirred tank bioleaching

Stirred tank leaching is reserved for the treatment of high-grade mineral concentrates and has been in commercial use for the past 20 years (Brierley, 1997). The overall leaching kinetics associated with tank leaching is higher than those found in heap leaching owing to control of an optimum environment in stirred tanks with regards to pH and temperature (Okibe *et al*., 2003). The use of an agitator and a blower to promote a uniform solids suspension and improve oxygen mass transfer contributes to the increased leaching kinetics. Finely divided solids enhance mineral availability with the homogenous environment allowing for better solid – liquid contacting and microbial dispersion throughout the tank leaching process. The use of cooling coils or water jackets are required to maintain the ideal operating temperature (Brierley, 1997). Due to the corrosiveness of the acidic ferric sulphate, rubber lined or high grade stainless steel reactors are needed for tank leaching. One of the major constraints on the operations of stirred tank reactors is the quantity of solids (pulp density) that can be maintained in suspension (Whitlock, 1997). This is limited to ~

20% in mesophilic systems. At pulp densities higher than 20%, physical and microbial hurdles occur. The slurry becomes too thick for efficient gas transfer to occur and the increased shear forces induced by the impellers and the suspended solids create physical damage to microbial cells (Rawlings *et al*., 2003). As such, the limitation in solids concentration plus considerably higher capital and operating costs than heap reactors has restricted stirred tank reactors to high value minerals or mineral concentrates (Rawlings 2002).

2.2.2 Heap leaching

Heap bioleaching targets the extraction of marginal ores with a lower target mineral concentration. Heap reactors are cheaper to construct and operate than stirred tank reactors due to their lower set-up and maintenance costs (Rawlings *et al.*, 2003).

However, heap reactors are more difficult to monitor and manage when compared to stirred tank reactors. Conditions within stirred tank reactors seek to approximate homogeneity with aeration, pH, temperature, nutrient concentration and microbial growth being monitored. In heap reactors, efficient aeration of the heap is more difficult due to the low gas to liquid mass transfer rates in stationary bodies (Ritchie, 1997) and the varying pH gradients occurring due to the composition of stacked ore being a mixture of mineral and gangue material (Rawlings 2003). Consequently the microbial heat generation rates are poor (Petersen & Dixon, 2002) with a resultant decrease in leaching kinetics. While mineral decomposition takes days in stirred tank reactors, it may take weeks or months in heap reactors (Rawlings 2003).

To optimise heap leaching, a different set of process considerations need to be understood when compared with tank leaching. These include a better understanding of the hydrodynamics of solution flow through a heap and the influence of microbial dispersion and attachment to the ore during leaching (Petersen *et al.*, 2004).

2.3 Potential for heap bioleaching

In terms of tonnage, copper is currently the most important metal to be recovered by leaching (Brierley, 1997). During the past two decades world copper production has steadily increased from 9 million tons per annum in 1984 to 16 million tons per annum in 2005 (Watling, 2006). Current copper production through

hydrometallurgical processing of chalcocite and covellite contributes an estimated 20 to 25 % of world copper production (Watling *et al.*, 2004). Due to the resultant decrease in the high-grade copper ore deposits, the mining industry is now focused on the utilisation of remaining low-grade copper ore deposits found worldwide (Rawlings *et al.*, 2003). These low grade ores require the use of alternative metal extraction procedures owing to the prohibitive cost and energy requirements of traditional concentration operations for low grade ores.

The heap leaching process does not require milling or concentrating of minerals. Further it requires less energy than the traditional methods of roasting and smelting. It does not produce sulphur dioxide and prevents the release of toxic heavy metals in gaseous streams. The developments in heap leaching processes have mostly focused on the engineering field with little attention being given to the microbial interaction within the ore (Rawlings *et al.*, 2003). This work will investigate the attachment, loading and migration of microorganisms through a mineral environment to try and better understand their influence on the heap leaching process.

2.4 Mechanisms of leaching

2.4.1 The indirect and direct mechanism

The principle role of microbial involvement in the bioleaching process is the oxidative regeneration of ferric ion which forms the mineral leach agent and the oxidation of elemental sulphur product to sulphate (Watling *et al.*, 2004) as shown in Figure 2.2.

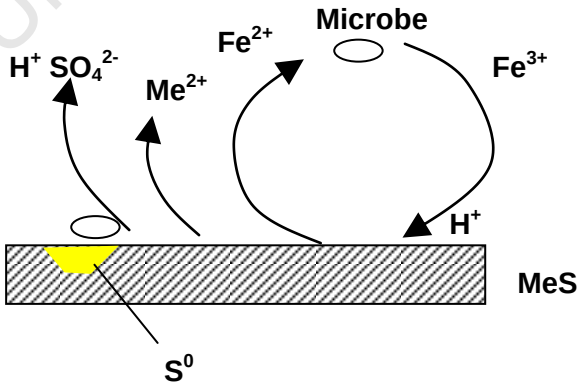

Figure 2.2: Schematic representation of microbial leaching of a metal sulphide (adapted from Petersen *et al*., 2004)

Two mechanisms for microbial leaching have been proposed by Silverman (cited in Crundwell, 2001). These are known as the direct contact mechanism and the indirect mechanism. The direct contact mechanism involves the leaching microorganisms being able to directly oxidise the sulphide mineral via a biological oxidant, without the requirements of ferric or ferrous ions (Crundwell, 2001). Much debate has surrounded the validity of the direct mechanism, which has been refuted by Schippers *et al.* (1996) and Tributsch (2001) as a leaching mechanism.

The indirect mechanism involves the microbial oxidation of ferrous to ferric ion (Nordstorm & Southoam, 1997). The chemical attack of the mineral sulphide by ferric and hydrogen ions, results in the dissolution of the mineral and the formation of ferrous ion and various forms of sulphur (Rawlings, 2002). The dissolution of the mineral releases the soluble metal sulphate into solution (Schippers & Sand, 1999) allowing it to be recovered via solvent extraction and electrowinning processes.

The indirect method of leaching has two categories namely contact and cooperative leaching (Rawlings *et al.*, 1999). With the contact mechanism microorganisms attach to the mineral sulphide surface (described in Section 2.9) as shown in Figure 2.3a (Rohwerder *et al.*, 2003). The firm attachment of microbes to the mineral surface occurs through the formation of an exopolymeric substance (EPS). The EPS acts as a controlled reaction zone between the bacterial membrane and mineral sulphide (Tributsch, 2001) in which reaction substrates may be concentrated. This reaction space aids in the microbial catalysed oxidation of ferrous to ferric ion and subsequent mineral leaching. The microbial attachment to or association with the mineral has been shown to leave corrosive pits along the mineral surface where ferric reduction has occurred.

With co-operative leaching (Rojas Chapana *et al*. 1998), bacteria attached to the mineral surface and free bacteria co-operate (Figure 2.3b). Ferrous ions and sulphur in suspension provide the energy source to maintain a planktonic bacterial population in the surrounding medium. The free-floating bacteria are able to oxidise the ferrous and reduced sulphur ions; thereby regenerating the ferric oxidant and sulphuric acid (Rohwerder *et al.*, 2003). Figure 2.3 (a) and 2.3 (b) illustrates the contact and cooperative leaching mechanisms.

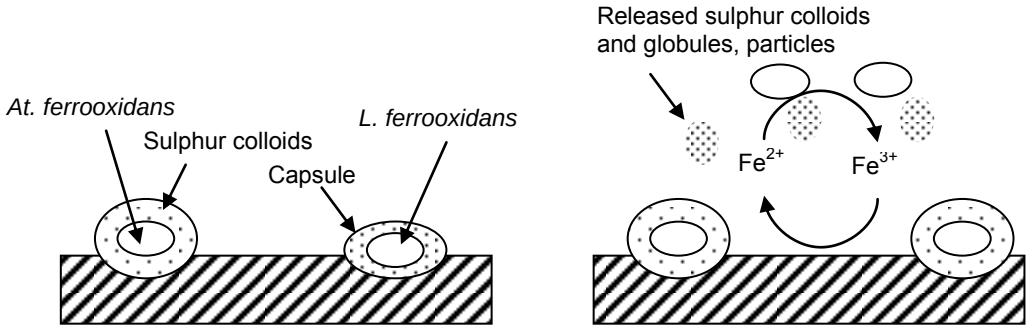

a) Contact leaching (attached bacteria) b) Co-operative leaching

Figure 2.3 (a) and (b): Contact and cooperative leaching mechanisms (adapted from Rawlings *et al.*, 1999)

2.4.2 Leaching pathways

The mineral dissolution reaction is not identical for all metal sulphides with the oxidation of different metal sulphides proceeding via different intermediates (Rawlings *et al.*, 2003). The oxidation of a sulphide mineral by ferric ions may proceed via a thiosulphate intermediate or a polysulphide pathway depending on the mineral solubility in acid (Schippers & Sand, 1999).

2.4.2.1 Thiosulphate pathway

In the thiosulphate mechanism, acid-insoluble metal sulphides such as pyrite (FeS_2) are exclusively solubilised through a ferric ion attack resulting in thiosulphate as the main intermediate (Equation 2.1) and sulphate as the main end product (Equation 2.2) (Rohwerder *et al.*, 2003).

$$FeS_2 + 6Fe^{3+} + 3H_2O \rightarrow S_2O_3^{2-} + 7Fe^{2+} + 6H^+ \qquad \text{Equation 2.1}$$

$$2S_2O_3^{2-} + 8Fe^{3+} + 5H_2O \rightarrow 2SO_4^{2-} + 8Fe^{2+} + 10H^+ \qquad \text{Equation 2.2}$$

During the course of pyrite oxidation, the ferric ion adsorbs onto pyrite, accepts an electron and is reduced to its ferrous form (Equation 2.1). The ferrous ion remains adsorbed onto the pyrite surface and can then be reoxidised to the ferric form, by transferring electrons to molecular oxygen via a microbial intermediate (Equation 2.2) (Schippers *et al.*, 1996). The oxidation of thiosulphate by ferric ions to sulphate and

protons is rapid (Hansford & Vargas, 2001). A postulated pathway of the oxidation of pyrite with intermediates is shown in Figure 2.4. Significant amounts (10 – 20%) of elemental sulphur are produced in the absence of sulphur-oxidising bacteria (Schippers *et al.*, 1999).

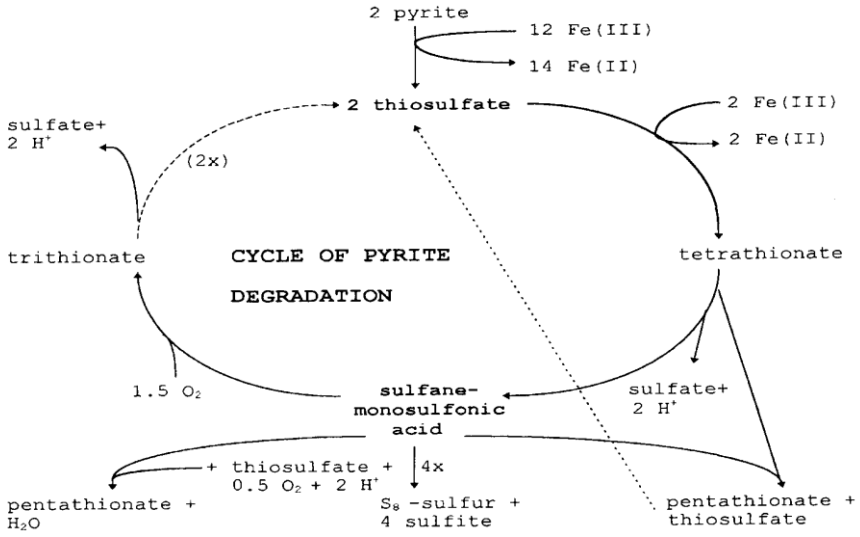

Figure 2.4: Cycle of oxidative pyrite by bacterial and/or chemical leaching (Schippers *et al.,* 1996)

2.4.2.2 Polysulphide and Sulphur Pathway

In the case of the polysulphide mechanism, acid-soluble metal sulphides, such as chalcopyrite, are solubilised by the combined attack of ferric ions and protons, with elemental sulphur as the main intermediate (Rawlings *et al.,* 2003) (Equations 2.3 to 2.5).

$$MS + Fe^{3+} + H^{+} \rightarrow M^{2+} + 0.5\ H_2S_n + Fe^{2+}\ (n \geq 2) \qquad \text{Equation 2.3}$$

$$0.5\ H_2S_n + Fe^{3+} \rightarrow 0.125\ S_8 + Fe^{2+} + H^{+} \qquad \text{Equation 2.4}$$

$$0.125\ S_8 + 1.5\ O_2 + H_2O \rightarrow SO_4^{2-} + 2\ H^{+} \qquad \text{Equation 2.5}$$

In the course of this process, more than 90 % of the sulphide is transformed into elemental sulphur in the absence of sulphur oxidising bacteria (Rohwerder *et al.*, 2003) due to the stability of sulphur under experimental and environmental conditions (Schippers & Sand, 1999).

In both pathways, the role of leaching microorganisms is the regeneration of ferric ions from ferrous iron. The ferric ion attacks the sulphide mineral as the oxidant for

sulphide leaching (Rohwerder *et al.*, 2003). Elemental sulphur is oxidised by microbes as this sulphur species is inert to abiotic oxidation in acidic environments. Consequently, elemental sulphur may accumulate in the course of metal sulphide dissolution if sulphur-oxidising bacteria are absent or inhibited. The production of sulphuric acid from reduced sulphur compounds is needed to regenerate protons consumed by the initial leaching processes via the polysulphide pathway (Rohwerder *et al.*, 2003).

2.5 Abiotic vs biotic heap leaching

The leaching of an ore can be done via abiotic or biotic heap leaching. When comparing these two types of leaching methods, it has been shown that the use of microorganisms increases the rate of oxidation of ferrous iron (Crundwell, 2001). This higher oxidation rate ensures an adequate or improved supply of the ferric mineral leach agent, increasing metal recovery to higher levels than that of chemical leaching under the same conditions (Watling *et al*., 2004, Qiu *et al*., 2005). Table 2.1 provides comparison of the ferrous iron oxidation rates in both systems (Nemati & Harrison, 2000).

Table 2.1: Oxidation rates of a biotic and abiotic system at 68° C (Nemati & Harrison, 2000)

Initial iron concentration ($kg.m^{-3}$)	Biological oxidation rate ($kg.m^{-3}$)	Chemical oxidation rate ($kg.m^{-3}$)
0.8	0.023	0.002
1.8	0.051	0.002
3.5	0.077	0.006
5.8	0.082	0.023
7.5	0.105	0.028
9.0	0.070	0.040

2.6 Microorganisms involved in heap leaching

Microorganisms commonly associated with a heap leaching environment at an operating temperature of 40 ^{o}C or less consist of a consortium of Gram - negative bacteria. These include *Acidithiobacillus ferrooxidans* (*At. ferrooxidans*); *Leptospirillum ferrooxidans* (*L. ferrooxidans*); *Acidithiobacillus thiooxidans* (*At.*

thiooxidans); *Acidithiobacillus caldus* (*At. caldus*) (Goebel & Stackebrandt, 1994; Kelly & Wood, 2000; Hallberg & Lindstrom, 1994; Coram & Rawlings, 2002; Hallberg & Johnson, 2001) and *Leptospirillum ferriphilum (L. ferriphilum)* (Coram & Rawlings, 2002). At temperatures greater than 50° C, bacteria belonging to the Gram - positive genera *Sulfobacillus* and *Acidimicrobium* become dominant (Clark & Norris, 1996a). Temperatures greater than 60° C yield a biomining consortia dominated by archaea rather than bacteria with the species of *Sulfolobus* and *Metallosphaera* being most prominent (Norris *et al.*, 2000). The mesophilic chemoautolithotrophic bacteria obtain their energy from the oxidation of ferrous iron (*At. ferrooxidans*, *L. ferriphilum* and *L. ferrooxidans*) or reduced inorganic sulphur compounds to sulphate (*At. ferrooxidans*, *At. thiooxidans* and *At. caldus*) (Kelly & Harrison, 1989). The production of sulphate results in the accumulation of sulphuric acid (Rawlings, 1997) with the concomitant effect that the pH of the environment is typically less than pH 3.0 and that all the bacteria are therefore obligately acidophilic (Norris & Johnson, 1998).

Several authors have compared the efficiency of bioleaching with pure and mixed cultures of leaching microorganisms (Plumb *et al*., 2008; Qiu *et al.*, 2005; Rawlings *et al.*, 1999; Hallman *et al.*, 1993). A faster leach rate of copper was observed on the sulphide mineral, chalcopyrite, when leached by a mixed bacterial population compared to the leaching of individual pure cultures under the same conditions (Qiu *et al.*, 2005). This is generally understood to be due to the symbiotic relationship formed between the cultures in the mixed population.

2.7 Bioleaching of chalcopyrite

Chalcopyrite ($CuFeS_2$), a primary copper sulphide is considered to be the most abundant copper bearing ore found worldwide (Rawlings *et al.*, 2003) and is a potential economically valuable source of copper to the mining industry (Madigan *et al.*, 1997). However, due to its refractory nature to chemical and biological leaching (Rodriguez *et al.*, 2003a), chalcopyrite leaching has yet to be implemented effectively on a commercial scale (Watling, 2006). There are, however, clear economic advantages to leaching chalcopyrite in order to satisfy the increasing demand for copper.

While the bioleachability of chalcopyrite has been demonstrated, it has been considered to be non-viable economically due to the long leach times required for

sufficient recovery of copper (Schnell, 1997; Stott *et al.*, 2001). Initial rapid leaching rates decline as a function of time, with bioleaching releasing only a portion of the copper value in chalcopyrite (Watling *et al.*, 2004). The main reason for the refractory nature of chalcopyrite is postulated to be the formation of a solid passive layer on the mineral surface (Rodriguez *et al.*, 2003a; Petersen & Dixon, 2005) at high solution potentials (>600 mV vs. Ag/AgCl) (Hackl *et al.*, 1995). The process of 'passivation' reduces the leaching effect by limiting both reagent contact and the diffusion of the metal into solution (Rodriguez *et al.*, 2003a).

Both sulphur- and iron- containing reaction products have been invoked as the cause of the slow dissolution process and passivation of chalcopyrite (Watling, 2006). These insoluble reaction products form on the chalcopyrite surface during the abiotic chemical leaching and bioleaching processes (Klauber 2003, Klauber *et al.*, 2001 and Parker *et al.*, 2004) under both aerobic and anaerobic conditions, suggesting a common leaching mechanism (Watling, 2006).

During the chemical oxidation of a sulphide mineral by ferric iron, the sulphide is oxidised to elemental sulphur (Equation 2.6). This sulphur may accumulate on the mineral surface and prevent further oxidation by blocking access of ferric iron to the sulphide mineral (Crundwell, 1997).

$$CuFeS_2 + 4Fe^{3+} \rightarrow Cu^{2+} + 5Fe^{2+} + 2S^0 \qquad \text{Equation 2.6}$$

Iron-hydroxy precipitates, most commonly jarosites [$MFe_3(SO_4)_2(OH)_6$], form in acidic ferric sulphate and mineral leaching environments (Equation 2.7). Jarosite precipitates form a physical barrier that prevents microbial access and slow the diffusion of ferric ion and reaction products to and from the mineral surface (Dutrizac, 1989; Stott *et al.*, 2000; Boon and Heijnen, 1993).

$$3\,Fe^{3+} + 2\,SO_4^{2-} + 6H_2O + M^+ \rightarrow MFe_3(SO_4)_2(OH)_6 + 6H^+ \qquad \text{Equation 2.7}$$

($M = K^+$, H_3O^+ or NH_4^+)

The rate of jarosite formation is constant within a pH range of 2.0 to 2.8. However below a pH of 2.0, the deposition of jarosite is reduced (Linge, 1976). At a pH of 1.1, jarosite precipitation was reduced significantly and the onset time of precipitation typically delayed by approximately 140 hours depending on solution concentrations.

The primary use of microorganisms in chalcopyrite bioleaching is to catalyse the reactions to regenerate the ferric oxidant and the oxidation of elemental sulphur to generate acid (Tshilombo *et al.*, 2002). Sulphur metabolising microbes can rapidly oxidise the sulphur layer, producing sulphuric acid (Equation 2.5) and reducing the pH of the environment thereby delaying the onset of jarosite precipitation (Watling, 2006).

In the process, iron-oxidising bacteria can reoxidise ferrous ions to ferric ions, thereby regenerating the oxidant in solution (Equation 2.8) to continue the leaching process at the minerals surface.

$$2Fe^{2+} + 2H^{+} + 0.5O_2 \rightarrow 2Fe^{3+} + H_2O \qquad \text{Equation 2.8}$$

Clark and Norris (1996b) demonstrated that the rate and extent of chalcopyrite leaching is increased with increasing temperature, requiring the presence of thermophilic microorganisms such as *Sulfolobus metallicus* and *Metallosphera sedula*. It has been observed that thermophilic leaching takes place in a low potential environment (380 – 500 mV Ag/AgCl) in which chalcopyrite passivation is not observed (Petersen *et al.*, 2001; Gericke *et al.*, 2001; Third *et al.*, 2000). Petersen and Dixon (2002) noted that heating a heap to thermophilic temperature ranges would require a succession of mesophilic and moderate thermophiles. While mesophiles and moderate thermophiles leach pyrite preferably over chalcopyrite at high potentials (600-700 mV vs. Ag/AgCl), heat generation allows progression to a hot heap. It is postulated that the presence of sufficient quantities of pyrite (~ 5 %) would be required. The leaching of chalcopyrite was then postulated to commence upon the introduction of extreme thermophiles and decrease of solution potentials once temperatures exceeded 60 °C. The linear rate of leaching observed on high temperature leaching was postulated to result from the low solubility of oxygen at these prevailing temperatures (Petersen and Dixon 2002; Petersen *et al.*, 2004). However conditions within a heap are highly variable (Plumb *et al.*, 2002) hence differing operating regimes exist. Consequently the understanding of the microbiology involved in the heap leaching process is integral to increasing the bioleaching rate of chalcopyrite in heap operations.

2.8 Current heap leaching practices

2.8.1 Prevalence of copper heap bioleaching

Current bioheaps predominantly leach secondary copper sulphides ores such as chalcocite and covellite. Table 2.2 shows a selection of heap operations found worldwide. The proliferation of bioheap leach operations during the last ten to fifteen years attests to the good performance and profitability of this technology (Brierley, 2001). However, little is known and understood about the microbiology of bioheap leaching.

Table 2.2: Commercial bioheap leach operations (Watling, 2006)

Plant / Location	Size (t / Day)	Operator	Ore grade (% Cu) / Mineral Type	Years in Operation
Lo Aguirre, Chile	16 000	Sociedad Minera Pudahuel	1.5 % / Chalcocite	1980 – 1996
Mt. Leyshon, Australia	1370	Normandy Poseidon	0.15 % / Chalcocite	1992 – 1995
Cerro Colorado, Chile	16 000	Rio Algom	1.4 % / Chalcocite, Covellite	1993 – Present
Girilambone, Australia	2000	Straits Resources	~ 3 % / Chalcocite, Chalcopryite	1993 – Present
Ivan, Chile	1500	Glamis Gold	2.1 % / Oxides, Sulphides	1994 – Present
Quebrada Blanca, Chile	17 300	Cominco	1.3 % / Chalcocite	1994 – Present
Andacollo, Chile	16 000	Dayton Mining	1.0 % / Chalcocite	1996 – Present
Dos Amigo, Chile	3000	Cemin	2.5 % / Chalcocite	1996 – Present
Cerro Verde, Peru	32 000	Cyprus-AMAX	0.7 % / Oxides, Sulphides	1996 – Present
Zaldivar, Chile	~20 000	Placer Dome / Outokumpu	1.4 % / Chalcocite	1998 – Present
S&K Copper Project, Myanmar	15 000	Myanmar Ivanhoe Copper	1.25 % / Chalcocite	1998 – Present

2.8.2 Practices of setting up and operating bioheaps

The construction of a heap leach begins with crushed ore being acidified with sulphuric acid and agglomerated in rotating drums to bind the fine material to coarser particles (Schnell, 1996). The agglomerated ore is stacked onto prepared pads in layers (Schnell, 1997). Aeration piping may be supplied to improve bioleaching rates (Rawlings, 2002). A leach solution is then applied to the top and percolates through

the heap. In time, leaching microorganisms colonise the ore and catalyse the regeneration of the leach agent, allowing the oxidation of the insoluble metal to its soluble form, releasing the metal of value into solution (Rawlings, 1998). External to the heap, the metal is recovered from solution by further processing (Schnell, 1997).

2.8.2.1 Crushing

The crushing of an ore to its optimum size depends on the mineralogy of the ore. This has a direct effect on the leaching variables (Brierley, 2001; Bruynesteyn & Duncan, 1974). While a finer particle size aids availability of mineral to leach agents, it also impacts porosity of the heap and increases crushing costs. Particle size range should be optimised for each ore type. Clayey ores should not be crushed to small particle sizes, whereas hard siliceous ore can withstand crushing to smaller sizes without generating fines which reduce heap porosity (Schnell, 1997). In general the finer the particle size the better the final recovery (Schnell, 1997).

2.8.2.2 Agglomeration

The agglomeration of crushed ore binds the fines of the mineral to larger sized particles (Schnell, 1997). An agglomerated moisture content of 7.5 % prevents mineral fines from hindering solution transport through the heap (Petersen & Dixon, 2003). The crushed ore can be agglomerated with sulphuric acid or with the effluent from the solvent extraction – electrowinning process (raffinate). The raffinate usually contains a small number of leaching microorganisms which assist in inoculating the heap (Brierley, 2001). Agglomerating techniques increase in complexity and expense as the amount of mineral fines increases per operation (O'Kane Consultants Inc., 2000). The agglomeration of the ore preconditions the heap for bacterial colonisation (Brierley, 2001) while creating a more homogenous heap to reduce preferential flow.

2.8.2.3 Height and aeration

Agglomerated ore is usually stacked in lifts at 2 to 10 meters high (Rawlings, 2002; Schnell 1997; Brierley, 2001) on impermeable irrigation beds lined with high density polyethylene to avoid loss of solution via evaporation (Rawlings, 2002). Aeration pipes are positioned below the lifts to provide forced aeration to minimise CO_2 and O_2 limitation, thereby improving the speed of the bioleaching process and stimulating the development of leaching microorganisms.

2.8.2.4 Irrigation

The heap is irrigated from drip points typically positioned in a 0.5 m grid over the heap surface. The industry standard for heap irrigation is 5 to 6 L /m^2 /hr (Schnell, 1997). This rate of irrigation does not cause saturation of the ore. The standard irrigation solution consists of raffinate which usually contains 1.5 to 6.0 g/L iron and a variety of other ions (calcium, magnesium, sodium, manganese, potassium, chlorides, etc). The initial leach solution usually includes ferric iron to initiate the leach cycle. The amount of iron in the leach solution varies from site to site depending on the ore composition and in some cases may be as high as 20 g/L (Petersen & Dixon, 2003).

2.8.2.5 Nurturing leaching microorganisms

Leaching microorganisms require ammonium, nitrogen and phosphate which is supplied as $(NH_4)_2SO_4$ (10 to 20 mg/L NH^+_4) and KH_2PO_4 (30 to 40 mg/L PO_4^{3-}) in the leach solution. Typically sufficient phosphate is present in the gangue materials and only ammonia may be required. Analysis of ore and leached solutions is required to determine level of nutrient supply (Schnell, 1997). An acidity of the leaching solution of pH 1.8 to 2.2 is required to allow suitable microbial growth. Typical solution acid concentrations used in the mining industry are 6.0 to 8.0 g/L H_2SO_4. With certain ores, significant acid consumption by gangue minerals may occur as the solution percolates through the heap, increasing the pH. In such cases, acid supplementation may be required (Schnell, 1997).

2.8.2.6 Effluent extraction

The pregnant leach solution containing copper ions is collected at the base of the heap and is either recycled to the top of the heap (irrigation leaching solution) or directed to a solvent extraction and electrowinning plant (SEx/EW) circuit for copper recovery. The stripped solution (raffinate) from the SEx/EW is returned to the heap for irrigation (Brierley, 2001).

Leach times vary, but are typically in the 200 day range for secondary copper ores. Recoveries are about 75 to 85% depending on mineral quality (Brierley, 2001). The

careful construction and operation of the heap reactor increases its efficiency. It is anticipated that continued improvements may enable the bioleach process to be carried out in a matter of months rather than years (Rawlings 2002).

2.9 Microbial attachment

It is recognised that the colonisation of the bioheap is aided by the adhesion of microbial cultures to the ore surface. Much debate has surrounded the initial adhesion of leaching bacteria to sulphide mineral surfaces. A number of mechanisms have been proposed to describe the initial attachment and the subsequent formation of biofilms. These include chemotaxis, electrostatic interaction, hydrophobicity, EPS formation and site specific attachment.

2.9.1 Chemotaxis

Chemotaxis is thought to play a major role in initial attachment of leaching bacteria (Rodriguez *et al.*, 2003b; Acuňa *et al.*, 1986). All bacteria involved in the leaching of sulphide minerals are motile and possess flagella (Adler, 1973; Kleene *et al*., 1979; Koshland, 1981; Kort *et al*., 1975). Motile microorganisms are attracted by certain chemicals and repelled by others by means of a chemosensory system which regulates motility by controlling the direction of flagellar rotation (Adler, 1973; Kleene *et al.*, 1979; Koshland, 1981). Signals for a number of attractants and repellents are processed by the transmembrane proteins which convert information received from the environment into signals that converge on the flagellar motor (Koshland, 1981; Kort *et al.*, 1975). The chemotatic response of *At. ferrooxidans*, *At. thiooxidans* and *L. ferrooxidans* using sulphur and ferrous iron as attractants has been shown by Rojas-Chapana *et al.* (1998) and Acuňa *et al.* (1986).

2.9.2 Hydrophobicity

The cell surface of *At. ferrooxidans* and the role it plays in the attachment to sulphide minerals has been investigated repeatedly (Shrihari *et al.*, 1991; Murthy and Natarajan, 1992; Blake *et al.*, 2001; Devasia *et al.*, 1996, Solari *et al.*, 1992). Surface properties of leaching bacteria proposed to affect adhesion to mineral sulphides include cell surface hydrophobicity and electrokinetic potential of the bacterium (Van Loosdrecht *et al.*, 1990).

The nature of the cell surface of *At. ferrooxidans* depends on the culture conditions (Ehrlich, 2002). *At. ferrooxidans* cells grown on elemental sulphur are more hydrophobic than cells grown on ferrous ion media (Devasia *et al.*, 1993; Blake *et al.*, 2001). A decrease in pH of growth caused an increase in the hydrophobicity of *At. ferrooxidans* (Solari *et al*., 1992). Devasia *et al.* (1993) hypothesized that this increased hydrophobicity of *At. ferrooxidans* would increase the adhesiveness of the bacterium to sulphide minerals. However, Sampson *et al.* (2000) showed that the higher hydrophobicity of the sulphur grown cells did not increase their attachment to pyrite since the less hydrophobic cells of *At. ferrooxidans* which had been cultured on ferrous iron and a chalcopyrite concentrate, respectively, exhibited a greater degree of attachment to pyrite. This suggests that hydrophobic interactions are not dominant in the attachment of microbes to metal sulphide surfaces (Gehrke *et al.*, 1998; Sampson *et al.*, 2000)

2.9.3 Electrostatic potential

In studies carried out by different authors, the electrostatic force between mineral surfaces and bacteria is the main factor in the initial bacterial attachment (Rodriguez, 2003b). Solari *et al*. (1992) investigated the electrophoretic mobility measurements on chalcopyrite, pyrite and *At. ferrooxidans* as a function of pH. Solari *et al*. (1992) reported that *At. ferrooxidans* cells grown on sulphur had an isoelectric point (IEP) or point of zero charge (pZc) of pH 3.0 while chalcopyrite had an IEP of pH 2.0. Pyrite, however, was shown to have a negative electrophoretic mobility below pH 4.0, with two IEPs at pH 4.5 and at pH 5.7. This was confirmed by *At. ferrooxidans* being electrostatically attracted to pyrite and chalcopyrite in the pH range of 2 to 3. The largest degree of cell adhesion was obtained for chalcopyrite with a 23 % coverage area, followed by pyrite with 20 % surface coverage (Solari *et al.*, 1992). However Solari *et al.* (1992) showed that below a pH of 2.2 *At. ferrooxidans* was not electrostatically attracted to chalcopyrite, due to the electrostatic repulsive barrier of the positively charged chalcopyrite below pH 2.0. In the case of pyrite, the electrostatic interaction would always be attractive because of the negative charge on pyrite below pH 2.0. Devasia *et al*. (1993) showed that depending on the media used to culture *At. ferrooxidans*, the IEP of ferrous grown cells was pH 2.0, while mineral sulphide grown cells had an IEP of pH 3.8. It was also reported that the interaction of *At. ferrooxidans* with pyrite and chalcopyrite shifted the IEP of the

mineral sulphides from pH 2.9 to 4.7 and pH 2.6 to pH 4.4 (Devasia *et al.*, 1993). This would indicate that the interaction of *At. ferrooxidans* with a mineral not only changes the electrokinetic behaviour of the bacterium but also that of the mineral with which it had interacted. This interaction would increase the attachment of bacterial cells to the mineral while decreasing electrostatic repulsion between the two bodies.

Karavaiko *et al*. (1995) investigated the charge of *At. ferrooxidans* and found that the increase of the negative value of the cell's electrophoretic mobility was characteristic of the exponential growth phase of the culture and the active oxidation of substrates. It was proposed that *At. ferrooxidans* picks up the negative charge from the oxidation of ferrous to ferric iron and elemental sulphur to sulphate, by the adsorption of ferrous and elemental sulphur ions by the ionogenic groups on the cells' surface (Barrett *et al.*, 1993; Balke *et al.*, 1989; Cox and Brand, 1982; Gromova *et al.*, 1983; Ingledew *et al.*, 1977; Karavaiko and Pivovarova 1973; Pivovarova *et al*, 1982). Karavaiko *et al*. (1995) found that cells with high values of a negative charge had higher metabolic activity. When metabolic processes in the cell stopped due to the exhaustion of substrate, the charge of the cell approached its IEP.

Bacteria influence charge of substrate and create a high redox potential in the medium. The charge of the substrate can be either lower or higher than that of the cell, but the activity of the oxidation process depends on the value of this difference and hence on the expense of energy for the electron migration from the valence zone to the zone of conductivity and their transport to the acceptors located on the cells surface (Karavaiko *et al.*, 1995). In conclusion, the primary attachment to pyrite is mediated by positively charged exopolymer-complexed ferric ions, allowing an electrochemical interaction with the negatively charged surface (Geesey and Lang, 1989 cited in Gehrke *et al.*, 1998).

2.9.4 Extracellular polymeric substance

The extracellular polymeric substance (EPS) mediates contact between the bacterial cell and the sulphide energy source (Gehrke *et al.*, 1995; Pogliani and Donati, 1999; Sand *et al.*, 1995). *At. ferrooxidans* and *L. ferrooxidans* cells grown on solid substrates such as pyrite, excreted up to tens times more EPS than cells grown on

ferrous media. The composition of the excreted EPS consisted mainly of neutral sugars and some uronic acids as shown in Table 2.3 (Gehrke *et al.*, 1995).

Table 2.3: Chemical composition of EPS from cells of *At. ferrooxidans* and *L. ferrooxidans* grown on pyrite (Gehrke *et al*., 1995)

Composition (µg/mg cell protein)					
Organism	Neutral Sugars	Hexosamines	Uronic Acids	Iron	Other Compounds
At. ferrooxidans	4535	0	313	57	N/D
L. ferrooxidans	1600	0	150	20	N/D

The content of neutral sugars, uronic acids, iron ions and unknown compounds amounted to 42%, 3%, 0.5% and 54% (w/w) respectively. Gehrke *et al*. (1995) reported that cells containing EPS and bound ferric ions attached to pyrite relatively quickly when compared to EPS-deficient cells. This delay could be attributed to the cellular regeneration of the EPS layer.

At. ferrooxidans and *L. ferrooxidans* grown on pyrite or ferrous ions, were shown by Gehrke *et al.* (1995) to incorporate ferric ions into their EPS. This rendered the surface charge of the cell positive under physiological conditions, whereas pyrite was negatively charged (Gehrke *et al.*, 1995; Blake *et al.*, 1995). Therefore it was concluded that the EPS-complexed ferric ions enabled the cell attachment to a pyrite surface primarily by electrostatic interaction. The ferric ion - complexed EPS played a role in the electrochemical dissolution of pyrite via the contact mechanism in which the EPS provides a reaction space in which dissolution can take place (Rohwerder *et al.*, 2003; Gehrke *et al.*, 1998; Crundwell, 2001).

Rohwerder *et al.* (2003) found that cells grown on sulphur contained less sugars and uronic acids but more fatty acids in their EPS than pyrite grown cells. These sulphur grown cells had a lower affinity for pyrite. This may have been due to the modified EPS composition, which lacked complexed ferric ions. Gerhke (1998) proposed that an exclusive hydrophobic interaction existed between sulphur grown *At. ferrooxidans* and sulphur. This is supported by experimental work of Blake *et al*. (2001). Surface proteins have also been implicated in the adhesion of bacteria to solids (Arredondo *et al.*, 1994) with a 40-kDa outer membrane protein being described for sulphur - grown *At. ferrooxidans* (Ohmura *et al.*, 1996) and an aporusticyanin protein for ferrous grown *At. ferrooxidans* cells (Blake *et al.*, 2001).

Ohmura *et al.* (1996) reported the adhesion of sulphur-grown *At. ferrooxidans* to sulphur is mediated by the 40-kDa protein positioned on the flagellum. This allowed the appendage to break through the energy barrier between the bacterium and mineral and resulted in the formation of disulphide bonds between the thiol groups of the protein and elemental sulphur. Flagella were only seen to occur on sulphur grown *At. ferrooxidans* (Ohmura *et al.*, 1996).

Cultures of *At. ferrooxidans* grown on ferrous iron produced a protein with a high affinity for pyrite (Blake *et al.*, 2001). Blake *et al.* hypothesized that the surface protein, aporusticyanin, acted as a cellular receptor for the adhesion of intact cells to the exposed iron atoms at the solid-liquid interface of the pyrite crystal lattice (Blake and Ohmura, 1999). Furthermore, the addition of ferrous ions to the binding mixture prevented the adhesion of either aporusticyanin or intact cells (Blake and Ohmura, 1999). Observations by Blake *et al.* (2001) and Blake and Ohmura (1999) are consistent with a model where aporusticyanin located on the surface of the bacterial cell acts as a mineral-specific receptor for the initial adhesion of *At. ferrooxidans* to a solid. Blake and Ohmura (1999) provided more evidence for this model where binding of the apoprotein to solid pyrite was accomplished by coordination of the unoccupied copper ligands with iron atoms at the exposed edge of the pyrite crystal lattice. Furthermore, the addition of ferrous iron to the binding mixture prevented the adhesion of either aporusticyanin or intact cells.

From this it can be concluded that leaching bacteria are able to adapt the composition and amount of EPS and surface proteins according to the growth substrate to allow for optimal adhesive properties. The attachment of leaching bacteria to a mineral surface was observed to form a monolayer rather than a multilayered biofilm (Edwards *et al.*, 1998 and Sanhueza *et al.*, 1999). A hypothesis for the formation of a monolayer biofilm is that the dominant microbes are aerobes, and formation of a thick film would restrict the diffusion of oxygen to the cell surface (Edwards *et al.*, 1998 and Sanhueza *et al.*, 1999). The EPS of leaching bacteria, together with bound ferric ions, constitutes a preferred reaction space in the vicinity of the cells, assisting further the attack on the metal sulphide (Gehrke *et al.*, 1995; Sand *et al.*, 1995). This is supported by evidence of dissolution pits being formed by the attached bacteria (Edwards *et al.*, 1998). Mineral dissolution by attaching microorganisms involves the recognition of high surface energy sites, mineral specificity, and specificity with respect to crystallographic orientation. Localised etch pits are absent on pyrite incubated with planktonic cultures and in controls. The

absence of etch pits indicates that without attachment, the primary pyrite dissolution mechanism involves the generation of dissolved ferric ion; with surface dissolution being evenly distributed. Physical degradation of pyrite was more extensive in samples with a higher degree of colonisation and EPS formation (Edwards *et al.*, 1998).

2.9.5 Crystal boundaries

It was observed by Sanhueza *et al.* (1999) that the oxidised pits on a mineral surface had a defined symmetry indicating that bacterial attack occurred preferentially in determined crystallographic directions. Sanhueza *et al*. (1999) proposed that this pit forming mechanism was strongly influenced by the orientation of the individual planes. Edwards *et al*. (1998) demonstrated that bacterial cells on pyrite had a non-random orientation, with the alignment of the cells being commonly parallel to the pyrite's crystallographic direction. The localization of attached cells and the development of micro-colonies were seen to occur at crystallographically controlled surface topographic features. Preferred sites were non uniformities on the mineral surface such as dislocations and grain-boundaries and noncrystallographic features such as scratches, micro-cracks and grooves (Bagdian and Myerson, 1986). This gives further evidence to the proposal that cells have a chemotactic sense that allows them to distinguish between favourable and unfavourable sites for association with the mineral surface (Acuña *et al*, 1992). Bengrine *et al*. (2001) proposed that the adsorption of microorganisms to a mineral was species and site specific as *At. ferrooxidans* and *L. ferrooxidans* competed for different binding sites on the same piece of mineral.

2.10 Studies around attachment and colonisation

2.10.1 Quantifying attached leaching microorganisms

The maximum amount of cells that can associate with the surface of a particle of a particular size is dependent on the orientation of the microorganisms on the mineral surface as well as the size of the bacteria. (Moon, 1995; Edwards *et al.*, 1998). The orientation of cells depends on whether the bacteria are positioned with their longest

axis parallel or perpendicular to the mineral surface. Table 2.4 below gives the typical sizes of *At. ferrooxidans*, *L. ferrooxidans* and *At. thiooxidans*.

Table 2.4: Size of mesophilic leaching bacteria (Rawlings, 2007)

Microbe	Shape	Size
At. ferrooxidans	Rod	0.5 – 1.0 µm
L. ferrooxidans	Vibriod	0.9 – 1.1 µm
At. thiooxidans	Rod	1 – 2 µm

To calculate the maximum number of cells that can associate with a particular surface area, this surface area should be divided by the surface area of a particular cell. Moon (1995) calculated that for a collection of spherical pyrite particles with diameter of 13.63 µm, the maximum attachment for cells orientated with their longest axis parallel to the mineral surface was 2.2×10^{17} cells/ton ore. For cells orientated perpendicular to the mineral surface, the maximum cell attachment was found to be 6.5×10^{17} cells/ton ore. However, the maximum number of cells associated with a particular piece of mineral is much lower due to the repulsive forces between like-charged microorganisms (Ohmura, 1993), the formation of a monolayer biofilm and the fact that only a certain percentage of the mineral is available to colonisation (Edwards *et al.*, 1998 and Sanhueza *et al.*, 1999). This is due to the tendency of microorganisms to associate themselves within non-uniformities on the mineral surface like surface dislocations and grain boundaries (Bagdian and Myerson, 1986). Research carried out by Chang and Myerson (1982) on the association of *At. ferrooxidans* to pyrite minerals showed that these bacteria only made use of 0.6 % of the surface area available on the pyrite surface. The rest of the surface area was not used as an association site by the bacteria that remained in solution. This may have been due to the remaining surface area not being suitable for microbial association.

Asai *et al*. (1992) determined by experiment, the maximum amount of *At. ferrooxidans* cells that can associate with pyrite of varying size fractions per Gram of ore. These values are shown in Table 2.5. As expected, cell association per mass of ore increases with increasing surface area available. However it is evidenced that full surface coverage is not achieved with a maximum loading of 6.6×10^{16} cells/ton being an order of magnitude less than the predicted loading for monolayer coverage.

Table 2.5: Saturation capacity of *At. ferrooxidans* on varying pieces of pyrite (Asai et al., 1992)

Particle Size (μm)	Maximum adsorption capacity per unit weight of pyrite
25 – 44	6.61×10^{10} cells / g-FeS_2
53 – 63	2.50×10^{10} cells / g-FeS_2
63 – 88	1.41×10^{10} cells / g-FeS_2
149 – 177	0.912×10^{10} cells / g-FeS_2

The quantification of bacteria attached to minerals is difficult to establish due to the formation of a biofilm on the minerals surface, the low cell densities found in the bioleaching system as well as the interference caused by the minerals ore during analysis (Moon, 1995). Counting directly using a microscope enumerated the free bacteria in solution. In order to determine the amount of attached bacteria, attached microorganisms have to be dislodged from the mineral surface by chemical and/or physical means (Coram *et al*. 2002). Alternatively, some epifluorescent techniques (Yeh *et al.*, 1986) and fluorescent antibody (FA) staining techniques (Gates and Pham, 1979) have been developed to enumerate attached bacteria directly. The inclusion of these methods would contribute significantly to the quantification of the attached microbial mass within a heap leach environment.

2.10.2 Studies on the attachment to a chalcopyrite concentrate

The attachment of bacteria to mineral surfaces as well as the selectivity of attached bacteria to sulphidic regions has been observed with the scanning electron microscope (Bagdian and Myerson, 1986; Murthy and Natarajan, 1992). Rapid initial adsorption rates have been reported (DiSpirito *et al.*, 1983; Myerson and Kline, 1983). Meyerson and Kline (1983) found that up to 90% of the microbes were absorbed within the first 5 minutes. Bagdian and Myerson (1986) found that up to 100% of the total bacterial population adsorbed within 2 minutes of inoculation provided sufficient surface area was available. Moon's data (1995) agreed with these results, where the *At. ferrooxidans* planktonic concentration decreased with time. Ohmura *et al*. (1993) described a 14% cell attachment of *At. ferrooxidans* to a chalcopyrite particle. The cell density of *At. ferrooxidans* was calculated to not exceed $6x10^6$ cells/cm^2. Experimental data gathered by Blake *et al.* (2001) indicated that approximately 66% of a inoculum attached within the first 10 minutes to pyrite. Cells cultured on ferrous ions adhered very tightly to pyrite with the average diameter of the pyrite used being 70-80 μm.

The addition of high concentrations of soluble ferrous ions in solution reduced the adhesion of iron grown cells to pyrite. Equivalent concentrations of ferric ions had no effect on adhesion of either iron- or sulphur- grown cells (Blake *et al*., 2001). Most leaching bacteria grow attached to surfaces of the mineral sulphide. In the case of a non-limiting surface space, more than 80% of an inoculum withdrew from the planktonic phase within 24 hours (Bagdian and Meyerson 1986; DiSpirito *et al.*, 1983; Gehrke 1998). However some cells remained in the planktonic state. More than 80 % of attached microbes adhere to sites of visible imperfections and to areas with low crystallisation (Andrews, 1987; Edwards *et al. 1998*, Escobar and Lazo, 2003; Escobar *et al*. 2003; 1998; Harniet, 2005; Plumb *et al*. 2008; Ohmura *et al.*, 1993; Sanhueza *et al.*, 1999).

2.10.3 Studies on a simulated heap environment

The heap bioleaching of marginal sulphide ores has become increasingly popular with the decline of available high-grade deposits. While heap leaching has been applied extensively, the rates and extents of leaching in full scale heaps have fallen below those achieved in laboratory columns (Petersen and Dixon, 2003). One of the constraints cited in meeting the expected performance is the optimal colonisation and activity of microorganisms in the heap. The attachment and migration of a viable microbial population in a heap can be studied *in situ* with difficulty or through construction of a simulated heap leach. A simulated heap leach allows for better operational control and monitoring of a heap undergoing microbial colonisation and establishment. To date, very limited studies on heap microbiology *in situ* have been conducted, especially on the mineral chalcopyrite. The data acquired from a simulated heap leach could assist in developing understanding for optimising heap operations and in the programming of a better heap leach modelling tool (HeapSim) with the end goal being a reduction in heap leach times and better operational understanding of the complex interactions between microorganisms and mineral in order to optimise the leaching process to improve leaching performance.

2.11 Study objectives

An attachment study was conducted to determine the association between the defined microbial species, *L. ferrooxidans* and a chalcopyrite concentrate. This mineral–microorganism selection was motivated by the dearth of available information in comparison to readily available description of the pyrite – *At. ferrooxidans* interaction. Further *Leptospirillum* has been identified as a key mesophilic leach organism and chalcopyrite as a mineral of importance. The attachment capability of the pure culture, was measured by conducting cell counts on the inoculum before and after elution through a chalcopyrite concentrate matrix. The goal of these adhesion experiments was to quantify the extent of adhesion of *L. ferrooxidans* to a chalcopyrite concentrate, the time period required and its ease of dislodgement.

Using this preliminary information the research presented in this thesis undertakes to elucidate the microbial interaction and association with a run of mine ore containing the mineral sulphide, chalcopyrite. The interaction between microorganisms and mineral in a heap bioleach context is poorly defined. Several authors (Petersen *et al.*, 2004; Clark and Norris, 1996b; Edwards *et al.*, 1999; Goebel and Stackebrandt, 1994; Tyson *et al.*, 2004) have recognised that in a heap bioleach there is a set of complex interactions of microbial types with solution conditions determining the selection of species. Limited knowledge of microbial colonisation tendencies exists with regard to the selection and cohabitation of various species, the interactions and symbioses between these and their propagation through a porous matrix and across the particle surface.

In the context of the current work, a number of objectives were set out to understand the interaction between mineral, ore and microorganisms in terms of their preferential attachment, their loadings as well as the ability for the microbes to propagate through a packed bed of ore. The following objectives will be addressed in this thesis:

1) The investigation of retention of individual microbial species in a packed bed reactor. In addition, the influence of solution conditions on microbial retention will be considered.

2) The flow of liquid from a single drip point will be investigated in a simulated packed bed reactor to determine the flow pattern and whether the attachment

and subsequent colonisation of mixed microbial species follows the same patterns as liquid flow through the reactor.

3) The influence of fluid flow and retention time within a bed on the solution chemistry and leach efficiency of the simulated heap will be investigated.

In addition to addressing the above objectives, the following research questions were formulated:

- To what extent does an iron and detergent solution influence the retention of a single microbial species in a packed bed?
- Does the colonisation of a heap from a single drip point follow hydrological flow patterns and to what extent can it be related to the inoculum size?
- Does varying the flow rates influence the extent to which an ore bed is colonised over an extended period of time and is this colonisation even?
- Does the use of recycled feed improve the leach ability of an ore bed?

3. Materials and methods

3.1 Chalcopyrite concentrates

A chalcopyrite concentrate, from BHP (Andina), with a size fraction of 100 % ≤ 22 µm, was used a source of iron and sulphur for oxidation by acidochemolithotrophic bacteria for maintenance of stock cultures.

A second chalcopyrite concentrate, obtained from Mintek, was wet sieved to a size fraction of between 106 and 150 µm. This was confirmed by laser diffraction using a Malvern Mastersizer particle analyser. The density of the Mintek concentrate was determined to be 4.1394 g/cm^3 using an AccuPyc 1330 V1.02 pycnometer. The elemental composition and mineralogical analysis of the Mintek sample is shown in Table 3.1 (Jaffer, 2001).

Table 3.1: Elemental and mineralogical analysis of Mintek chalcopyrite concentrate

Element	Concentrate (%)
Copper	29.4
Iron	31.3
Sulphur	33.8
Mineral	
Chalcopyrite	66
Pyrite	11
Pyrrhotite	<1
Sphalerite	3
Quartz	18
Fe Oxides	2

3.2 Chalcopyrite ore

A chalcopyrite ore was supplied by Rio Tinto from the Kennecott Utah Copper operation in North American mine with a size fraction range from less than 1 mm to 50 mm. An elemental composition of the ore showed it contained 0.48 % copper, 2.9 % iron and 0.68 % sulphur (Watling *et al*. 2005).

3.3 Microbial cultures

Four microbial stock cultures, supplied by CSIRO Land and Water (Perth, Australia), were used in this research. These included 3 mesophiles; *Acidithiobacillus ferrooxidans*, *Acidithiobacillus thiooxidans* and *Leptospirillum ferrooxidans* and a moderate thermophile *Acidithiobacillus caldus*. Two mesophiles (*At. ferrooxidans* and *L. ferrooxidans*) and the moderate thermophile (*At. caldus*) were grown at 37^{o}C and 45^{o}C respectively in 1 L temperature controlled, stirred tank reactors aerated at 2L/min and agitated at 500 rpm. A schematic representation is shown in Figure 3.1. *At. thiooxidans* was grown in a 1 L Erlenmeyer flask inside a shake incubator at 25^{o}C and agitated at 200 rpm.

The temperature of the reactors was maintained, by circulating warm water from two different water baths. Each reactor was fitted with a four blade stainless steel pitched blade with impeller, a set of four 10 mm wide Perspex baffles to prevent vortex formation, a condenser to reduce evaporation and a sparger with four downward facing holes 1 mm in diameter that provided air from the bottom of the reactor. Compressed air was supplied at a rate of 2 L/min.

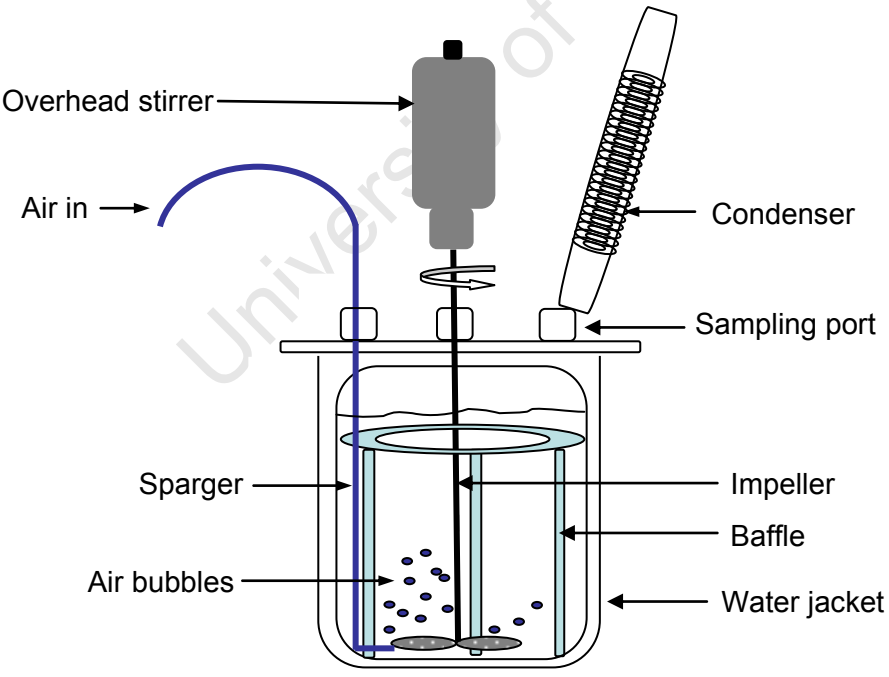

Figure 3.1: Schematic representation of the bioreactor (Reproduced with permission by Nemugumoni, 2008)

The growth media for the bacterial stock cultures are shown in Table 3.2. A 5 % solids loading of the chalcopyrite concentrate was supplied to the *At. ferrooxidans, L.*

ferrooxidans and *At. caldus* bioreactors. The required trace metals were supplied by the mineral concentrate itself. Elemental sulphur (5 g/L) was supplied to *At. thiooxidans* in the shake flask. The pH of the media was adjusted to pH 2.5 for the bio reactors and pH 4.6 for the shake flask by the addition of 1 M H_2SO_4.

Table 3.2: Growth media for microbial stock cultures

Compound	Concentration (g/L)			
	At. ferrooxidans	*L. ferrooxidans*	*At. caldus*	*At. thiooxidans*
$(NH_4)_2SO_4$	3	3	3	3
KCl	0.1	0.1	0.1	N/A
K_2HPO_4	0.5	0.5	0.5	N/A
$MgSO_4.7H_2O$	0.5	0.5	0.5	0.5
$Ca(NO_3)_2.4H_2O$	0.01	0.01	0.01	N/A
Na_2SO_4	1.5	1.5	1.5	N/A
$FeSO_4.7H_2O$	0.4	0.4	N/A	N/A
KH_2PO_4	N/A	N/A	N/A	3
$CaCl_2.2H_2O$	N/A	N/A	N/A	0.25

The stock cultures were sub-cultured twice monthly, with 300 ml of culture being drawn and replaced with 300 ml of respective media. Once a month, 5 g of the chalcopyrite concentrate or elemental sulphur was added to the stock cultures. The cell concentrations in the reactors were monitored by periodic cell counts and maintained in the range of 5 x 10^8 cells/ml. Before sub-culturing took place, distilled water was added to bring the volume to the initial 700 ml level to compensate for evaporative loss.

3.5 Experimental protocol for microbial attachment

Microbial attachment to the concentrate was investigated in a series of mini-columns (10 mm diameter x 50 mm height), constructed from 5 ml auto pipette tips. The chalcopyrite concentrate (10 g) was slurried with distilled water and the slurry loaded into the 5 ml small column reactor; the reactor base of which was plugged with glass wool. This minimised air pockets and ensured homogenous packing of the bed. The void volume of a packed column was 2 ml. A pure culture of *L. ferrooxidans* was used as the inoculum (2 ml). This was followed by 15 minute intervals of 2 ml washes at room temperature for each of the attachment runs. To investigate cell attachment, various solutions were passed through the inoculated columns with the eluted volumes being quantified. It has previously been reported by Ohmura *et al.* (1993) and Devasia *et al.* (1993) that association with the mineral phase is influenced by the availability of ferrous iron in the liquid phase. A 10 x 9K basal salts medium (Table 3.5), a ferrous and ammonium sulphate solution (44.2 g/L $FeSO_4.7H_2O$ and 30 g/L

$(NH_4)_2SO_4$), and a detergent medium (Triton-X100 0.05 % in 9K medium) were used in this study. At the end of each run, the ore was washed for 1 hr at 60°C with 1% Tween-20 to detach any remaining microorganisms on the concentrate. Each run was repeated five or six times. A summary of the experimental parameters is shown in Table 3.5.

Table 3.4: 10 x 9 K basal salts medium

Compound	Concentration (g/L)
$(NH_4)_2SO_4$	30
KCl	1
K_2HPO_4	5
$MgSO_4.7H_20$	5
$Ca(NO_3)_2.4H_2O$	0.143
Na_2SO_4	14.52
dH_2O	1000ml

Table 3.5: A summary of the experimental sample elutes through a chalcopyrite concentrate matrix

	Attachment Runs		
Steps of run	1	2	3
1	Inoculated (2ml)	Inoculated (2ml)	Inoculated (2ml)
2	Basal salts (2ml)	Basal Salts (2ml)	Basal Salts (2ml)
3	Basal salts (2ml)	$FeSO_4$+$(NH_4)_2SO_4$ (2ml)	$FeSO_4$+ $(NH_4)_2SO_4$ (2ml)
4	Basal salts (2ml)	dH_20 (2ml)	Triton-X100 (2ml)
5	Basal salts (2ml)	dH_2O (2ml)	dH_20 (2ml)
6	Tween (10ml)	Tween (10ml)	Tween (10ml)

3.5.1 Attachment run 1

A *L. ferrooxidans* inoculum of 10^8 cells was used to inoculate the four repeat runs of attachment run 1. Elution stages included repeated additions of the 10 x 9K basal salts media (Table 3.4) to the chalcopyrite concentrate matrix.

3.5.2 Attachment run 2

Attachment run 2 was repeated five times with an inoculum of 10^8 cells of *L. ferrooxidans*. Following elution of planktonic cells with basal salts, it included steps

in which a $FeSO_4.7H_20$ (4.42 g/100ml) and $(NH_4)_2SO_4$ (3g / 100ml) solution were eluted through the column as shown in Table 3.5.

3.5.3 Attachment run 3

For attachment run 3 an inoculum of 10^8 cells of *L. ferrooxidans* was used and the experiment repeated four fold. In addition to basal salts elution and elution in the presence of ferrous iron attachment run 3 consisted of a step in which a 0.05 % Triton-X100 detergent solution was eluted through the matrix, prior to the 1 % Tween wash step (Table 3.5).

3.6 Simulated heap set-up

A simulated heap environment was constructed in a plastic container with a height of 43 cm, diameter of 32 cm and a volume of 25 litres. The container was packed with 36 kg of acid agglomerated chalcopyrite ore. The agglomeration was carried out by mixing the ore and acid water in a large container prior to the packing of the ore. The ore was agglomerated with 70 ml water containing 4.3 ml of concentrated H_2SO_4 per kg of dry ore. This corresponded to a total moisture content of 7.5 % (Petersen and Dixon, 2003). The heap was divided into two layers comprised of nine distinct regions as shown in Figures 3.2 and 3.3. Two Perspex rings (10 cm height) were placed at the bottom of the container to separate the inner, middle and outer layers. The layers were segregated into their respective regions by a line of silicone between the Perspex rings, corresponding to the diagram in Figure 3.3. The simulated heap was fed drop wise above region 1 in a temperature controlled environment (37^{o}C) with a feed solution consisting of 2 g/L iron (1.3 g/L ferrous iron, 0.7 g/l ferric iron, 7.5g 98% H_2SO_4) (Petersen and Dixon, 2003). A Master Flex Pump 1 was used to pump the feed solution into the container.

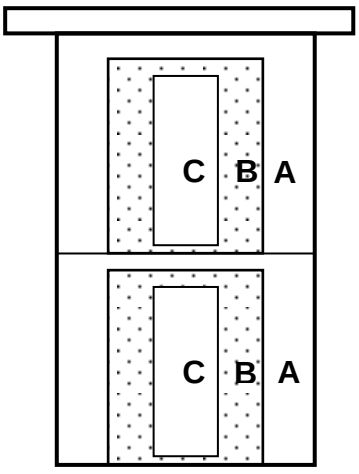

Figure 3.2: Division of reactor into upper and lower layers with shade cloth being used to segregate the divisions (A – Outer region; B - Middle region; C - Inner region)

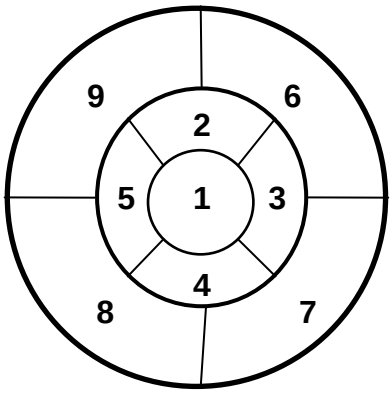

Figure 3.3: Numbered points for sample collection on underside of container

Eluted samples were collected by funnels below the 1 cm sample holes at the base of the reactor. Each sample point corresponded to a region of ore. Nine 25 L containers were used to collect 0.01 L to 5 L leachate samples for analysis.

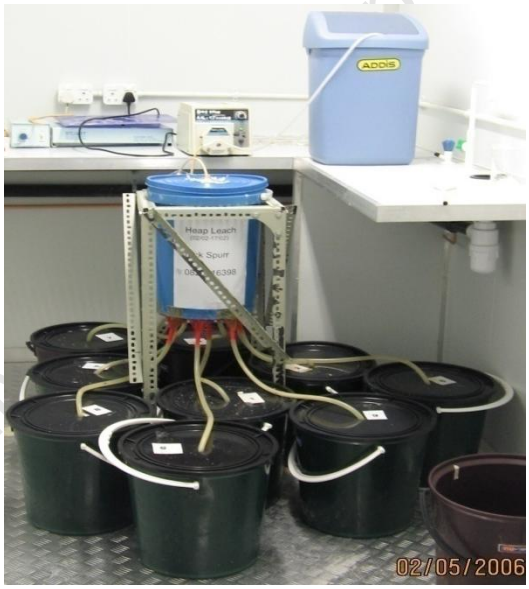

Figure 3.4: Simulated heap reactor set-up

3.7 Experimental protocol for simulated heap leaches

Four simulated heap leaches were conducted in this study. Reactors one to four were each loaded with 36 kg of agglomerated chalcopyrite ore. The ore was agglomerated with 70 g of water containing 8 g concentrated sulphuric acid per kg of

dry ore, with a solution pH of 0.6. The moisture content was 7.5%, which corresponded to operating conditions at a mine site (Petersen and Dixon, 2003)

3.7.1 Heap leach 1

The agglomerated ore of heap leach 1 was washed for 24 hours with the feed solution described in Section 3.6 prior to inoculation. A mixed mesophilic bacterial population (*At. ferrooxidans* and *L. ferrooxidans*) of 1.52 x 10^{12} cells was combined with the feed solution and pumped through the reactor over a 24 hour period. A low flow rate of 1.5 ml/min (1.12 L/hr/m^2) was used to feed the reactor for the 15 day duration of the leach. After each 24 hour period, leachate was collected and analysed for volume, pH, redox, ferrous iron, total iron and copper. For the first five days cell counts were conducted daily, thereafter cell counts were performed every third day.

3.7.2 Heap leach 2

Agglomerated ore in heap leach 2 was acid washed (30ml 98% H_2SO_4 in 30 L H_2O) over a 48 hour period. The heap was then inoculated with a mixed mesophilic culture of *At. ferrooxidans* and *L. ferrooxidans* with a cell number of 3.04 x 10^{11} cells. This was applied directly to the heap at a flow rate of 21 ml/min (15.5 L/hr/m^2). A feed solution of 30 litres was then fed to the reactor daily at the same flow rate for the duration of the leach. The leach was carried out for a period of 5 days, with volume, pH, redox, ferrous iron, total iron, copper and planktonic cell number per region being determined. To determine an optimum method for cell dislodgement from leached ore, a mechanical disruption procedure and a detergent washing method were compared for all 18 regions as described in Section 3.8.8.

3.7.3 Heap leach 3

Agglomerated ore for heap leach 3, once loaded into the reactor, was inoculated. The inoculum consisted of a mixed mesophilic culture comprised of *At. ferrooxidans* and *L. ferrooxidans* at a total cell number of 5.46 x 10^{11} cells. The inoculum was fed into the reactor at a constant rate of 21 ml/min (15.5 L/hr/m^2). A feed solution was then pumped daily into the reactor until the end of the experiment on Day 30. From Day 15 to 30, the eluted leachate was collected and fed back into the reactor the following day. Daily samples were taken of the pre-recycled and recycled solution

and analysed for volume, pH, redox, ferrous iron, total iron and copper. Microbial counts were performed for the first five days and then every third day on the eluted samples.

Upon completion of the leach, the reactor was unpacked and region-specific leached ore was washed to detach any remaining microorganisms to determine the cells attached per region of ore. The washing process has been described previously in Section 3.8.8.

3.7.4 Heap leach 4

Agglomerated ore, once loaded into the reactor was washed through with 1 L of acid water (H_2SO_4 pH 1.8) at a feed flow rate of 6 ml/min. A mixed mesophilic bacterial population (2.61 x 10^{11}) of *At. ferrooxidans* and *L. ferrooxidans* was used to inoculate the heap. The reactor was fed daily with a feed solution at a rate of 6 ml/min (5 L/hr/m^2) until the end of the leach (Day 58). A total cell number of 7.70 x 10^{10} cells of *At. thiooxidans* was inoculated into the reactor on Day 51. Recycling of the feed solution commenced on Day 18 and ended on Day 46. The microbial colonisation of the ore was analysed by the cell separation method previously described in Section 3.8.8. The compositional analysis of the precipitate was investigated through separate water and acid washes (Section 3.8.9). This was done to determine if copper formed part of the precipitate and if the precipitate was water or acid soluble. A total acid digest of an unleached and leached samples was performed to determine the elemental composition prior to and after microbial leaching had occurred. A summary of parameter and experimental analyses performed is shown below in Table 3.7.

Table 3.7: Summary of the parameters and experimental analyses performed on the simulated heap leaches 1 - 4

	Simulated heap leach number			
Control Parameters	1	2	3	4
Inoculum (total cells)	1.52×10^{12}	3.05×10^{11}	5.46×10^{11}	8.57×10^{11}
Inoculation volume (ml)	220	900	1000	1000
Feed volume per day	2.2 L	30 L	30 L	8.64 L
Flow rate (ml/min)	1.5	21	21	6
Duration (Days)	15	5	30	58
Feed recycle (Days)	No	No	15-30	18-46
Analyses undertaken				
pH	x	x	X	X
Redox	x	x	X	X
Volume collected per outlet	x	x	X	X
Cell counts	x	x	X	X
Microbial species composition				x
Ferrous iron	x	x	X	x
Total iron, copper	x	x	X	x
aluminium, potassium				x
Post operational analyses				
Microbial colonisation		x	X	x
Precipitate analysis				x
Total acid digestion				x

3.8 Analytical methods

3.8.1 Volume

The volume of eluted samples from the simulated heap leach was measured gravimetrically on a Mettler-Toledo scale. The dry weights of the sample containers were taken prior to the start of the experiment with the resultant volume being calculated by difference.

3.8.2 pH analysis

pH readings were taken using a Metrohm 961 pH meter and probe. The probe was calibrated daily at pH 1, 7 and 9 with an analytical error of less than 5 %.

3.8.3 Redox potential

The redox potential was measured to determine the ratio of Fe^{3+} to Fe^{2+} in liquid samples. The redox potential was measured using a Crison GLP 21 Eh meter equipped with a platinum ring electrode. The direct measurement is redox potential with the offset for Eh being 207 at 25 °C.

3.8.4 Ferrous iron determination

3.8.4.1 Titration method

Ferrous iron was initially determined by titration, based on the reaction of potassium dichromate ($K_2Cr_2O_7$) and a barium diphenylamine sulphonate indicator. According to Equation 3.1, the reaction is between the dichromate ion and the ferrous ion which is oxidised to ferric ion (Vogel, 1989) in acidic solutions.

$$Cr_2O_7^{2-} + 6Fe^{2+} + 14H^+ \rightarrow 2Cr^{3-} + 6Fe^{3+} + 7H_2O \qquad \text{Equation 3.1}$$

Five ml of a sample was pipetted into a 125 ml conical flask. 10 ml of spekker acid (1600 ml dH_2O, 600 ml 98% H_2SO_4, 600 ml 85% H_3PO_4) and 3 drops of the barium diphenylamine sulphonate indicator were then added to the sample. This was titrated with 0.0149 M potassium dichromate until the first permanent colour change from yellow to purple occurred. The concentration of ferrous iron was quantified using Equation 3.2

$$[Fe^{2+}](g/l) = \frac{[K_2Cr_2O_7] \times V_T \times 55.84 \times 6}{V_{SOL}} \qquad \text{Equation 3.2}$$

where: $[K_2Cr_2O_7]$ = concentration of $K_2Cr_2O_7$ (M)

V_T = titration volume (ml)

V_{SOL} = volume of solution in flask (ml)

A sensitivity limit of 125 mg/L restricted uses of the titration method for Fe^{2+} determination.

3.8.4.2 Spectrophotomeric method

The spectrophotomeric method was introduced to overcome the detection limit. This method is based on the formation of orange red complexes when ferrous iron is mixed with 1-10 phenanthroline ($C_{12}H_8N_2.H_2O$). The reaction (Equation 3.3) occurs when three molecules of 1-10 phenanthroline chelate one molecule of ferrous ion resulting in a colour change. The orange red complex is quantified spectrophotometrically by absorbance at 510 nm. A 1 ml sample was added to 2 ml of 0.03968 M acetate buffer and 2 ml of 0.02 M 1-10 phenanthroline solution (0.1 g 1-10 phenanthroline ($C_{12}H_8N_2.H_2O$) / 100 ml dH_2O). A dilution series was made to establish a calibration curve (shown in Appendix A).

$$Fe^{2+} + 3\ (C_{12}H_8N_2.H_2O) \rightarrow [(C_{12}H_8N_2)_3.Fe]^{2+} + 3H_2O \qquad \text{Equation 3.3}$$

3.8.5 Copper, total iron and ferric iron determination

Atomic adsorption spectroscopy was used to determine copper and total iron in solution. A Varian Spectra AA – 30 was used with an air pressure of 3.5 bars and acetylene at 1.5 bar for sample analysis. Copper and iron wavelength measurements were 324.7 nm and 371 nm respectively. Ferric iron was determined by the difference between total iron and ferrous iron.

3.8.6 Cell counting

Cell counts were conducted by direct microscope counting using a Helber Bacteria Thoma counting chamber. The grid consisted of 16 large squares with each large square divided into 16 small squares. The depth of the chamber was 0.02 mm with an area of 1 small square being 2.5 x 10^{-3} mm^2. Cells were enumerated under an Olympus BX40F optical light microscope at a 1000x magnification.

The resultant cell concentration per ml was calculated using the following Equation 3.4.

$$C_N = \frac{c * (N/n)}{D * A} * d * 10^3 \qquad \text{Equation 3.4}$$

where: C_N = cell concentration (cells ml)

C = number of cells counted per large square (16 small squares)

N = total number of large squares = 16

n = number of large squares where cells were counted

D = depth of the chamber (0.02 mm)

A = total area of the counting chamber (0.64 mm^2)

d = dilution

The standard error for cell counting was calculated to be 9 % for 6 replicate samples.

3.8.7 SEM

Scanning electron microscopy was used to investigate cell morphology from the bioreactors and the attachment of microorganisms to the ore. Samples were taken to the Physics Dept. at UCT for analysis. Cells were fixed to a 0.45 µm Nucleopore (Millipore) filter by 3% gluteraldehyde. A 30% solution of ethanol in water was then passed through the filter and the filter was left to stand for 15 minutes. This procedure was repeated for 50, 70, 90 and 100% ethanol. This was done to dehydrate the samples. The filters were then taken through the critical point drying process prior to being coated with gold/palladium plasma and viewed using a JEOL JSM-840 scanning electron microscope under varying magnifications.

3.8.8 Cell separation from leached ore

Attached cells were removed from the ore using a mechanical disruption method, modified from Plumb *et al*. (2006). A 50g sample of region specific ore was vortexed at top speed on a vortex genie for 10 seconds in 50 ml 9K media (pH 1.8) (Rodriguez et al 2003b) . The slurry was centrifuged at 800 rpm for 1 minute. The supernatant was then removed. This was repeated five times after which a sample from the pooled volume was counted. The vortexed ore was then agitated, on a rotary shaker (145 rpm), in 50 ml of a 1% Tween-20 detergent solution for 1 hour at 65^oC. This method of ore agitation was applied to heap leaching experiments 2 and 3. A 0.1 % Tween-20 concentration was used for heap leaching experiment 4 under the same conditions to minimise cell disruption.

3.8.9 Water and acid soluble precipitate from leached ore

During the simulated heap leach a precipitate was seen to have coated the ore. The composition of the precipitate was investigated by a series of water and acid washes. Each sampled region of ore was agitated with water with a separate sample being agitated with acid. The sample (50g) of region-specific ore and 50 ml of distilled water or 50 ml of 1M HCl was slurried and shaken at 30^{o}C for 1 hour on a rotary shaker. Dissolved concentrations of iron, copper, aluminium and magnesium were analysed by AAS (Atomic Adsorption Spectroscopy). This was done for all 18 samples of leached ore from the leaching reactor 4.

3.8.10 Total acid digests of ore

Acid digestions were conducted on previously acid washed leached ore. Samples were milled and acid digested for elemental analysis. Each sample was weighed out to 0.5 g in a 250 ml Erlenmeyer flask. This was then digested with 10 ml of HCl / HF mixture and boiled until the volume was approximately 2 ml. HNO_3 (10ml) was then added and boiled until the volume was approximately 2 ml. $HClO_4$ (5ml) was finally added and boiled until the volume was 2 ml. The sample was then transferred quantitatively to a 100 ml volumetric flask and made up to 100 ml with distilled water. This was filtered and the metal concentration of the filtrate was determined by AAS filtrate was then read on the A.A. The percentage of element concerned was calculated as follows:

$$\% \text{ Element in sample} = \frac{R \text{ (in ppm)}}{100 \times (\text{sample mass})} \qquad \text{Equation 3.5}$$

4. Results and discussion

4.1 Analysis of column attachment studies

A series of attachment studies were conducted to determine the degree of attachment of *L. ferrooxidans* to chalcopyrite concentrate in the presence of abundant mineral surface area. Further these studies allowed for ease of dislodging of cells and validation of the methodology for the analysis of total cell population adhered to the mineral.

The attachment study involved a series of plastic columns loaded with 10 g of chalcopyrite concentrate (106 – 150 µm) and slurried to ensure homogenous packing. The packed columns had a height of approximately 10 cm and a void volume of 2 ml. The columns remained saturated and the liquid in the void volumes could only be displaced by the addition of more liquid to the top of the column. The columns were inoculated with 2 ml of a known cell concentration of *L. ferrooxidans*. To determine cell attachment efficiencies on the ore, elutions of cells from the ore were performed by using a basal salt medium to displace planktonic cells from the void volume. A ferrous and ammonium sulphate solution was used to remove cells in response to nutrient chemotaxis or altered surface properties and a detergent medium was used to dislodge cells adhered to the ore as described in Section 3.8 and Table 3.6. The eluted volumes prior to inoculation were kept for further analysis. In certain cases, multiple elutions with one or several eluents were performed. Finally the ore was removed from the columns and washed with agitation for 1 hour at 160 rpm, in 10 ml of 1 % Tween–20 at 65^{o}C to remove all cells. The three main attachment studies are discussed below.

4.1.1 Attachment run 1

Attachment run 1 consisted of repeat ore elutions with the basal salts medium to differentiate attached and planktonic cells. It was repeated four times. Typical results are shown in Table 4.1. Some 3.5 % of cells inoculated were displaced on the first volume replacement, illustrating a planktonic void volume location. Further washes failed to remove any significant proportion (< 10 %) of microorganisms added to the column as inoculum, across all runs. However the final Tween wash released more than 90 % of cells inoculated, as shown in Table 4.1.

Table 4.1: Cells released from packed column on elution basal salts

Run 1		
L. ferrooxidans inoculation number : 4.25 x 10^8 cells per 2 ml		
Steps	Cells released	% Released
1 – Inoculation	0.00	0
2 – Basal salt	1.50 x 10^7	3.5
3 – Basal salt	7.5 x 10^6	1.8
4 – Basal salt	2.5 x 10^6	0.6
5 – Basal salt	5.0 x 10^6	1.2
6 – Tween wash	4.0 x 10^8	94.1

These results agree well with previous attachment studies carried out in shake-flasks with similar mineral compositions and sizes (Bevilaqua *et al.* 2004; Gonzalez *et al.*, 1999; Lizama *et al.*, 2003, Harniet *et al*. 2005, Solari *et al*. 1992, Devasia *et al*. 1996, Rodriguez *et al*. 2003(b)) as these authors also showed similar total attachment sizes and time scales.

To test the adhesive properties of *L. ferrooxidans* during the attachment phase, the concentrate was pre-washed with 1 % Tween-20 and inoculated. Up to 13 % of microorganisms inoculated were released (Table 4.2) on the first wash confirming a planktonic location. However the percentage range of cell removal from the first basal salt washes of previous experimental runs were represented by the range between 3 and 12 %. This suggests that the Tween-20 washed concentrate had similar properties to the mineral itself, thereby not affecting the attachment of *L. ferrooxidans*. Samples of the Tween washed data is found in Appendix D.

Table 4.2: Tween-20 treated concentrate prior to a basal salt wash

Run 1		
L. ferrooxidans inoculation number : 8.72 x 10^8 (cells/2ml)		
Steps	Cells released (cells/2ml)	% Released
1 – Inoculation	3.13 x 10^6	0.6
2 – Basal salt	1.13 x 10^8	13
3 – Basal salt	1.56 x 10^7	1.8
4 – Basal salt	1.06 x 10^7	1.2
5 – Basal salt	6.25 x 10^6	0.7

4.1.2 Attachment run 2

Attachment run 2 expanded the study to consider the properties of the liquid eluent, specifically including the energy source, ferrous iron. The study was done in duplicate. Ferrous iron and ammonium sulphate eluent were passed through the columns after the inoculation with 10^8 *L. ferrooxidans* cells and washing with basal salts medium. This had little effect on the detachment of cells as < 8 % of the cells associated with the ore was released (Table 4.3).

Table 4.3: Cells released with iron and sulphate media wash

Run 2		
L. ferrooxidans inoculation number : 5.94 x 10^8 (cells/2ml)		
Steps	Cells released (cells/2ml)	% Released
1 – Inoculation	6.25 x 10^5	0.1
2 – Basal salt	4.56 x 10^7	7.7
3 – Iron and ammonium sulphate	2.94 x 10^7	5.0
4 – Distilled water	8.75 x 10^6	1.5
5 – Distilled water	1.00 x 10^7	1.7
6 – Tween wash	5.69 x 10^8	95.8

4.1.3 Attachment run 3

Attachment run 3 consisted of four experimental runs where the loaded ore was rinsed through with 0.05 % Triton–X100 detergent solution after inoculation of 10^8 *L. ferrooxidans* cells. The detergent solution of Triton–X100 had minimal effect as less than 5 % of the inoculum were released (Table 4.4).

Table 4.4: Cells released with a Triton–x wash

Run 3		
L. ferrooxidans inoculation number : 8.72 x 10^8 (cells/2ml)		
Steps	Cells released	% Released
1 – Inoculation	6.88 x 10^6	0.8
2 – Basal salt	1.00 x 10^8	11.5
3 – Iron and ammonium sulphate	2.19 x 10^7	2.5
4 – Triton-X100	4.00 x 10^7	4.6
5 – Distilled water	4.44 x 10^7	5.1
6 – Tween wash	6.50 x 10^8	74.5

4.1.4 Discussion of mineral attachment studies

The results of the study of attachment to mineral concentrates suggest that significant attachment of > 90 % of *L. ferrooxidans* with the chalcopyrite mineral occurs within 15 minutes. The subsequent slow passage of liquid through these columns had minimal detachment ability. However a small percentage (0.5 to 13 %) of microorganisms was seen to be eluted through with each liquid passage. This suggests that some microorganisms are weakly adhered to the mineral itself with a dynamic equilibrium being sought between attached and planktonic cells. To achieve detachment of the majority of cells from the ore, repeated agitation in the presence of the detergent Tween in a slurry configuration, with good contacting was required. The similarity in nature of both detergents would suggest that the contact method of the detergent with the ore matrix has a major impact on cell dislodgement. Agitation under turbulent conditions achieves more of a detachment capability than the liquid passage through the ore bed under laminar conditions. These attachment experiments did not investigate the dynamic equilibrium between sessile and planktonic microorganisms within the ore matrix. This equilibrium has been suggested previously in shake flask studies by Escobar *et al*. (2003) and Plumb *et al*. (2008).

4.2 Analysis of simulated heap leaches

While there is limited work reported on microbe – mineral contact, there is a dearth of rigorous study on microbial colonisation of heap systems, with these being limited to field sampling of heaps or large columns. Based on this, the analysis of simulated heap leaches follows.

Four simulated chalcopyrite heap leaches were conducted to investigate a heap leaching environment. Each heap leach was constructed by packing 36 kg of acid agglomerated ore into a cylindrical reactor, in a temperature controlled room, at 37^{o}C. Using internal divisions, the ore was split into nine regions comprised of the inner, middle and outer regions. The inner region had a core radius of 5 cm. The middle region represents an annulus between radii of 5 and 10 cm and the outer region, the annulus from 10 to 15 cm. Leaching feed solution was introduced through a single point located above the inner region. Each heap leach was differentiated based on the flow rate and duration. The fourth leach was the most extensively analysed,

including post-operational investigation of the ore. Therefore leach four is discussed first, with significant findings from the preceding experiments following, to avoid repetition.

4.2 Analysis of simulated heap leach 4

The industry standard rate for heap irrigation is 5 to 6 L/m^2/hr (Petersen & Dixon, 2003). When the surface area of the reactor was taken into account, a flow rate of 8.64 L per day or 6 ml/min was derived for reactor four. This corresponded to 5 L/m^2/hr. The eluted volumes were collected from outlets from each region in the inner, middle and outer zones. A feed recycle period began on Day 18 and lasted for 28 days. To initiate the recycle period, eluted volumes from Day 16 and Day 17 were collected and stored in two separate containers. The collected volume from Day 16 was used to start the recycle, being reintroduced into the reactor as feed for Day 18. This was followed by the collected volume from Day 17 being fed into the reactor as feed on Day 19. The process of recycling the collected outflow was repeated until Day 46. During the recycle period the volume of collected feed decreased due to evaporative loss. Fresh feed was used to make the volume up to 8.64 L on Days 28, 29, 31 and 37. At the end of the recycle period on Day 46, fresh feed was again introduced at a rate of 8.64 L per day until the end of the experiment. During the experimental run, liquid eluted from the outlet points was collected and quantified daily with respect to volume, pH, redox potential, total iron, copper and planktonic cell number.

4.2.1 Volume elution

Volumes eluted on a daily basis from the outflow points in the inner region (1); middle region (2-5) and the outer region (6-9) are displayed in Figure 4.1. The majority of the liquid (30 to 85%) was collected from the inner region (point 1). Over the first 15 days the volume collected from point 1 decreased from 6.9 L to 3.6 L. The decline in volume collected from the inner region could be attributed to the increased wetting of the middle and outer regions which resulted in greater radial diffusion occurring (Bouffard & Dixon 2001). Figure 4.2 shows the concomitant increase in volume collected from the middle and outer regions. The middle region increased from 1.4 L to 2.7 L per day while the outer region increased from 0.7 to 1.9 L per day. From Day 15 to 19, a relatively stable outflow rate was maintained for the inner region. This may be possibly due to the bed reaching saturation. During the recycle period, the volume of the collected outflow decreased due to evaporation. From Day 28, the recycled feed was made up to the desired feed volume intermittently to correct for

evaporation, resulting in a reasonably constant volume being eluted. At the end of the recycle period, on Day 46, the daily addition of fresh feed was resumed. A pseudo steady state was reached with regards to liquid flow as liquid collected from the inner, middle and outer region remained relatively consistent with a deviation of < 10 % around the mean value over that time period.

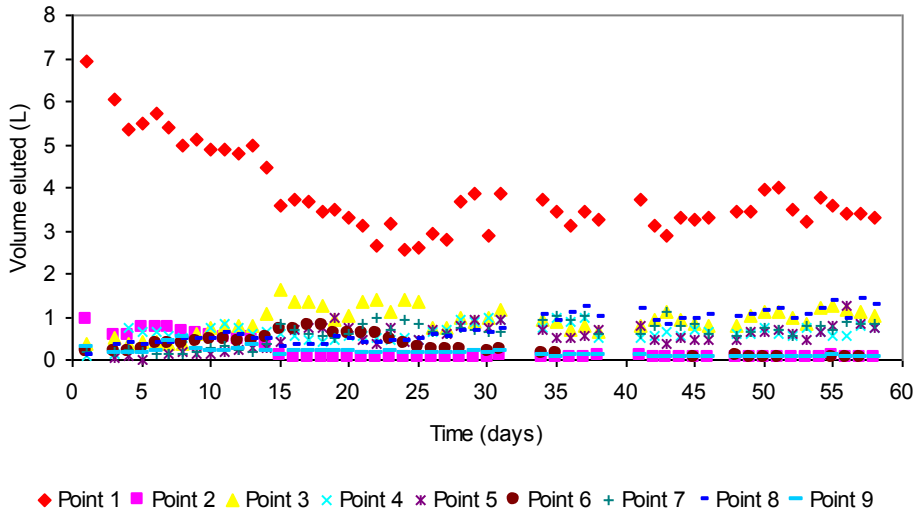

Figure 4.1: Daily flow collected from inner (point 1), middle (points 2-5) and outer (points 6-9) region outlet points

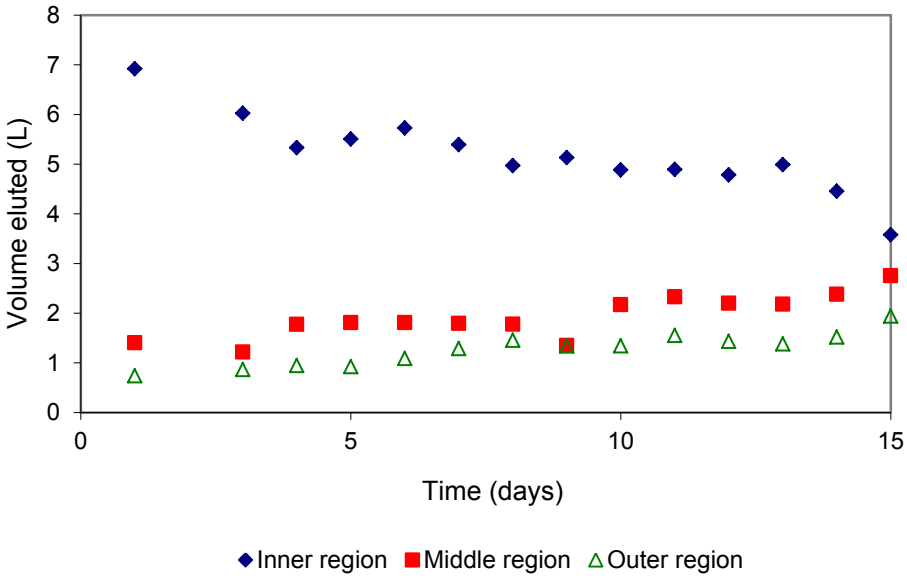

Figure 4.2: Total volume eluted per day for the inner, middle and outer regions from Day 1 to 15

Regional flow rates of the middle and outer elution points are shown in Figure 4.3. From Day 1 to Day 34 it can be seen that the majority of volume eluted is primarily from the middle region shown in red. However a gradual build up in flow is seen to occur in the outer region shown in green, for the same period. After Day 34,

equilibrium in volume elution is established between the middle and outer regions. This could be attributed to the radial diffusion of flow reaching a steady state between the inner, middle and outer regions. The volume occupied by each region, together with flow rate, influences the residence time. The inner region (point 1) has a volume of 3377 cm^3, while the individual points of the middle and outer regions occupy 2532 cm^3 and 4423 cm^3 respectively.

The regional flow rates in Figure 4.3 also show that a decrease in elution volume from an outflow point affected the flow rate of adjacent regional points. This can be seen for the middle region where point 2 showed a steady decline in elution from Day 6, with a sudden drop at Day 14. The volume from point 2 was transferred to outlet point 3, where an increase in volume was observed over the same period. Watertight partitions at the base of the reactor meant that the shift in the fluid flow was due to leakage between the regions, as a result of the base not being absolutely level. Point 6 in the outer region also showed a decrease in volume eluted from Day 18, with a sudden drop at Day 22, while points 7 and 8 showed an increase over the same period. Mineral precipitation is thought to be a likely cause of these changes in flow pattern. Mineral precipitation is discussed in greater detail later on Section 4.2.4.

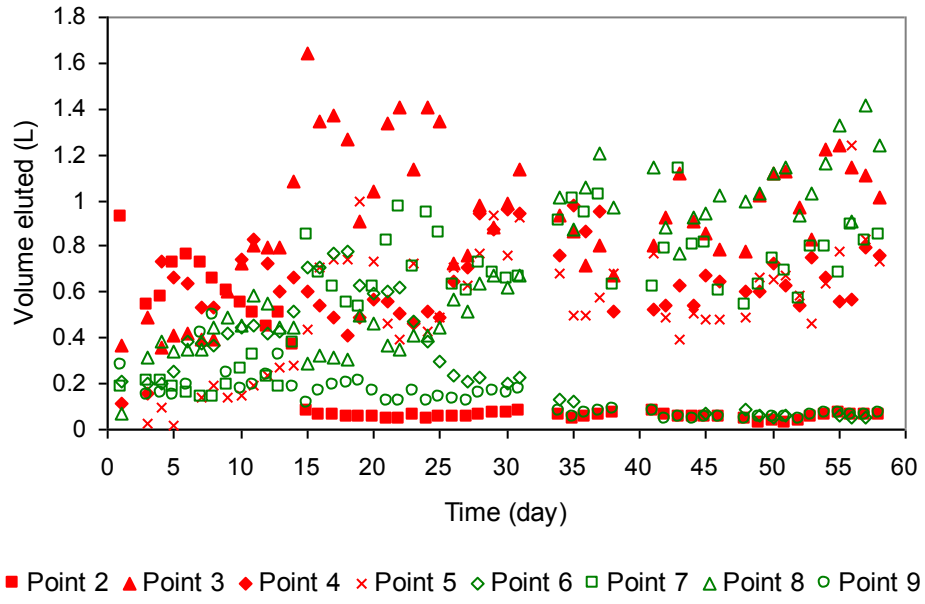

Figure 4.3: Middle (red) and outer (green) regional daily flow rates during the 58 day leach period

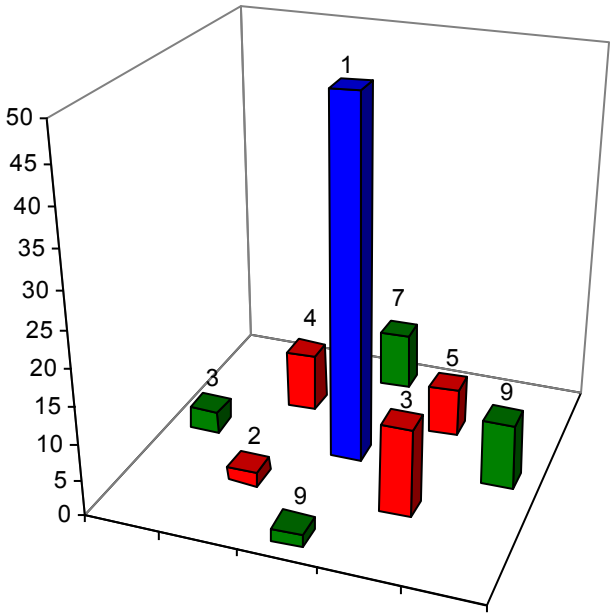

Figure 4.4: Percentage volume eluted from points within the inner, middle and outer regions

The cumulative percentage volume eluted for all regions over the 58 day duration is shown in Figure 4.4, with the inner region being displayed in blue, the middle region in red and the outer region in green. As can be seen, some 49 % of flow passed through the inner region, while 29% (2% at point 2), (12% through point 3), (8% through point 4) and (7% through point 5) passed through the middle region and 22% (3% through point 6), (8% through point 7), (9% through point 8) and (2% through point 9) was collected from the outer region. A conical shaped flow pattern is observed (Figure 4.4) and is consistent with liquid migration from saturated zones to unsaturated regions occurring (Petersen and Dixon 2003). This is evidenced in reactor 4 by the increase in associated volumes for the middle and outer regions eluted over time.

4.2.2 Residence time

Residence time was calculated by dividing the assumed interstitial volume of a region, by the volumetric flow rate of the eluent for that collection point on a daily basis. This is shown in Equation 4.1 where:

$$T = V_p / Q \qquad \text{Equation 4.1}$$

V_p is the void volume occupied by each regional point and Q is the volumetric flow rate from that corresponding point (Appendix C). This calculation was an approximation as it assumed that the liquid phase is radially distributed immediately upon entry into the bed, rather than conically as typically found from single point irrigation. Further ideal plug flow was assumed.

Residence time data for the inner, middle and outer regional points are displayed in Figures 4.5a and 4.5b. Two scales are used to illustrate this data with Figure 4.5a showing a low residence time of 0 to 200 hours and Figure 4.5b showing a high residence time of 0 to 800 hours. At the start of the experiment the inner region is shown to have the highest percentage volume eluted with the concomitant lowest residence time (Figure 4.5a). This can be attributed to the early saturation of the inner region, with the result that lateral diffusion of the liquid would occur radiating from the inner region to the less saturated parts of the reactor. Due to the ore not being fully saturated at the start of the leach period, high residence times can be associated with the middle and outer regions due to this lack of volume out flow. Points 4 and 7 illustrate this trend from having initially high residence times of 132 and 189 hours on Days 1 and 7 to residence times of 20 hours and 31 hours on Day 58 respectively.

a.

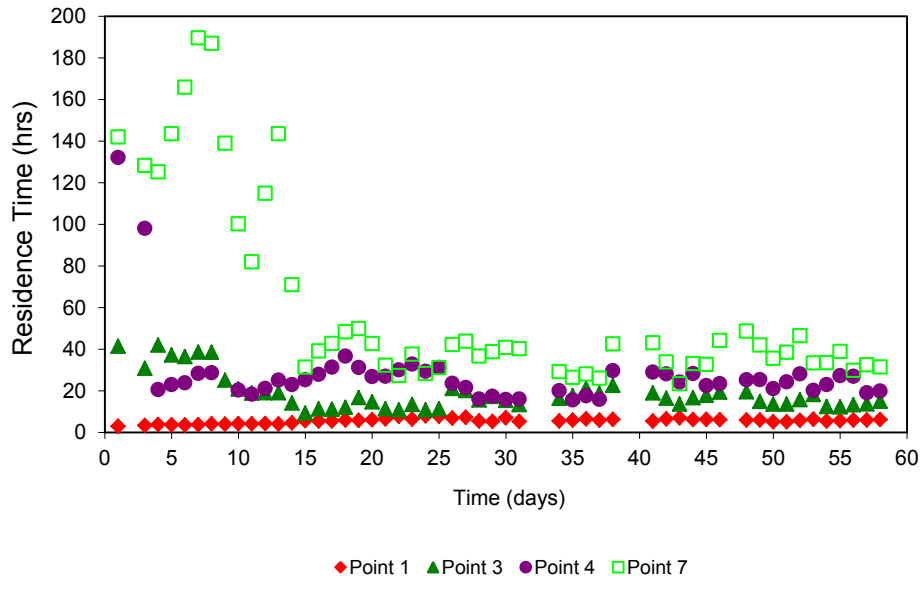

b.

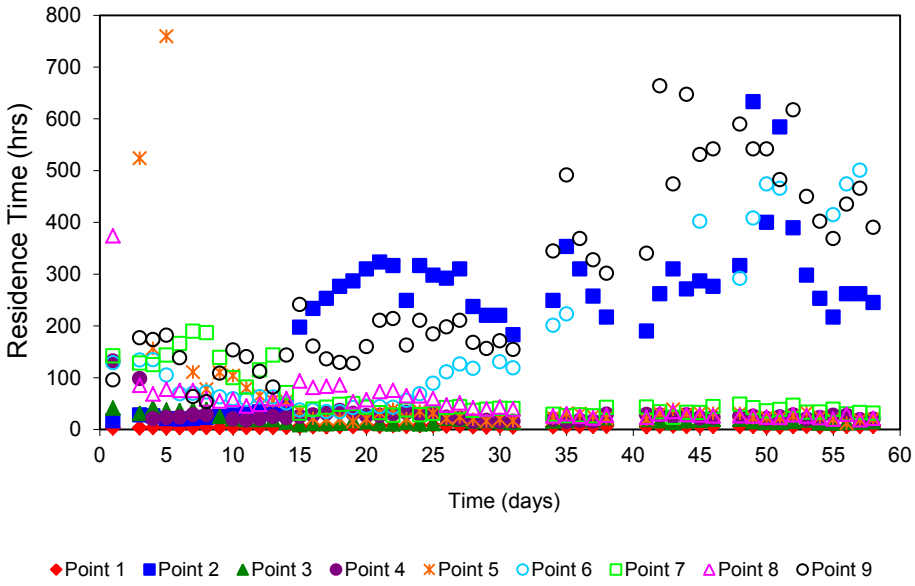

Figure 4.5: Residence times in each of the nine zones of the bed, estimated as a function of duration of experiment (b) and scaled to show high residence time

4.2.3 pH analysis

The pH data for the feed and collected leachate from the simulated heap leach are displayed in Figure 4.6. During the period when fresh feed was made up, the feed pH is seen to be relatively consistent with a pH variation of 0.25 units. During the recycle phase, the feed pH was measured from the pooled volume collected from two days before. An increase in feed pH is seen during the recycle phase. This is attributed to the decrease in free acid in solution as a result of the repeated passage through acid consuming regions of the bed. At the end of the recycle period on Day 46, fresh feed was made up daily, which continued until the end of the leach period.

The highest pH values at the commencement of the leach period for Days 1 and 3 were from point's 5, 7 and 9 (Figure 4.6). However, these points were below pH 2.0 by Day 4 indicating that a rapid decrease in pH was occurring for these initially high acid consuming zones. A decline in pH, with the exception of point 7 over Days 5 to 7, continued until the start of the recycle period on Day 18. During recycle, the pH increased at a rate of 0.04 units per day until Day 27. The decrease in pH between Day 27 and 30 resulted from the addition of fresh feed to the recycled volume to make up the required volume of 8.64 L. The addition of fresh feed resulted in a nett increase in H^+ ion concentration which lowered the solution pH. However from Day 30 the pH continued to rise, albeit at a slower rate of 0.02 units per day. This could

be attributed to the blocking of acid consuming regions of the ore through the formation of mineral precipitates. From Day 47, the pH decreased, reaching a stable state around Day 51 with the pH remaining between pH 1.13 and 1.69 for all elution points, until the end of the leach period.

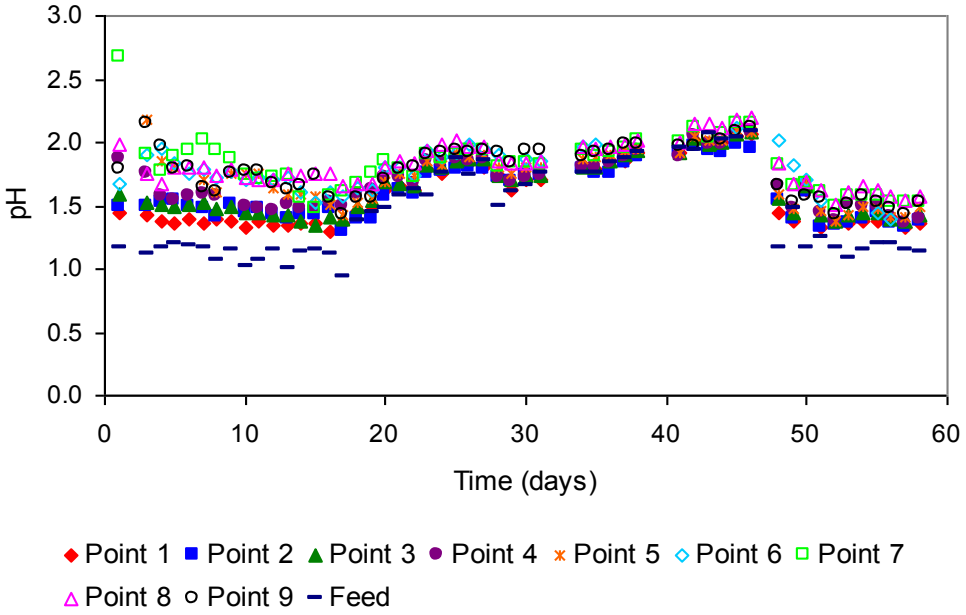

Figure 4.6: Daily eluted pH readings for outlet points 1 to 9

The pH profile over the first 18 days is seen to be region specific with the lowest and highest pH values associated with the inner and outer region respectively (Figure 4.6). The inner region pH range was relatively constant around pH 1.37 for Days 1 to 18 with an average difference of 0.25 between the feed pH and point 1. The middle region points 2 to 5, were characterised by a higher pH range of 1.45 to 1.68 during the pre-recycle period, with point 5 showing a pH drop at Day 8. Figures 4.7 and 4.8 illustrate the pH decrease at point 5 and 7 respectively with a corresponding decrease in residence time associated with this point. The outer region points, 6 to 9, displayed the majority of high pH readings during the pre-recycle period of Figure 4.6, with a pH range of 1.43 to 2.68. The highest initial pH reading of pH 2.68 occurred at point 7 on Day 1. This could be attributed to its low flow rate of 0.187 L (Figure 4.3) and an associated high residence time of 141.9 hours. An increase in pH over Days 4 to 7 for point 7 can be related to an increase in residence time over this period as shown in Figure 4.9. A decrease in pH for point 7 from Day 8 to 11 can also be attributed to a decrease in residence time for the same period. In each case where there is an increase or decrease in pH there is a concomitant increase or decrease in residence time respectively. This trend is consistent throughout all regions of the reactor but is more clearly seen in regions where a significant change

in residence time and resultant pH change occur as seen in Figures 4.7 and 4.8. The influence of mineralogy on pH and its relationship with residence time is explored in Section 4.2.4.

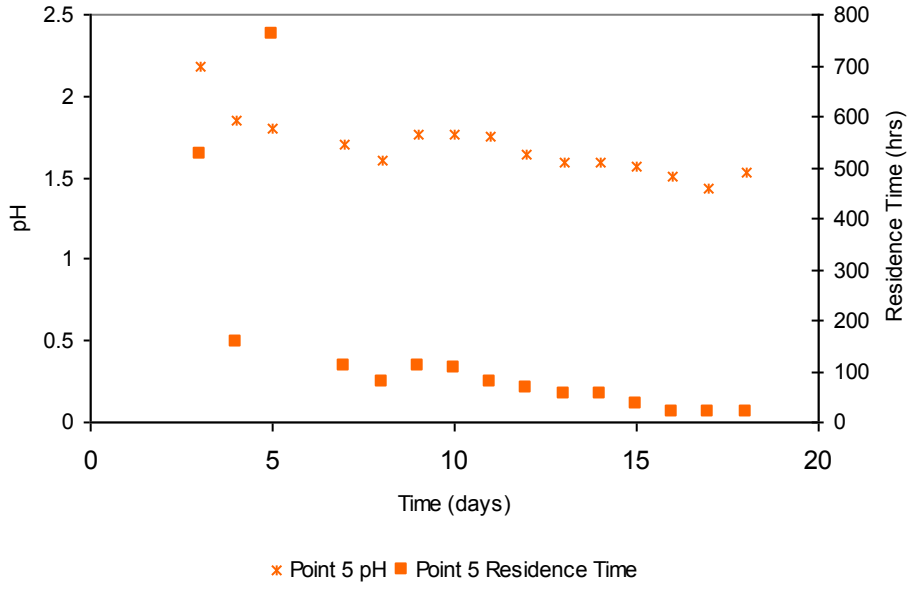

Figure 4.7: pH and residence time for point 5 from Day 1 to 18

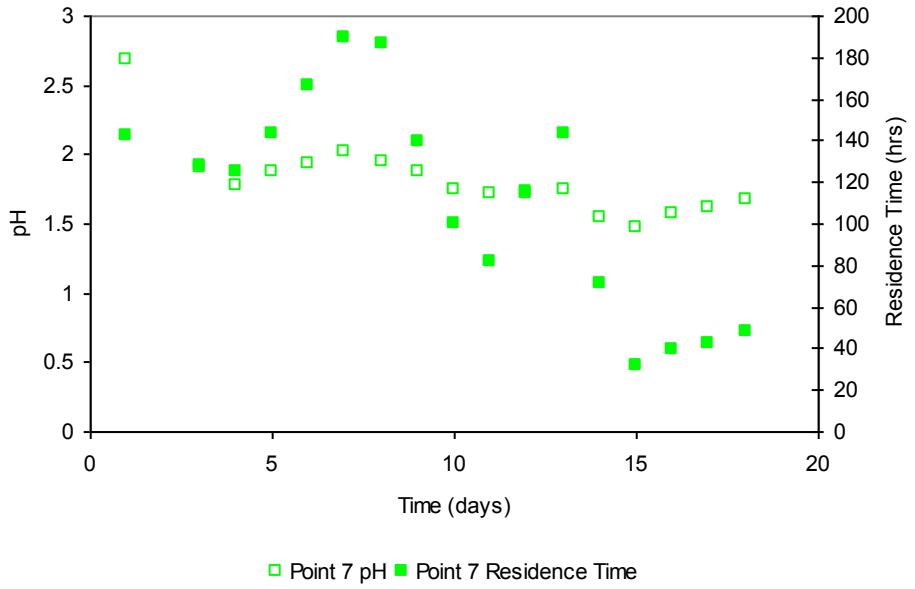

Figure 4.8: The relationship between pH eluted and residence time for point 7

Upon commencement of the recycle period on Day 18, a steady increase in pH was seen for all regions (Figure 4.6). This can be attributed to a reduction of free acid in solution as no acid was added to the recycled feed. A decrease in feed pH is seen on Day 28 owing to fresh feed solution being added to the recycled feed to bring the

feed solution back to its original volume of 8.64 L. This resulted in a decrease in pH of the eluted samples over Days 28 and 29. Thereafter the pH rose from Day 30 until the end of the recycle period on Day 46, with little influence of the feed volume adjustment on Days 31 and 34. Tables 4.5 to 4.8 show the effect of fresh feed addition to the concentration of H^+ and the theoretical pH of the new feed when added to the reactor on Days 28, 29, 31 and 34. These days were chosen as the volume correction using new feed exceeded 1 L.

Table 4.5: Theoretical H^+ concentration and increase in H^+ ions during the replenishment of the recycle feed on Day 28 (Recycle bin 1)

	Volume (l)	H^+ concentration (M)	Total H^+ in solution (mole)
Eluent collected (L) Day 26	6.627		8.86×10^{-2}
Feed addition Day 28 (L)	2.084	7.9×10^{-2}	1.65×10^{-1}
Total volume (L)	8.711		2.54×10^{-1}
H^+ concentration		2.92×10^{-2}	
Theoretical pH of feed		1.54	

Table 4.6: Theoretical H^+ concentration and increase in H^+ ions during the replenishment of the recycle feed on Day 29 (Recycle bin 2)

	Volume (L)	H^+ concentration (M)	Total H^+ in solution (mole)
Eluent collected (L) Day 27	6.391		8.91×10^{-2}
Feed addition Day 28 (L)	2.340	7.9×10^{-2}	1.85×10^{-1}
Total volume (L)	8.731		2.74×10^{-1}
H^+ concentration		3.14×10^{-2}	
Theoretical pH of feed		1.50	

Table 4.7: Theoretical H^+ concentration and increase in H^+ ions during the replenishment of the recycle feed on Day 31 (Recycle bin 2)

	Volume (L)	H^+ Concentration (M)	Total H^+ in solution (mole)
Eluent collected (L) Day 29	8.150		1.66×10^{-1}
Feed addition Day 31 (L)	1.112	7.9×10^{-2}	8.78×10^{-2}
Total volume (L)	9.262		2.54×10^{-1}
H^+ concentration		2.74×10^{-2}	
Theoretical pH of feed		1.56	

Table 4.8: Theoretical H^+ concentration and increase in H^+ ions during the replenishment of the recycle feed on Day 34 (Recycle bin 1)

	Volume (L)	H^+ concentration (M)	Total H^+ in solution (mole)
Eluent collected (L) Day 30	7.293		1.31×10^{-1}
Feed addition Day 34 (L)	1.515	7.9×10^{-2}	1.2×10^{-1}
Total volume (L)	8.808		2.51×10^{-1}
H^+ concentration		2.84×10^{-2}	
Theoretical pH of feed		1.54	

Note: Due to unforeseen circumstances volume elution was not measured for Days 31 to 33.

The replenishment of the recycled feed with new feed over Days 28 to 34, kept the pH of the eluting volume relatively constant for all regions. However after Day 34, there is a general increase in eluting volume pH, which may be due to the lack of significant (>1 L) fresh feed being added to the recycled feed. From Day 47 to the end of the leach period, fresh feed with a consistent composition was added daily to the reactor. A pseudo steady state with respect to pH of the eluent, from Day 51, was observed for all elution points.

4.2.4 Mineralogical analysis

To better understand the influence of mineralogy on the solution pH in the reactor, a mineralogical analysis was conducted on the ore. A QEMSCAN analysis of an ore sample prior to agglomeration revealed a number of mineral phases which could potentially consume acidity, resulting in the observed increase in pH. These minerals, along with their relative reactivity in an acid environment are shown in Table 4.9.

Table 4.9: Mineral dissolution rates and their reactivity to a low pH environment (Sverdrup, 1990 and Kwong, 1993a, 1993b)

Dissolution rate	Mineral type	Relative reactivity at pH 5	Average % in ore
Dissolving	Calcite	1.0	1.6
	Apatite		0.9
Intermediate	Biotite	0.4	21
weathering	Chlorite		3.2
Slow weathering	Plagioclase	0.02	7.9
Very slow weathering	Orthoclase	0.01	39.5
Inert	Quartz	0.004	19.2

Agglomeration of the ore with 8 g of sulphuric acid resulted in a slurry pH of pH 0.6. Based on the low percentage composition of the carbonate mineral (2.5%) and its reactivity below pH 5, all the available carbonate mineral may have reacted with the acid during the agglomeration phase. The dissolution of calcite, shown in Equation 4.2, may explain the relatively high pH values recorded on Day 1.

$$CaCO_{3(s)} + 2H^{+}_{(aq)} \rightarrow H_2CO_{3(aq)} + Ca^{2+}_{(aq)} \quad \text{Equation 4.2}$$

The calcium concentration in the leachate was not measured, so the rate of calcite leaching could not be quantified. As residence time increased during the leach, the contact time between liquid and mineral also increased allowing the dissolution of gangue mineral to impact on the properties of the liquid phase in the reactor. Due to the greater proportion of the mineral gangue being comprised of biotite ($KMg_{1.5}Fe_{1.5}AlSi_3O_{10}(OH)_{2(s)}$), plagioclase ($CaAl_2Si_2O_{8(s)}$) and orthoclase ($KAlSi_3O_{8(s)}$) at 21%, 7.9% and 39.5% respectively; much of the acid consuming ability of the ore can be attributed to the dissolution of these minerals as shown in Equations 4.3 to 4.5 (Ritchie, 1994; Busenberg and Clemency, 1976).

$$KMg_{1.5}Fe_{1.5}AlSi_3O_{10}(OH)_{2(s)} + 7H^{+} + {}^{1}/_{2}H_2O \rightarrow K^{+} + 1.5\ Mg^{2+} + 1.5\ Fe^{2+} + H_4SiO_4 + {}^{1}/_{2}Al_2Si_2O_5(OH)_{4(s)} \quad \text{Equation 4.3}$$

$$CaAl_2Si_2O_{8(s)} + 2H^{+}_{(aq)} + H_2O_{(aq)} \rightarrow Ca^{2+}_{(aq)} + Al_2Si_2O_5(OH)_{4(s)} \quad \text{Equation 4.4}$$

$$KAlSi_3O_{8(s)} + H^{+} + {}^{9}/_{2}H_2O \rightarrow K^{+} + 2H_4SiO_4 + {}^{1}/_{2}Al_2Si_2O_5(OH)_{4(s)} \quad \text{Equation 4.5}$$

The reduction in free acid during the recycle period resulted in the increase in pH of the eluent owing to the acid being consumed by the slow weathering minerals described above. The observed changes in flow pattern and residence time were most likely due to the precipitation of ferric iron salts such as ferric iron hydroxides and jarosite. The significant change in volumes eluted from particular regions coincides with the onset of this precipitate suggesting that the precipitation of ferric iron salts blocked preferential liquid flow paths and diverted the liquid flow from one region to another. An example of this can be seen in the volume elution profiles for points 2 and 3 from Day 6 where the volume eluted from point 2 decreased with a concomitant increase in volume elution for point 3.

4.2.5 Microbial attachment

The role of microorganisms in a leaching environment is to regenerate ferric iron and acid through the oxidation of ferrous iron and sulphur. The dynamics of bioleaching, whereby active bacteria account for the formation of these oxidised species in solution, is coupled to cell growth and biomass concentration (Ahonen & Tuovinen, 1995). Bacterial attachment to the mineral is characterised by an initial rapid stage, with various authors (Curutchet & Donati, 2000; Gericke *et al*. 2005; Harniet *et al*. 2005) having reported extents of attachment of 60 to 75% by *At. ferrooxidans* and *L.*

ferrooxidans on pyrite and chalcopyrite mineral occurring within the first 100 minutes of inoculation in an agitated slurry. Gericke *et al*. (2005) and Harniet *et al*. (2005) reported equilibrium of cell attachment 70 to 80% occurring after 4 to 6 hours on a 2% Chalcopyrite ore. As the first cell counts in the simulated heap leach occurred after 24 hours, it can be assumed that equilibrium had been reached. Calculated attachment efficiencies are shown in Table 4.10. The assumption was made that an even distribution of inoculum followed the same flow patterns as that of the feed distribution over the first 24 hours in order to determine the theoretical number of cells entering each region. The percentage attachment was calculated as the quotient of the number of cells eluted per region. The residence time was calculated through the assumption that the entire volume within each region which could hold liquid was fully saturated at the start of the leach. This assumption aggravated the high residence times seen for the outer region due to the small volume eluted from these points in the 24 hour period. Initially, limited flow through preferential channels occurred in the middle and outer region, with much of the middle and outer region remaining unsaturated. This can be seen for points in the middle and outer regions with calculated theoretical hydraulic residence times being significantly more than 24 hours despite leachate collection after 24 hours. The assumption of fully saturated regions at the start of the leach is incorrect as shown by the flow profiles in Figure 4.3 and Figure 4.4 for the middle and outer regions; however this provided a first order approximation of the approximate residence times for these regions. Longer times were needed for each region to become fully saturated, as seen by the lack of even volume distribution. Despite inaccuracies residence times for the middle and outer regions are several times higher than the inner region with a high flow rate and low residence time. It can therefore be assumed that an increase in attachment efficiency could be related to the increase in residence time per point analysed.

Table 4.10: Cell elution and attachment over the initial 24 hour period of Day 1

Collection points	% Volume eluted	Theoretical cell no. entering region	Eluent cell no.	Cells attached per elution point	% cells attached
1	0.763	2.00×10^{11}	4.33×10^{10}	1.56×10^{11}	78.33
2	0.102	2.67×10^{10}	1.01×10^{10}	1.66×10^{10}	62.08
3	0.040	1.06×10^{10}	2.41×10^{09}	8.18×10^{09}	77.25
4	0.013	3.32×10^{09}	1.37×10^{09}	1.95×10^{09}	58.83
5	N/A	N/A	N/A	N/A	N/A
6	0.023	5.94×10^{09}	5.15×10^{08}	5.43×10^{09}	91.33
7	0.021	5.39×10^{09}	3.51×10^{08}	5.04×10^{09}	93.50
8	0.008	2.05×10^{09}	2.00×10^{08}	1.85×10^{09}	90.25
9	0.031	7.99×10^{09}	1.73×10^{08}	7.82×10^{09}	97.83

The number of cells eluted daily per region is shown in Figure 4.9. As can be seen most cells eluted from the inner region. Cells eluted from the inner region show an

erratic planktonic cell number, possibly due to the new mineral environment, the establishment of flow channels, the limited surface availability and the creation of new mineral surface sites available for cell attachment by the dissolution of the acid soluble gangue exposing more mineral. A decrease in cell number eluted for Day 3 could be attributed to the possible increase in active mineral sites becoming available for microbial attachment due to the elution of the carbonate gangue mineral. Thereafter the number of cells eluted increased, possibly due to the maximum available surface area of the ore being reached. The analytical error for cell counting was calculated to be 9 % for replicate samples. The increase and decrease in cell number seen in Figure 4.9 could therefore not be attributed to counting error. Due to the compact nature of the graph, error bars were not included as this would hinder observable trends seen. The ore void of cells may be attributed to cell growth. Under optimal conditions the doubling time for *At. ferrooxidans* and *L. ferrooxidans* is 4.6 hours (Das *et al*. 2005) and 11 to 12 hours (Okibe *et al*. 2003) respectively. As such, a growing population of cells would lead to a consistent elution of cells and not an erratic pattern as seen in Figure 4.9 which cannot be explained.

Table 4.11: Specific growth rates for At. ferrooxidans and L. ferrooxidans

Author	Media	Microbe	Growth rate	Doubling time
Kai *et al*. 2007	9K media without $Fe2^{+}$	*At. ferrooxidans*	0.086 h^{-1}	8.06 hr
Lusty *et al*. 2006	Iron free media with thiosulphate	*At. ferrooxidans*	0.151 h^{-1}	4.6 hr
Das *et al*. 2005	Cell inoculum measured 9k Media	*At. ferrooxidans*		4.6 hr
Akbar *et al*. 2005	Basal salt media with 1% Pyrite	*At. ferrooxidans*	0.108 hr^{-1}	6.41 hr
Tupikina *et al*. 2005	Silverman-Kundgren Media sulpplemented with Fe^{2+} and a 1% pulp density pyrite	*At. ferrooxidans*	0.01 0.016	64.2 hr 43.3 hr
Okibe *et al*. 2003	Chalcopyrite concentrate	*L. ferrooxidans*		11 – 12 hr
Romero *et al*. 2003	BRS medium with sulphate	*L. ferrooxidans*	0.105	6.82 hr

Table 4.11 reviews the doubling times of *At. ferrooxidans* and *L. ferrooxidans* in a similar environment to that of the stirred tank reactors used to inoculate the leach reactors. It was assumed that the increase in cells eluted during the first five days was not due to cell growth as these cells were assumed to be in lag growth phase. However, 2.61×10^{11} cells were inoculated into the reactor, with a total of 3.01×10^{11} cells being eluted after 5 days. Throughout the initial 5 day period, most of the cells counted were rod-shaped indicating the possible washing out of *At. ferrooxidans* during this time. The post operational analysis of ore using restriction enzyme

analysis indicated no presence of *At. ferrooxidans* associated with the ore (unpublished data), suggesting that a population shift occurred with the washing out of *At. ferrooxidans*. This could be related to the rapid increase and consistently high redox potential values associated with this leach as discussed in Section 4.2.6. The recycle period from Day 18 was characterised by an increase in cell number eluted. This can be related to the recycled feed containing a planktonic cell population being reintroduced into the reactor. However from Day 27 to Day 36, the planktonic cell number decreased, possibly due to planktonic cells becoming entrapped in the mineral precipitate associated with this period. Equilibrium in cells eluted is seen to occur from Day 38 to Day 46. Thereafter a spike in cells eluted is seen on Day 49. This can be attributed to the switch from recycle feed to fresh feed with the associated increase in ferrous concentration in solution and the possibility of dissolution of the mineral precipitate by fresh acid releasing the entrapped cells therein (Escobar and Lazo, 2003). Thereafter a steady state in cells eluted is once again maintained until the end of the leach period (Appendix B).

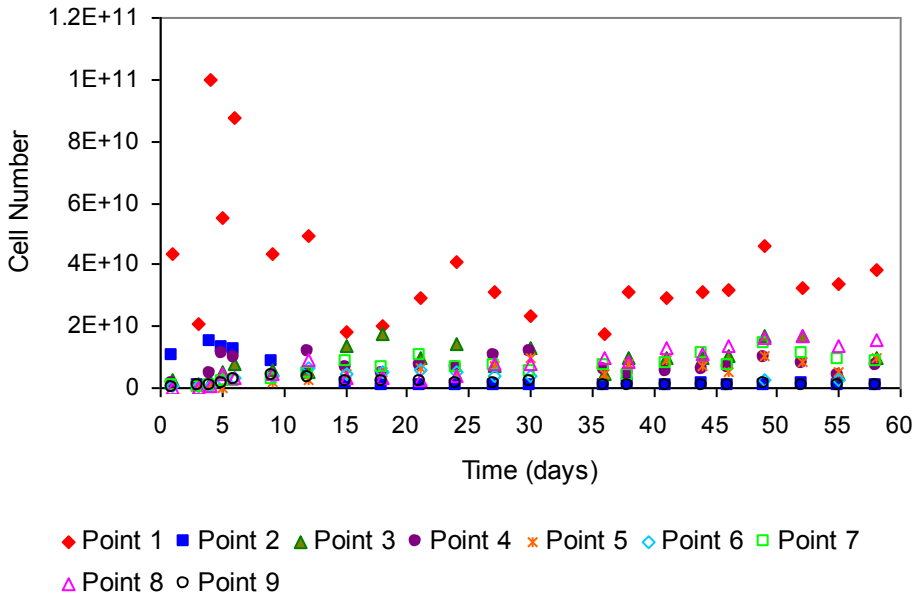

Figure 4.9: Cell elution profile for the duration of the experimental leach

4.2.6 Redox potential

The redox potential was measured daily for the collected leachate and is shown in Figure 4.10. From Day 1 redox readings show a rapid increase, stabilising around 600 mV for all points from Day 6 till Day 48. The rapid increase in the ferric to ferrous ion ratio is indicative of an active microbial population oxidising ferrous to ferric in

solution (Ahonen & Tuovinen 1995). High levels of ferric iron have been reported by various authors (Brunet-Battaglia 1998; Norris 1987) to inhibit *At. ferrooxidans* competitively which could explain the high number of rod shaped microorganisms counted during the first 5 days of the leach.

Redox potential of eluent from all the collection points on Day 1 was below that of the feed redox, with the outer region points 7 and 9 having the lowest redox values recorded. The acid agglomeration of the ore promoted the formation of ferrous irons through the abiotic leaching of the ore and enhanced the leaching effect of soluble ferric irons on exposed chalcopyrite. These conditions created a decrease in soluble ferric iron relative to that of the feed as seen in Figure 4.10. However, from Day 5 the redox potential of collected eluent from all points except 5 is above that of the feed redox. This indicates that the increase in the formation of ferric iron occurred from the oxidation reaction of ferrous iron to ferric iron. The low redox potential reading of point 5 may be attributed to a reduced microbial presence and oxidative activity within this region which could be related to the low volume outflow of the region. A greater volume outflow is seen for point 5 from Day 6 with a resultant increase in the redox potential. This indicates that an increase in the ferric ion concentration occurred in solution through a greater microbial oxidation of ferrous to ferric iron, with the result that the redox potential of this point increased to above that of the feed solution. However by Day 9 a steady state in the redox potential is seen for all elution points.

During the recycle period the redox potential for all eluents remained constant around 600 mV with the feed solution climbing steadily from Day 18 and remaining so until Day 46. A decrease in feed redox potential is seen on Day 28 which can be attributed to the volume adjustment with fresh feed. Little effect is seen on the redox potentials of the eluted volumes for the regional points.

At the end of the recycle period on Day 46 and at which daily fresh feed to the reactor was resumed, the feed redox potential and that of eluted volumes for points 1, 2, 3, 5, 6 and 9 decreased owing to the addition of fresh ferrous iron in solution decreasing the ratio of ferric to ferrous iron. However the redox potential at points 4, 7 and 8 did not change. The reason for this could not be explained as measurements were not taken on Day 47 due to human error. However the redox following Day 48 rapidly approached and maintained its previous redox potential of around 600 mV until the end of the leach period (Appendix B).

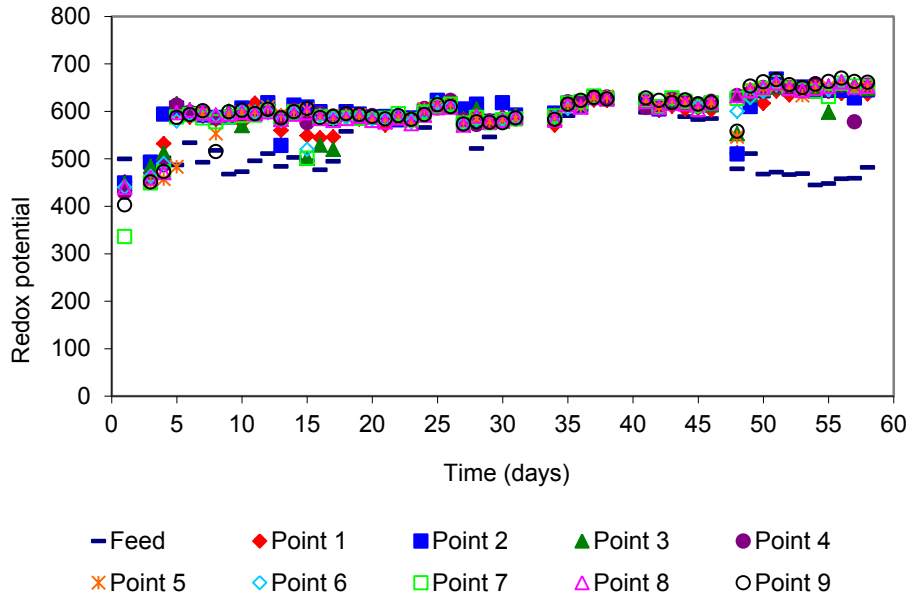

Figure 4.10: Daily redox measurements of collected eluted volumes

4.2.7 Iron elution

The iron concentrations from the feed and collected volumes were measured daily for the duration of the experimental leach. These are shown in Figure 4.11. The iron concentration eluted was region specific with the inner and middle regions maintaining a slightly higher iron concentration than for the outer region. The majority of the iron in solution was in the ferric form which would account for the high redox potential associated with this leach (Appendix B).

As shown in Figure 4.11 the iron concentration decreased from the start of the recycle period on Day 18. This could be attributed to the deposition of the iron species in the form of ferric hydroxide or jarosite. Toro *et al*. (1988) studied the nature of iron precipitation during the bio-oxidation of iron and from material balance calculations, found that ferric hydroxide was initially formed which upon aging was converted to jarosite. As an XRD analysis was not performed, the identification of this mineral precipitate is uncertain, but several authors (Stott *et al*. 2001, Petersen *et al*. 2001) account for the formation of ferric hydroxide and jarosite precipitation at these high redox potentials.

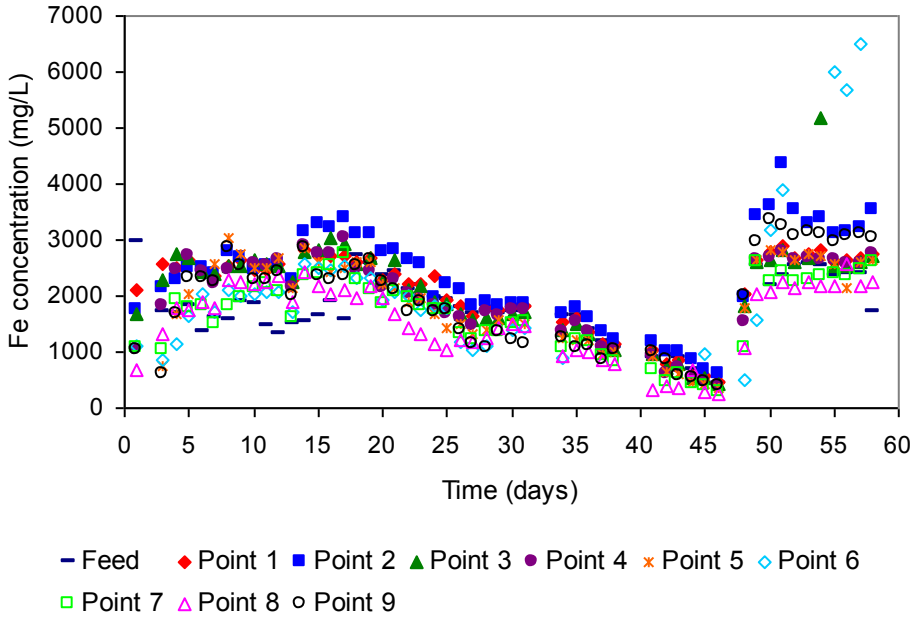

Figure 4.11: Daily iron concentration collected from the feed and eluted volumes of the inner, middle and outer regions

At the end of the recycle period, the iron concentration increased over a short time period due to the addition of fresh feed containing 2 g/L iron in solution into the reactor on Day 48. However, partial dissolution of the mineral precipitate may have occurred as the iron concentration increased to double the pre-recycle iron levels. Most notable is point 2 and point 6 showing the highest iron eluted for this period. A greater variance in iron concentration was also seen in these regions during the post-recycle period for all regions.

4.2.8 Copper elution

Copper concentration in the eluent from each region is shown in Figure 4.12. The concentration of copper in eluent form in the inner region is seen to be lower than that of the outer region throughout the leaching period. However, based on the volume of eluent through this region, the inner region accounted for the largest amount of copper released as shown in 4.13.

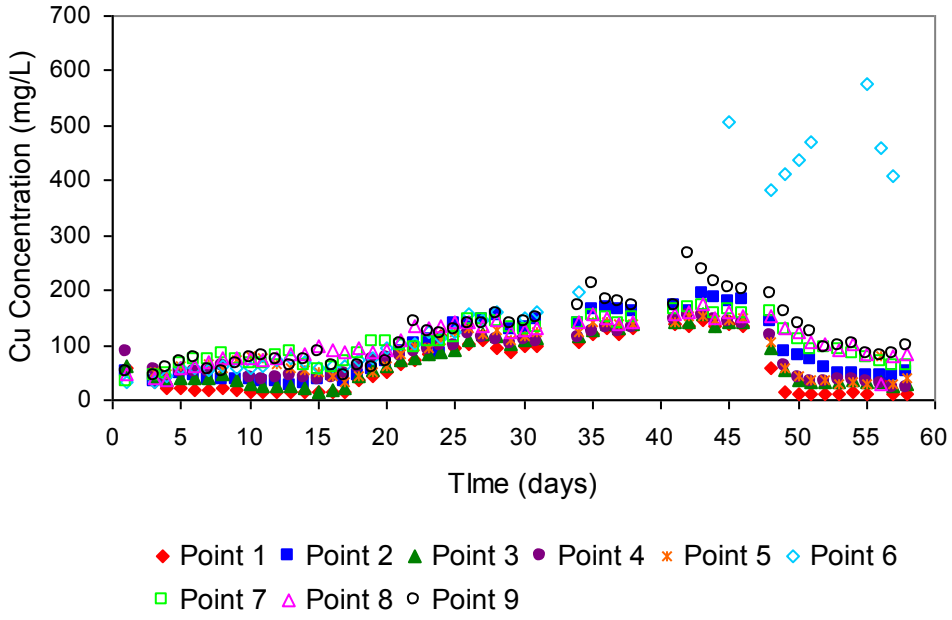

Figure 4.12: Daily copper concentrations eluted from inner, middle and outer region points

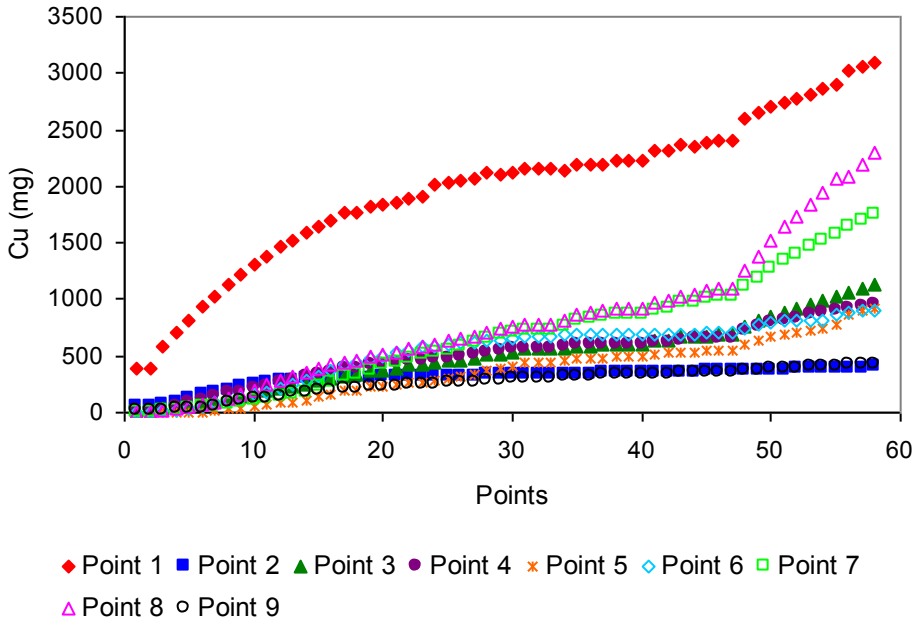

Figure 4.13: Cumulative copper released daily per point for inner, middle and outer regions

Figure 4.13 shows an increase in the cumulative release of copper from the reactor for all regions. The increase in copper eluted for points 7 and 8 begins from Day 10 and Day 25 respectively. The increase for point 8 can be related to the volume eluted, as the volume increased from 447 ml to 1239 ml by the end of the leach.

However the volume outflow of point 7 is less significant than point 8 with a concomitant lower copper output.

The total copper collected from the leach run is shown in Figure 4.14. Table 4.12 shows the percentage copper leached with regards to the ore mass of each region. As can be seen the three highest amounts of copper eluted are from points 1, 8 and 7. This can be related to the elution, ore volume, region mass and residence times of these points. Point 1 had the highest elution rate with the smallest ore volume and lowest residence time as compared to the middle and outer regions. This could also be attributed to the dripper point being directly above the inner region, allowing for ferric iron and acid to interact with the surface of the ore in this region releasing more copper. Points 7 and 8 had similar elution rates to points 3 and 4; however the ore mass occupied by these outer regional points was greater with concomitant higher copper percentages being found in these regions releasing more copper upon oxidation of the ore as shown in Table 4.12. Outer regional points 6 and 9 display significantly less copper leached, primarily due to the low volumes eluted (Appendix B).

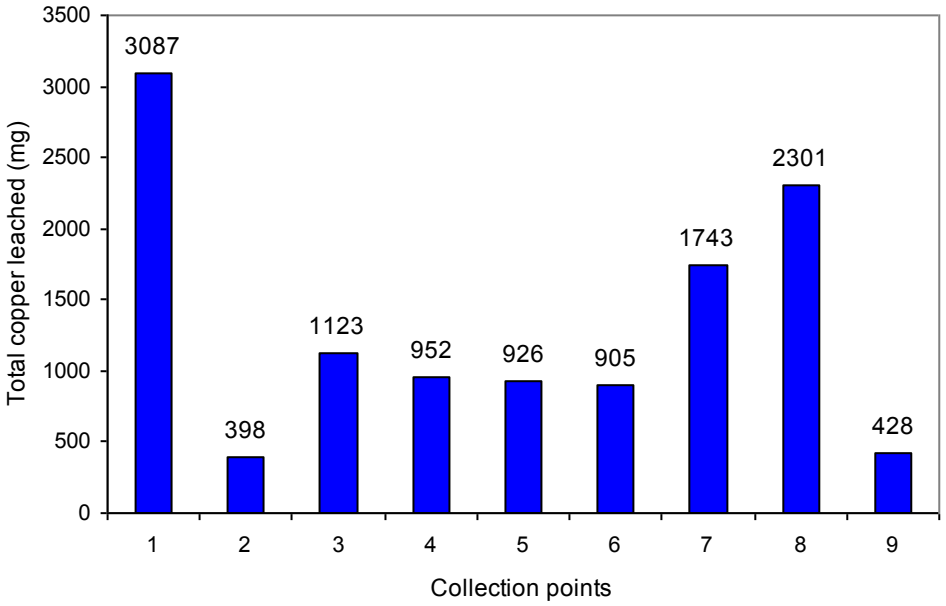

Figure 4.14: Total copper leached for eluted volumes collected for the duration of the leach experiment

Table 4.12: Comparison of copper leached per mass region of ore

	% Copper recovery per region								
Regions	1	2	3	4	5	6	7	8	9
% Cu	36	7	15	13	21	9	19	22	4

The outer region points 7 and 8 eluted more copper than the middle region points as the volume of ore occupied by this region was greater. As a result a greater percentage of copper would have resided within this region, which was released upon oxidation of the ore (Table 4.12). The volume eluted through points 7 and 8 was also significantly higher than through points 6 and 9, which would account for these two points having the highest copper elution values. During the recycle phase of the run, copper leaching continued due to the sufficient amount of ferric ion in solution. However a decrease in copper leaching rate was seen to occur during the recycle phase as shown in Figure 4.15. This could be related to the affinity copper has for binding to jarosite (Brierley and Brierley 2001; Acevedo 2000, Olumbambi *et al*. 2007). It was visually noticed that during this time, jarosite formation increased within the reactor with some collection points becoming blocked. However at the start of the fresh feed period on Day 46 an increase in copper in solution is seen which can be attributed to the partial dissolution of the jarosite precipitate by the fresh acid in the feed releasing the bound copper.

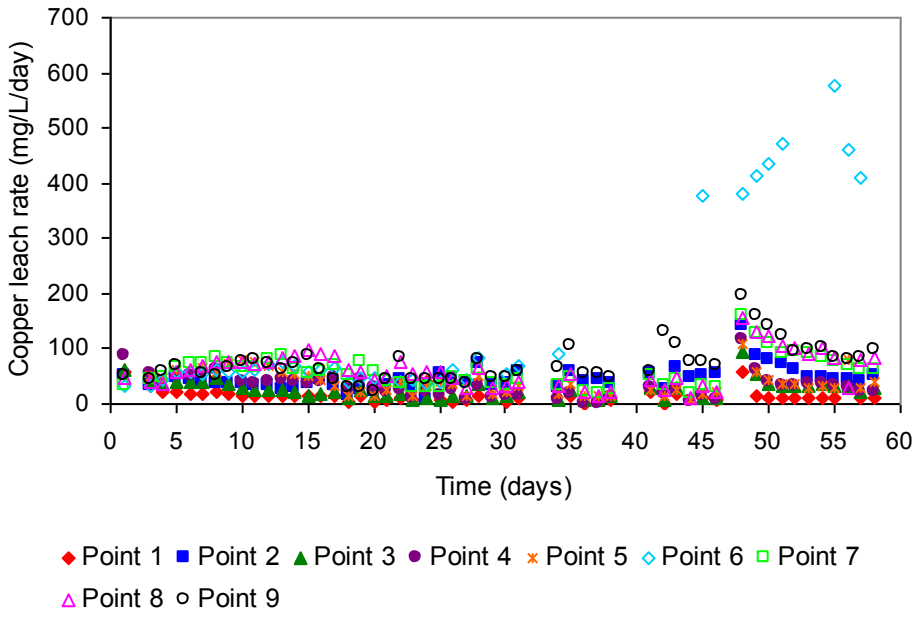

Figure 4.15: Daily copper leaching rate for eluted volumes collected

4.2.7 Post operational analysis

The post operational analysis of reactor four included the estimation of adhered cell number and the compositional analysis of mineral precipitate. A series of agitation of the mineral ore in liquid slurries and Tween washes as described in Section 3.7.8, were used to dislodge attached bacteria from the surface of ore samples. The detachment protocol was determined previously to remove at least 90 % of ore

adhered cells (data not shown). The enumeration of planktonic cells occurred by direct microscope counting. The attached cell number per region of ore is shown in Figure 4.16 for the top level.

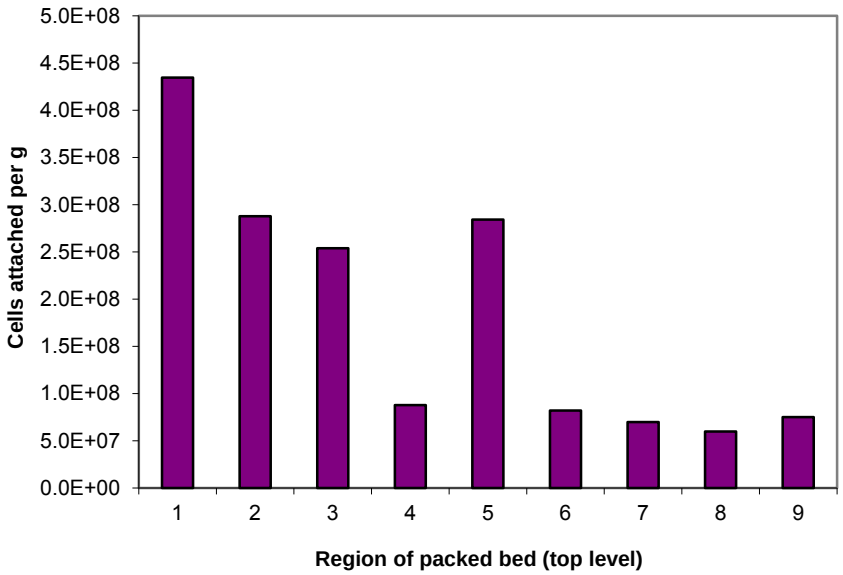

Figure 4.16: Number of attached cells per gram for the top level

Figure 4.16 shows the highest attached cell number occurred within the inner region. The dripper, through which the inoculum on Day 1 was introduced into the reactor, was positioned directly above the inner region. Prior to the unpacking of the leached ore, a biofilm was seen to have formed directly beneath the dripper as shown in Figure 4.17. This film was removed and is awaiting further analysis.

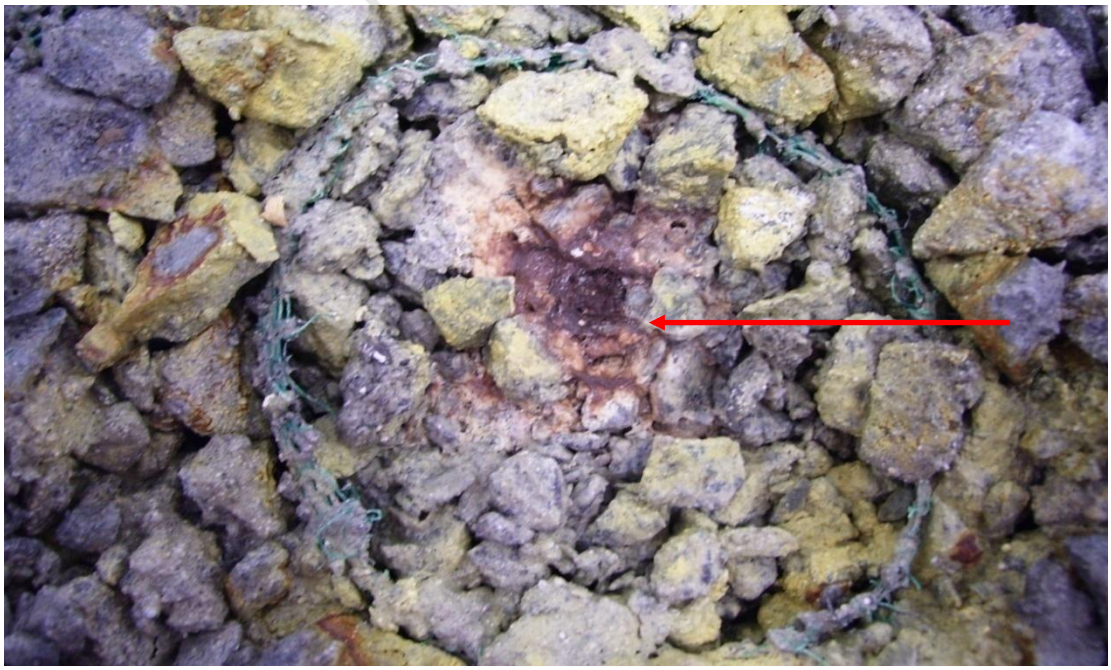

Figure 4.17: Biofilm formation beneath dripper during post operational analysis of reactor 4

Various authors (Bevilaqua *et al.* 2004; Gonzalez *et al.*, 1999; Lizama *et al.*, 2003) have shown that rapid cell attachment occurs within the first 24 hours, indicating that initial cell attachment would have occurred primarily within the inner region. The recycling of the feed solution from Day 18 to Day 46, with microbial populations ranging from 5.94 x 10^6 to 2.09 x 10^7 cells/ml, can also be assumed to have reinforced the creation of a primary corridor of attached microorganisms through the inner region. This would help to explain the relatively large number of microbes associated with this region during the unpacking and analysis of the ore. As such, the migration of microbes through the reactor can be assumed to have originated from the solution flow through the inner region. The decline in the number of attached microbes for the middle and outer regional areas (Figure 4.16) might therefore be attributed to the reduced volume elution with a corresponding lack in planktonic cell number being distributed within the migrating solution.

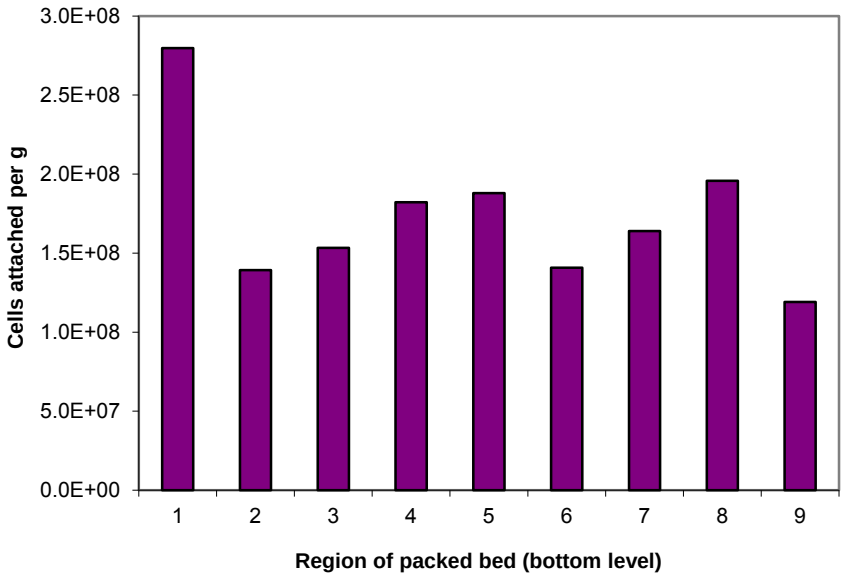

Figure 4.18: Attached cell number per gram of regional ore for the bottom layer

The inner region is shown by Figure 4.18 to still comprise the highest cell attachment suggestng that a primary corridor of cells extends through the inner region. This would indicate that attachment by microorganisms within the first 24 hours is important as the majority of cells adhere within the first 30 cm of the reactor. Even with repeated microbial populated recycle elutions, the primary cell attachment occurred and stayed within the first 30 cm of the bed of ore. This is shown by the

estimated adherence of cells within the first 24 hours of the inner region being very similar to the number of cells attached at the end during post leach agitation.

A greater cell attachment is seen to occur in the middle and outer regions which could be attributed to a greater solution flow occuring through these regions. Analysis of the adhered microorganisms from the top and bottom layers of ore (Figure 4.19) revealed a conical liquid flow pattern as evidenced by the decrease in spread of attached micro-organisms from the inner top layer (4.35 x 10^8 cells/g) to the outer top layer (1.44 x 10^7 cells/g) of the reactor. However a decrease in the cell number of 2.80 x 10^8 cells/g can be seen to occur from the bottom inner region to 1.19 x 10^8 cells/g for the bottom outer region sections. It can be seen that the majority of adhered microorganisms occurred in the bottom outer regions of the reactor, with little microbial activity occurring in the top outer reaches of the ore bed.

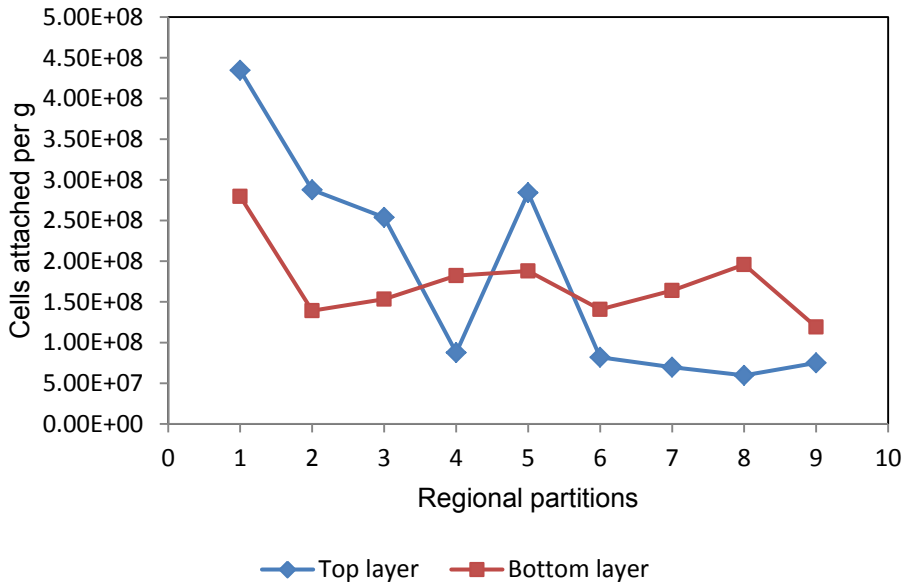

Figure 4.19: Microbial attachment per regional area of ore for the top and bottom layers of the reactor

The attachment of microbes to copper bearing ore is understood to enhance the rate of copper dissolution (Crundwell, 2001; Watling *et al*., 2004). Figure 4.20 shows total copper leached per regional ore area when compared to the regional microbial attachment of the ore by colonising bacteria. Total copper leached is shown to be the highest for the inner region which displays a relatively high sessile population (Figure 4.20). This could be partly attributed to the high volume throughput as well as the resident microbial population. It is interesting to note that for regional point 2 there is a drop in cell number with a corresponding decrease in copper leached confirming

the link in cell adhered number and copper leaching rate. However for regions 7 and 8 there is an increase in the amount of copper leached with a slight increase in the sessile cell population. This could be explained by the assumption that attached microorganisms were evenly distributed through the top and middle layers of the ore bed. As we know that the majority of microbes in the outer region tended to be in the bottom layer, the relatively low number of microbes attributed for points 7 and 8 could be related to the fact that the mass of the top layer of ore was taken into account for calculating the number of attached microorganisms per region. Evidence for this is shown in the decrease of copper leached from the inner region to the outer region as seen in Figure 4.21.

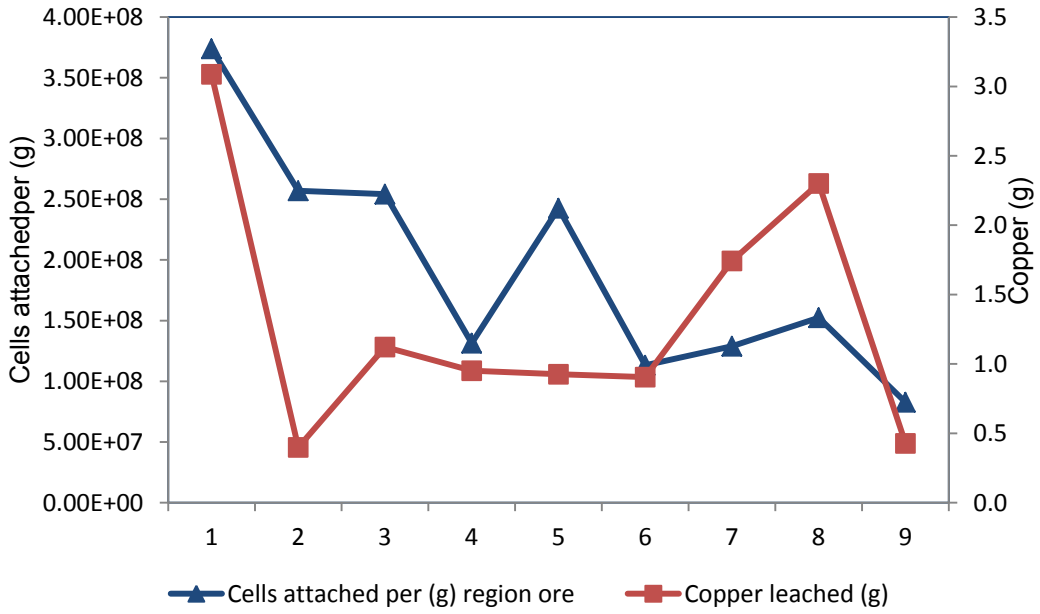

Figure 4.20: Copper leached per regional ore with microbial attachment

Figure 4.21 gives the copper leaching efficiency per region ore with the precipitate of copper included. The greatest copper leaching occurs within the inner region where the greatest elution rate and microbial adherence occurred. A significant amount of leached copper is retained within the bed either by adsorption to or entrainment within precipitated jarosite. Figure 4.21 indicates that the proportion of retained copper is greatest in the outer regions becoming insignificant in region 1. This follows the trend observed for pH and reinforces the relationship between jarosite precipitate and retention of leached copper.

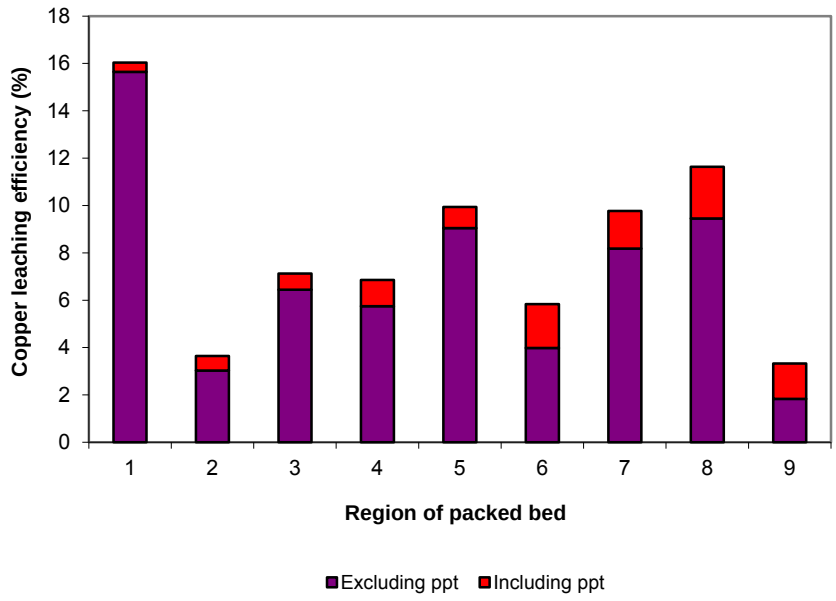

Figure 4.21: Copper leaching efficiency per region ore including precipitate

A table comparing the release of iron and copper following agitated washes with water and 1M HCl is shown below.

Table 4.13: Comparison of metal release by acid and water washing

	Acid Wash				% copper released by water wash	
	Iron released (mg)		Copper released (mg)		Top layer	Bottom layer
	Top layer	Bottom layer	Top layer	Bottom layer		
1	1814	1874	36	41	64.31	57.47
2	1574	931	55	25	72.20	70.26
3	2541	1235	88	31	60.92	84.45
4	2122	1606	133	51	29.69	65.22
5	1353	1002	59	32	48.71	61.64
6	2229	2731	211	205	5.01	36.98
7	1753	2985	236	103	2.09	50.15
8	1940	2818	405	128	0.77	34.27
9	1582	2781	203	147	6.25	45.39

The acid wash released significant amounts of iron and copper as a result of precipitate dissolution. This result is interesting as no copper precipitation should have occurred given the prevailing solution pH values. Both the top and bottom layers released relatively large amounts of iron suggesting a fairly even distribution of iron containing precipitates. Copper liberation showed a distinct pattern, with significantly more copper being released from the outer regions. This suggests an interaction between copper ions and the precipitated jarosite, particularly where liquid flow rates were lower. It has been previously reported that copper adsorbs to jarosite

with a relatively high affinity (Brierley 2001; Acevedo 2000). This would account for the significant retention of copper within the bed. A second phenomenon could be the entrainment of copper ions within the jarosite matrix during precipitation. The percentage of copper released by water washing is shown to be relatively high for the inner region decreasing towards the middle and outer regions. Less than 1% of the iron released by the acid wash came into solution following the water wash, confirming the insolubility of the jarosite (data not shown). This implies that the copper was adsorbed to the jarosite surface, with agitation releasing it into solution. Towards the outer region, relatively small amounts of copper were released by water washing, indicating that entrainment within the jarosite is more pronounced and agitation did little to release it into solution. This may be attributed to the lower flow rate which could increase the chance of leached copper being entrained, rather than merely adsorbed to the surface.

This result suggests a potentially significant amount of leached copper may not be recovered is situations where ferric iron precipitation is occurring.

4.3 Analysis of simulated heap leach 3

The flow rate for reactors 3 and 2 were determined by using the industry standard flow rate of 5 L/m^2/hr. It was assumed that 4 drip points, separated 50 cm apart were included in the 1 m^2 areas with the resultant flow rate for each point being 1.25 L/hr or 21 ml/min for each drip point. This flow rate was applied to reactors 3 and 2. However if the surface area of the reactor with relation to the industry standard flow rate of 5 L/m^2/hr, was taken into account and was up scaled to 1 m^2, the resultant flow rate would be equivalent to 15.5 L/hr/m^2. This is three times higher than the industry standard of 5 L/hr/m^2, indicating that for reactors 3 and 2, a very high flow rate was used.

The volumes eluted were collected on a daily basis for each region and outlet point. A recycle period of 15 days was initiated from Day 15 of the leach and ended at the termination of the leach on Day 30. No topping up of the recycled feed with fresh feed occurred during this time. Analysis of heap leach 3 involved the leachate being measured for pH, redox potential, volume, planktonic cell number, total iron and copper eluted.

4.3.1 Volume elution

Volumes eluted on a daily basis were collected and are displayed in Figure 4.23 below. Similar to reactor 4, the highest volume elution is seen to occur through the inner region (point 1). A total volume of 391 L passed through the inner region and accounted for 53 % of the total volume percentage eluted for the entire leach period. The gradual decline in volume elution from the inner region can be attributed to the increased lateral diffusion of feed to the middle and outer regions of the reactor. This is shown in Figure 4.24, where a low volume elution graph, which excludes the elution volume of point 1, is displayed. With the exception of point 4, the saturation of ore is reached by Day 8 for all regions. The higher volume outflow through point 4 could be related to a preferential flow channel being created during the packing of the reactor and the subsequent settling of the ore.

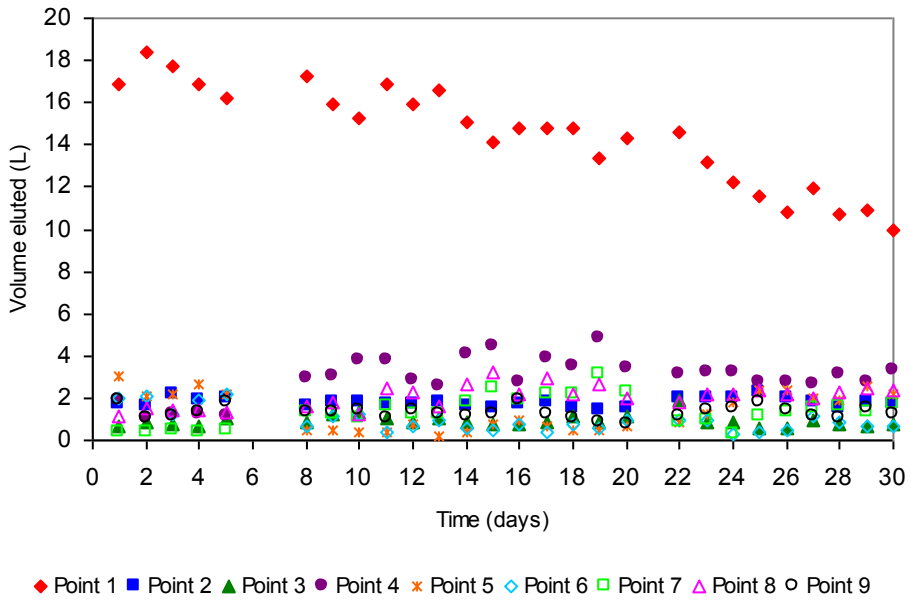

Figure 4.23: Daily volume elution from inner (point 1), middle (points 2-5) and outer (points 6-9) region outlet points

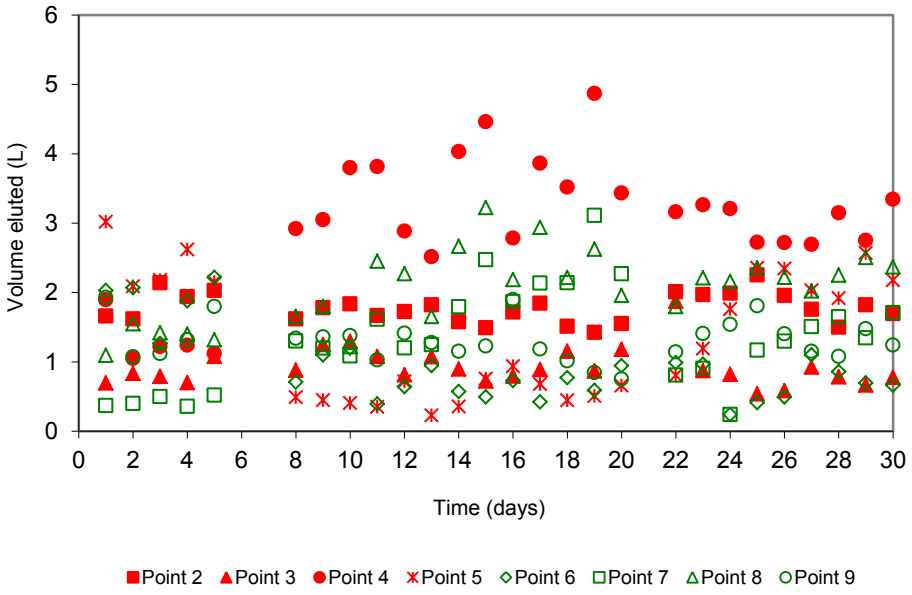

Figure 4.24: Middle (red) and outer (green) regional flow rates

During the recycle period from Day 15 to Day 30, the inner region elution volume decreased from 15.1 L to 9.9 L (Figure 4.25). This can be attributed to the overall decrease in feed volume due to feed evaporation without introduction of volume correction. During this same period, the elution volume of the middle region remained relatively constant from 7.4 L to 7.9 L, while the outer region showed a slight decrease in volume eluted from 7.4 L to 5.9 L.

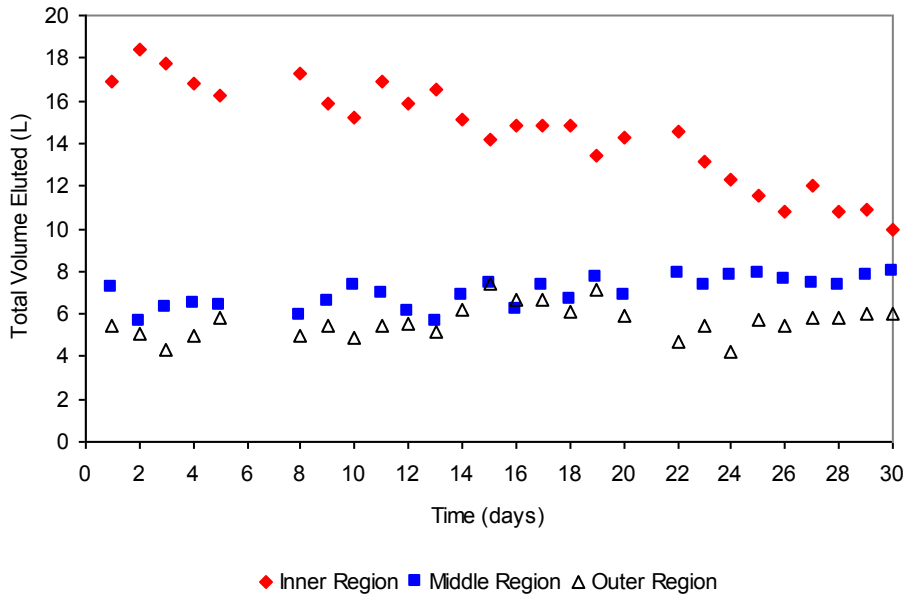

Figure 4.25: Total volume eluted for inner, middle and outer regions from Day 1 to 30

Inter-regional liquid transfer is seen to occur between Days 8 and 11. The inner region shows a decrease in volume eluted from 17.2 L to 16.8 L, while the average volume for each middle region elution point increased from 1.4 L to 1.7 L over the same period. The outer region remained relatively constant with only a slight increase of 0.1 L between those days. This shows that the transfer of feed occurred between the inner, middle and to a lesser extent, outer region prior to the start of the recycling period.

The cumulative percentage of volume eluted for all regions over the 30 day leach period is shown in Figure 4.26. The inner region is displayed in blue with the middle and outer regions being displayed in red and green. Some 53 % of feed solution passed through the inner region, while 26 % (7 % at point 2, 3 % through point 3, 11 % at point 4, 5 % through point 5) passed through the middle region and 21 % (3 % through point 6, 5 % at point 7, 8 % through point 8, 5 % through point 9) passed through the outer region.

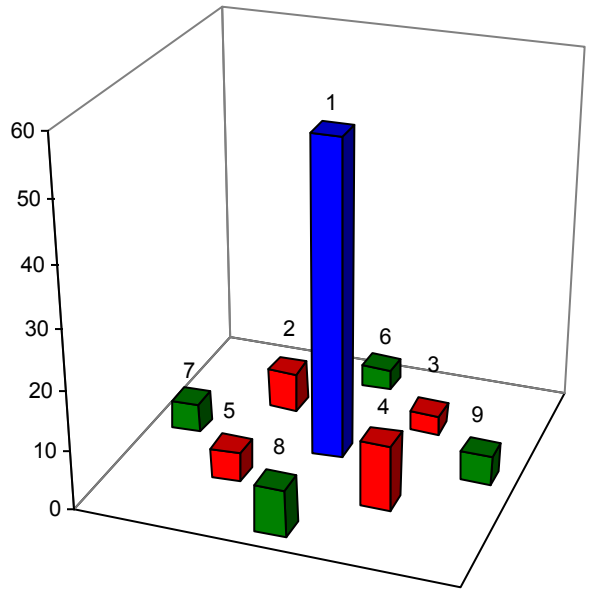

Figure 4.26: Percentage volume eluted from points within the inner, middle and outer regions

4.3.2 Residence time

The higher flow rate (21 ml/min) associated with reactor 3 would be expected to produce shorter residence times in comparison to reactor 4. This is shown in Figure 4.27, where the highest residence time is 109 hours for points 6 and 7 on Day 24. The slightly higher residence times associated with the middle and outer regions at the start of the leach, as compared to the inner region residence times, could be

attributed to those regions not being saturated at the start of the leach. The recycling of the feed solution from Day 15 and the decrease in feed volume did not significantly influence residence times associated with elution points in the inner, middle and outer regions. A comparison of the average residence times associated with reactors 4 and 3 for the inner, middle and outer regions is shown below in table 4.14.

Table 4.14: Average residence times for the inner, middle and outer regions for reactors 4 and 3

	Inner region	Middle region	Outer region
Reactor 4	5.3 hrs	75.9 hrs	95.6 hrs
Reactor 3	1.4 hrs	13.1 hrs	25.7 hrs

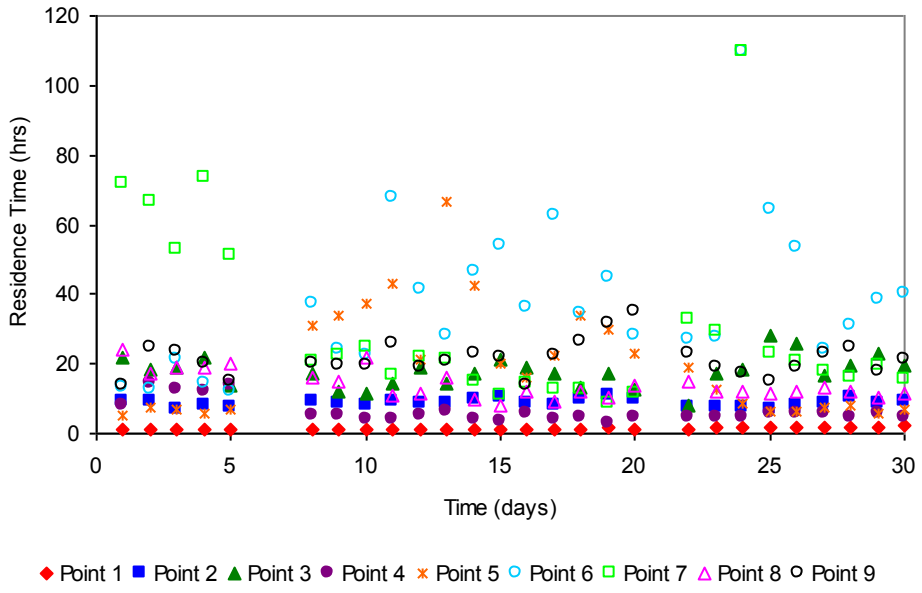

Figure 4.27: Residence times associated with elution points within the inner, middle and outer regions of the ore bed

4.3.3 pH analysis

The pH data from reactor 3 is shown in Figure 4.28. The overall pH profile is seen to be region specific with the lowest and highest pH values being associated with the inner and outer regions respectively. During the pre-recycle period, a general decline in pH is seen to occur on Day 2. This may be attributed to the continued washing out of excess hydrogen ions associated with the ore during the acid agglomeration phase. This was seen to occur for reactor 4 as well however the durations of these declines differed based on flow rates of the two reactors.

The initial high pH value eluted from point 7 until Day 8 in the outer region can be related to the relatively high residence time associated with this point. With an increased flow rate of feed coupled to reactor 3, pH variability decreased for all elution points, primarily due to the relatively low residence times associated with each elution point as compared to residence times experienced by reactor 4. This is evidenced by the pH range of reactor 3 extending from pH 1.14 for the inner region to pH 1.58 for the outer region whereas the pH range for reactor 4 extended from pH 1.37 for the inner region to pH 2.68 for the outer region prior to recycling of the feed.

The recycle period, from Day 15 shows a gradual increase in eluent pH for all regional points. Unlike reactor 4, the recycled feed was not topped up with fresh feed intermittently. Due to this the increase in pH during the recycle period can be attributed to the repeat interaction of recycled feed with acid consuming regions of the ore. As a result of the high flow rate and relatively short residence times associated with reactor 3, the overall pH never increased to above pH 2.0.

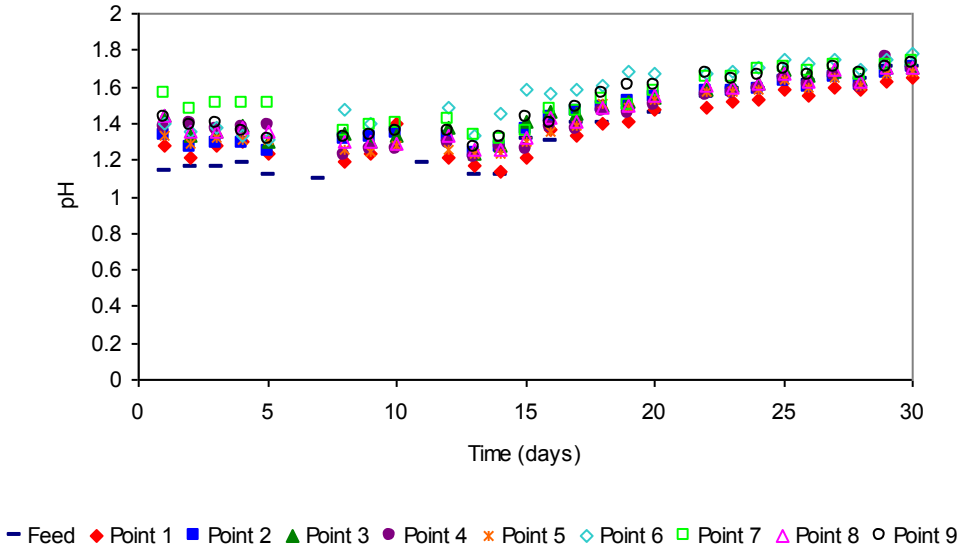

Figure 4.28: Daily eluted pH readings for elution points 1 to 9

4.3.4 Microbial attachment

The number of cells eluted over the 30 day leach period is shown in Figure 4.29. A significant decrease (92 %) in cells eluted is seen to occur on Day 2 from the inner region. This may be attributed to a high percentage of inoculum cells not adhering to the ore within the first 24 hours. This might be attributed to the growth conditions of the micro-organisms in the stirred tank reactors given in Section (3.3) and their introduction into a complete mineral environment at a high flow rate. However, some

viable cells do remain attached to the ore which would account for the slow increase in cell number due to cellular growth.

From the start of the recycle period on Day 15, an increase in cells eluted is seen to occur. However from Day 20 a decrease in cell number eluted is seen. This may be attributed to the possible entrapment of cells by the mineral precipitate. During the recycle period, from Day 19, a lower pH value is eluted from the inner region compared to that of the feed pH (Figure 4.30). This may suggest that an increased level of microbial activity within the inner region has occurred by the indication of a lower pH reading possibly through the oxidation of sulphur to sulphuric acid.

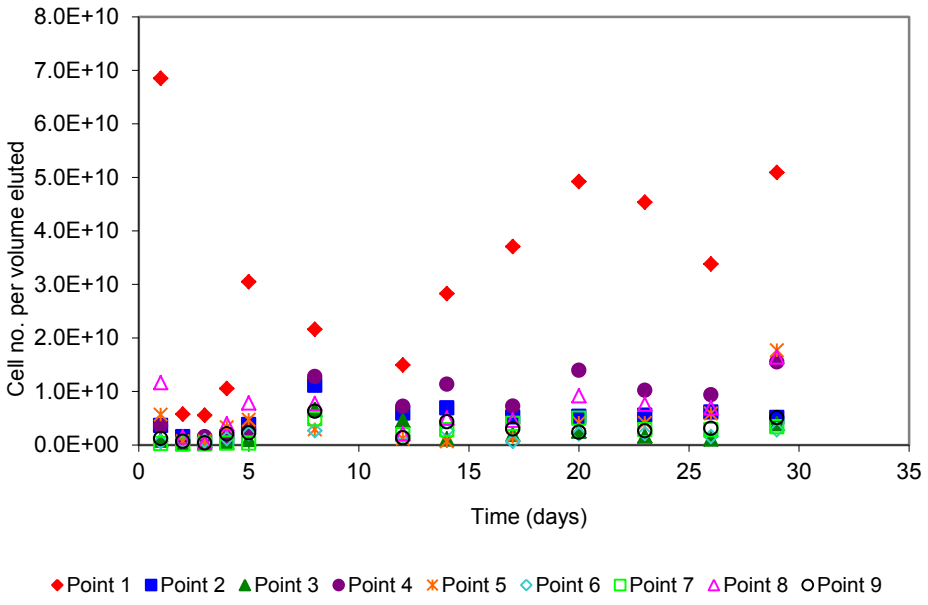

Figure 4.29: Daily cell elution profile for the duration of reactor 3 leach

Compared to reactor 4, the higher flow rate associated with reactor 3 increased the penetration of feed throughout the reactor with the resultant increase in cell attachment occurring within the middle and outer regions.

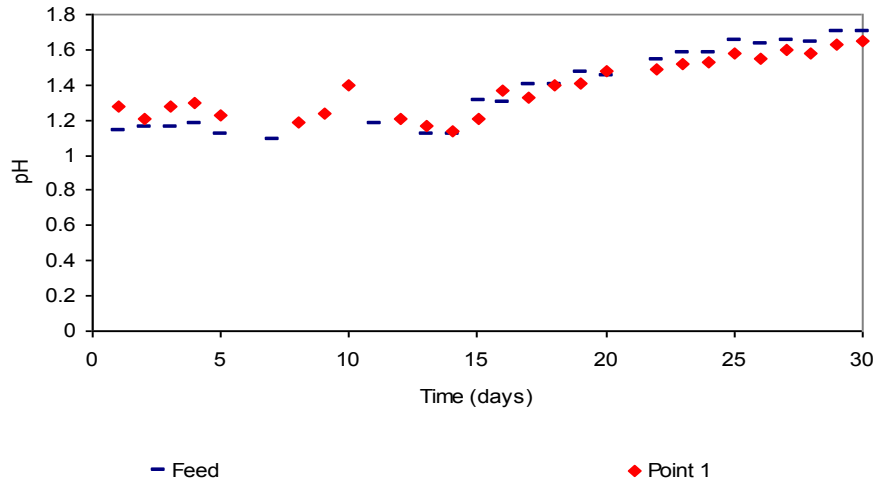

Figure 4.30: Comparison of feed and inner region pH

4.3.4 Redox potential

The redox potential of the leachate collected was measured daily and is shown in Figure 4.31. Initial redox potential readings from the inner, middle and outer elution points are lower than that of the feed. This could be attributed to the acid agglomeration of the ore and the initial chemical leaching of chalcopyrite through the oxidation of ferric to ferrous iron. The increase in the redox potential of eluted volumes above the feed redox from Day 5 may be indicative of an active microbial population.

However from Day 8 and 9 to Day 14, a drop in the redox potential for all elution points is seen to occur. This decrease in redox readings could be attributed to the rate of leaching of chalcopyrite through the oxidation of ferric to ferrous iron exceeding the rate of bio-oxidation of ferrous iron until the start of the recycle period.

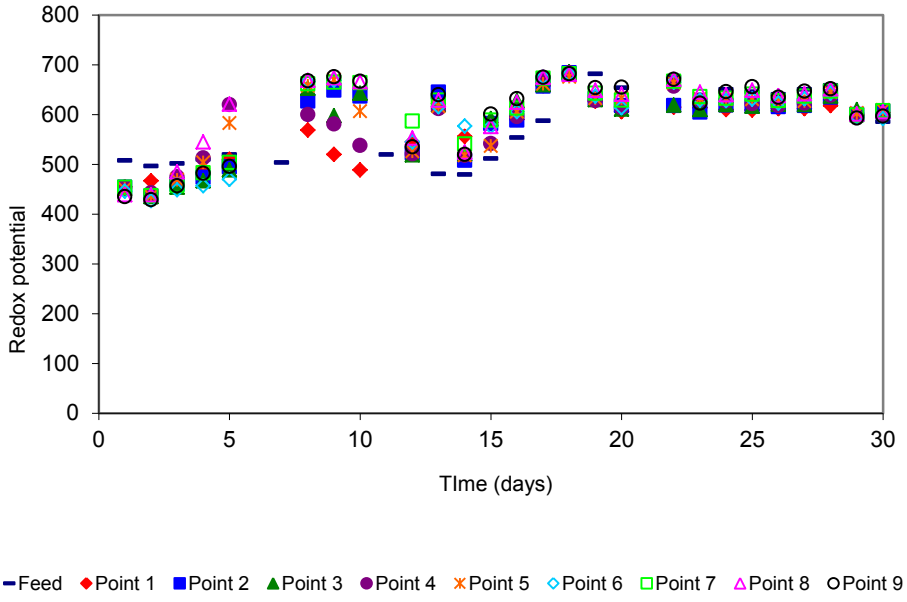

Figure 4.31: Redox potential as a function of leach time for reactor 3

At the start of the recycle period on Day 15, there is an increase in redox potential for all elution points. This is related to the recycling of the feed solution and the lack of topping up with fresh feed. From Day 20 the overall redox potential remains around 600 mV for all elution points. This may be indicative of a reduced level of chalcopyrite leaching occurring as the redox potential remains relatively stable.

4.3.5 Iron elution

The iron concentrations from the collected volumes were measured for the duration of the experimental leach of reactor 3 (Figure 4.32). From Day 2 to Day 12, a steady decline in the iron concentration is seen to occur from the inner region. This could be related to the deposition of iron species in the form of ferric hydroxide or jarosite. Conversely from Day 5 to Day 12 the iron concentrations in the middle and outer regions were seen to increase.

From the start of the recycle period on Day 15, the iron concentration for point 1 is seen to increase from 2833 mg/L to 3106 mg/L. This may be related the overall decrease in feed volume, due to evaporation, which would concentrate iron species in solution. Absence of volume correction in the recycled feed may have contributed to the increase in iron eluted as the fresh feed would have diluted the concentrated iron in the recycled feed. During the recycle period there is a general decline in the amount of iron eluted from the middle and outer regions. This may be due to the build

up of ferric hydroxide and jarosite precipitates as the average redox potential for the middle and outer regions were 624 mV and 636 mV respectively.

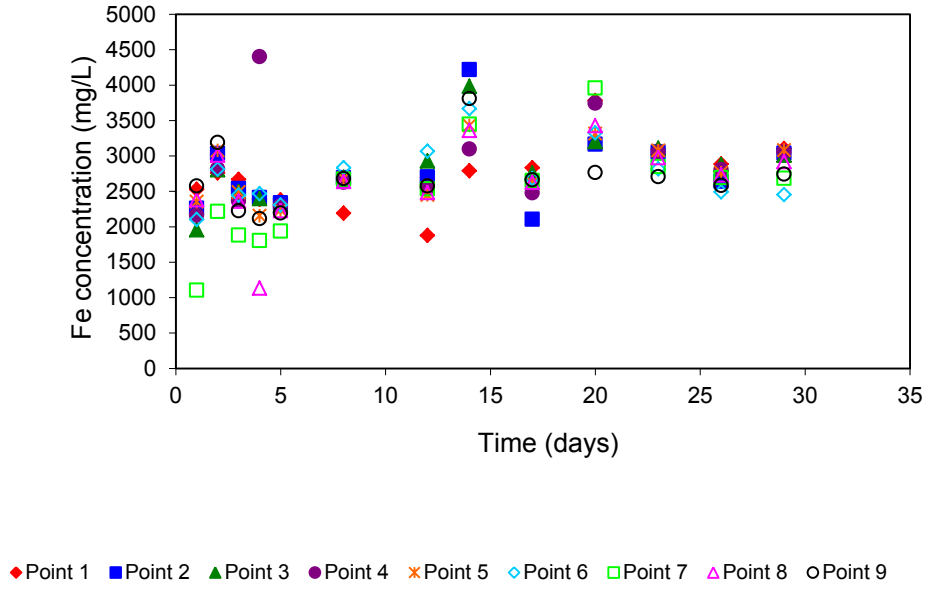

Figure 4.32: Daily iron collected from the eluted volumes of the inner, middle and outer regions

4.3.6 Copper elution

Copper concentrations in the eluent were taken from each region as shown in Figure 4.33. The decrease in copper elution for all regional points could be attributed to the initial washing out by the feed solution of soluble copper during the acid agglomeration phase of the reactor set up. This would explain the relatively high levels of copper eluted with a decline occurring from Day 2.

However up until Day 17, the copper concentration in the eluent from the outer region is greater than the inner region (Figure 4.34). This may be related to the greater area of the outer region, compared to the inner region and the increased residence time for the outer region, allowing an increased contact time between mineral and feed to occur. Thereafter the inner region is seen to have eluted more copper. This may be related to the inner region showing the lowest redox potential and pH readings than the feed and the middle and outer region elutions over this time period. This may indicate that the microbial population is actively growing and leaching chalcopyrite. This can also be correlated to the increase in the number of planktonic cells eluted over the same time period.

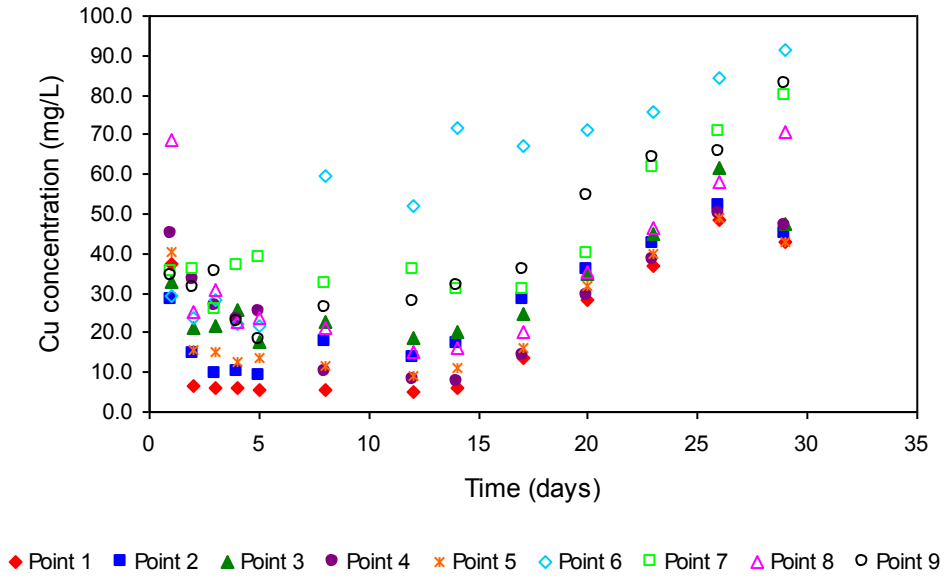

Figure 4.33: Copper leaching rate for eluted volumes collected

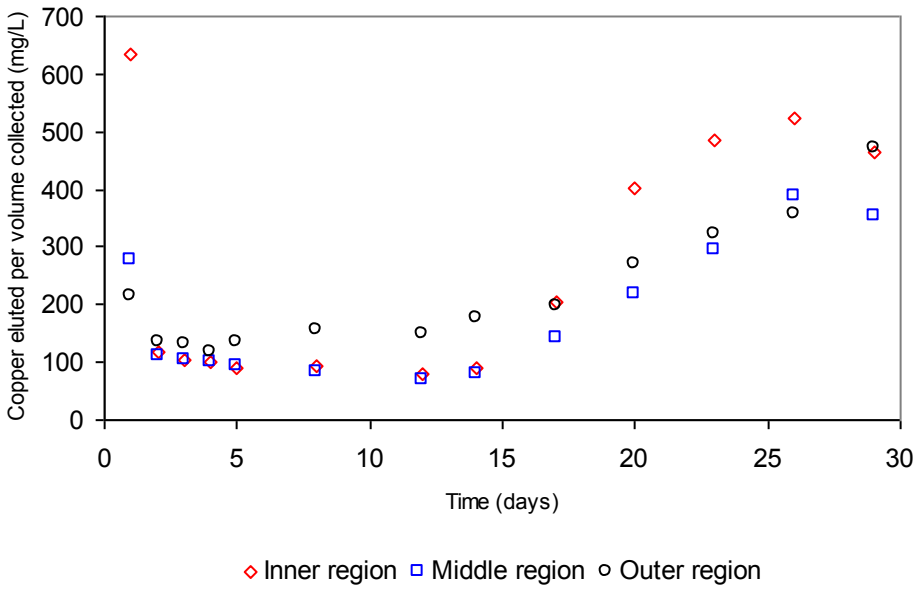

Figure 4.34: Comparison of copper leached across the radial regions

4.3.7 Post operational analysis

In the post operational analysis of reactor 3, the ore-associated cell number per region ore was determined by dislodging the bacteria from the surface of collected ore samples as described in Section 3.7.8. The attached cell number per top and bottom layer regions ore are shown in Figure 4.35 and 4.36.

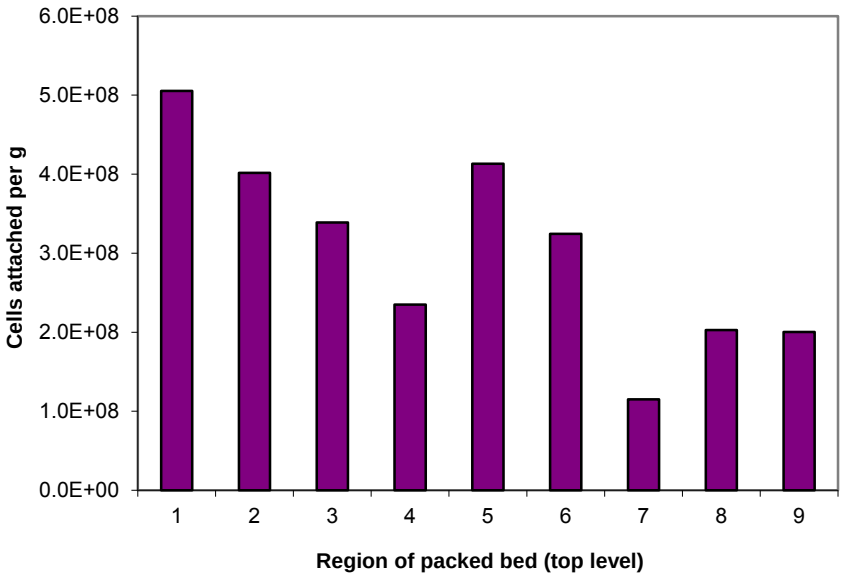

Figure 4.35: Attached cell number per gram of top layer regional ore

The highest cell concentration is seen to occur in the inner region of reactor 3 with an estimated cell number of 5.05 x 10^8 cells per gram ore. This is similar to reactor 4 where the highest cell concentration of 4.35 x 10^8 occurred within the inner region. Regional areas are also less defined in terms of cell adherence with less differentiation between the middle and outer region of the top layer. Figure 4.36 shows the cell adherence pattern for the bottom layer of reactor 3.

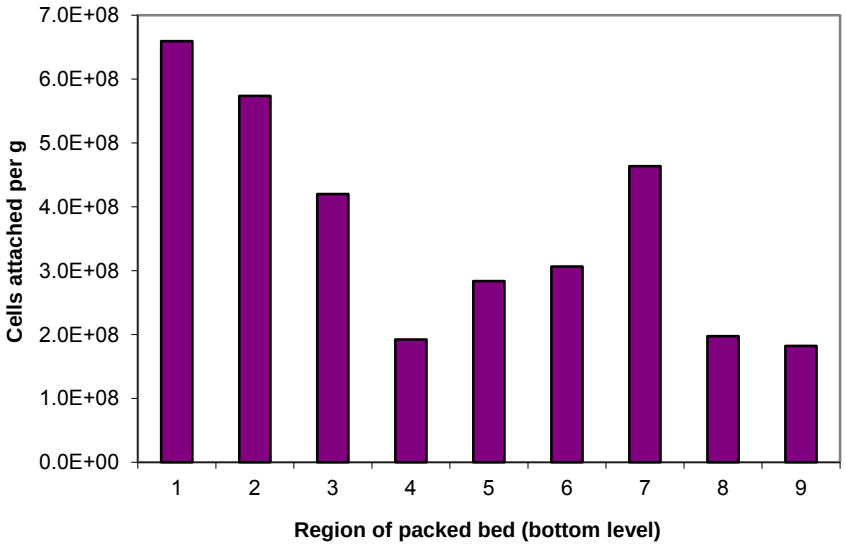

Figure 4.36: Attached cell number per gram of bottom layer region ore

A higher cell association number is seen to occur at a lower level with 6.59 x 10^8 cells per gram ore for the inner region. A greater cell association number is also seen to be found in the bottom region when compared to reactor 4. This could be due to the higher cell inoculum used for reactor 3 with two orders of magnitude.

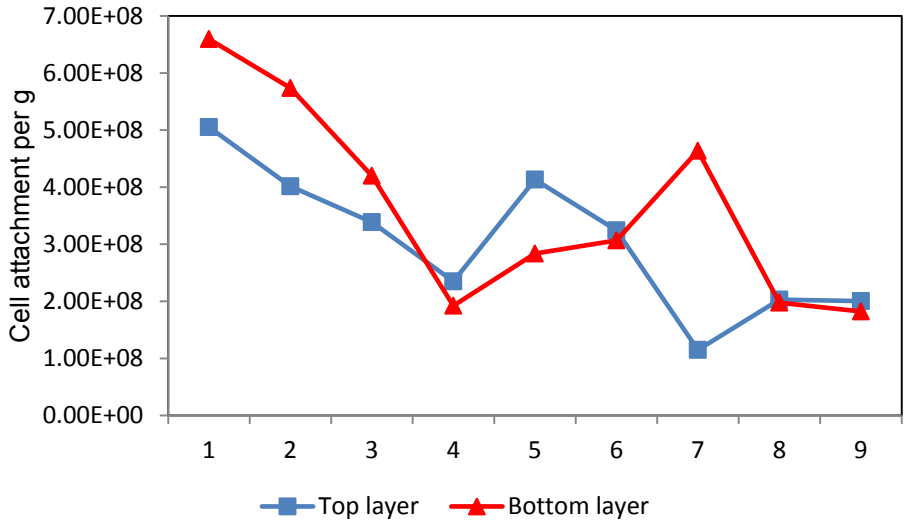

Figure 4.37: Comparison of top and bottom layer cell attachment per g ore

Figure 4.37 shows the comparison of the top and bottom layers of cells attached per g of ore. Figure 4.37 shows relatively more cells being found attached in the bottom layer of the inner region than the top layer. This could be related to the higher flow rate washing some cells of the inner region with more cells attaching when the flow rate decreased lower down the reactor.

An increase in residence time for the middle and outer regions did not correspond to an increase in cell number for these regions (Figure 4.37). This could be due to the assumption that residence time was calculated for the entire volume of that region, whilst it was shown that little microbial activity occurred in the outer top layer of the reactor. When the residence times of reactor 4 and reactor 3 were compared (Figure 4.38), residence times for reactor 3 were much less than reactor 4 which can be attributed to the higher flow rate.

On comparing the microbial populations across reactors 3 and 4 in Figure 4.38, it is seen that the population of reactor 3 is greater. This could be explained by the larger cell number of 4.91 x 10^{11} cell used to inoculate reactor 3 with compared to the inoculum of 2.62 x 10^{11} cells for reactor 4. Further the higher flow rate associated with reactor 3 may have increased liquid percolation and thereby the microbial

presence throughout the reactor which is reflected in the higher cell number found in the middle and outer regions of the ore bed when compared to reactor 4 (Figure 4.38).

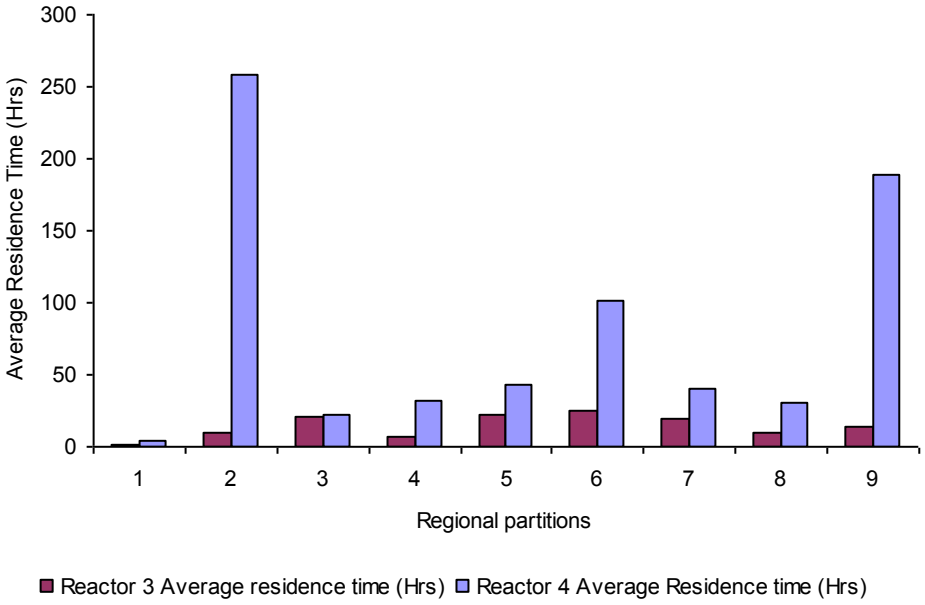

Figure 4.38: Comparison of reactor 4 and reactor 3 residence times for all regions

The comparison in cell associations is shown in Figure 4.39 at the varying flow rates. At the higher flow rate, more microbes are seen to be associated with specific regions of the ore. This could be related to the larger inoculum size used at the start of the leach of reactor 3. A greater microbial association is seen with the ore at the higher flow rate, however as leaching is mostly a kinetic process this would have little influence on the leach solution as the redox potentials for both leaches were relatively high.

Figure 4.40 compares the total daily eluted copper values for reactors 3 and 4 for a 30 day leach period. The lower flow rate of 8.64 L/hr leaches more copper than the higher flow rate of 15.5 L/hr during this period. This could be related to the diminished residence time and subsequent shortening of the mineral-liquid interaction associated with reactor 3 as shown in Figure 4.38. The higher flow rate also reduces the amount of microorganisms associated with the top layer thereby reducing any lateral microbial diffusion which may occur.

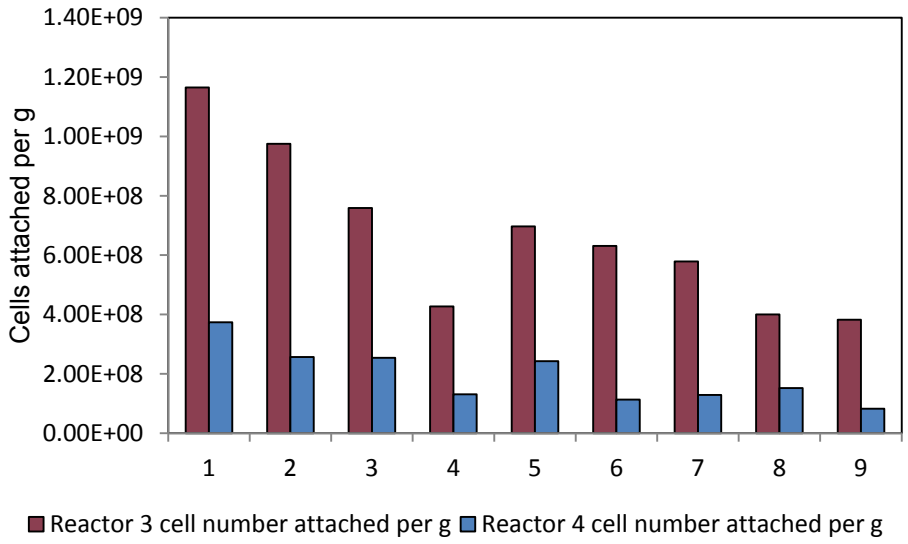

Figure 4.39: Comparison of reactor 4 and reactor 3 cell attachment numbers for all regions

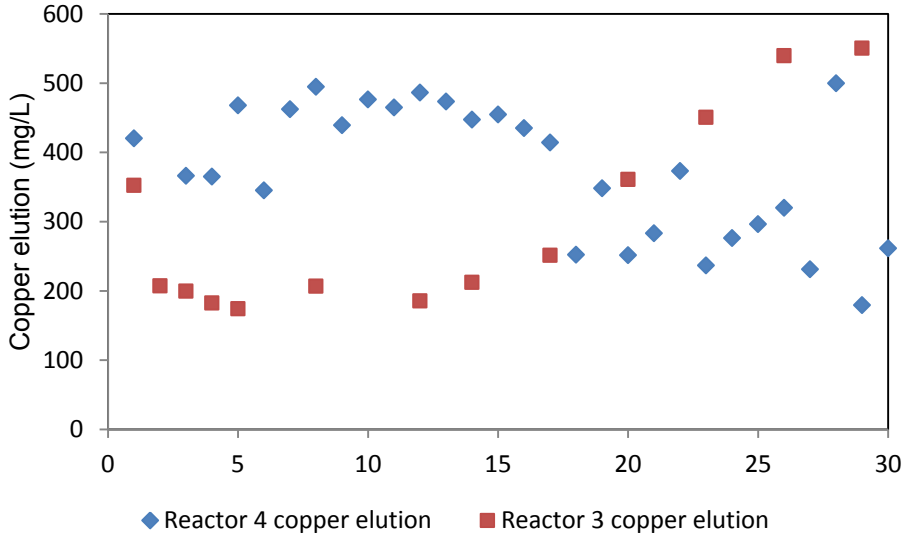

Figure 4.40: Comparison of copper elution from reactor 3 and reactor 4

4.4 Analysis of simulated heap leach 2

The reactor set-up for heap leach 2 involved a 48 hour acid washing of the ore prior to inoculation of a mixed mesophilic culture. The same feed rate as reactor 3 was used, namely 30 L per day at a flow rate of 21 ml/min. The duration of this leach was 5 days during which time the eluted volumes for each regional point were measured for pH, redox potential, ferrous iron, total iron, copper and planktonic cell number.

4.4.1 Volume elution

The volumes eluted for reactor 2 over the 5 day period are shown in Figures 4.41 and 4.42. As can be seen, the volume elution profile tends to be region specific with the inner region eluting 35 % and the outer region eluting 4 % of the total. However on Day 1, points 3 and 4 from the middle region have higher elution volumes than point 1. The increase in the inner region elution on Day 2 may be attributed to the settling of the ore and the development of flow channels. The settling of ore was also seen to have affected the elution from point 5, as after Day 1 elution stopped from this point. This point was visually seen to be blocked by loose ore which was probably impeding liquid flow. Little lateral diffusion is seen to occur from the inner region due to the relatively short duration of this leach. The initial uneven elution profile as shown by points 1, 3 and 4, when compared to that of reactors 3 and 4 may be explained by the uneven setting of reactor 2. This would explain the preferential volume elution through points 3 and 4 as the reactor tilted towards those points. This is supported by Figure 4.42, whereby the total volume eluted from the middle region was consistently higher than that of the inner region which does not hold with the volume elution profiles seen for reactors 3 and 4. The reactor base was corrected and stabilised for heap leach runs 3 and 4.

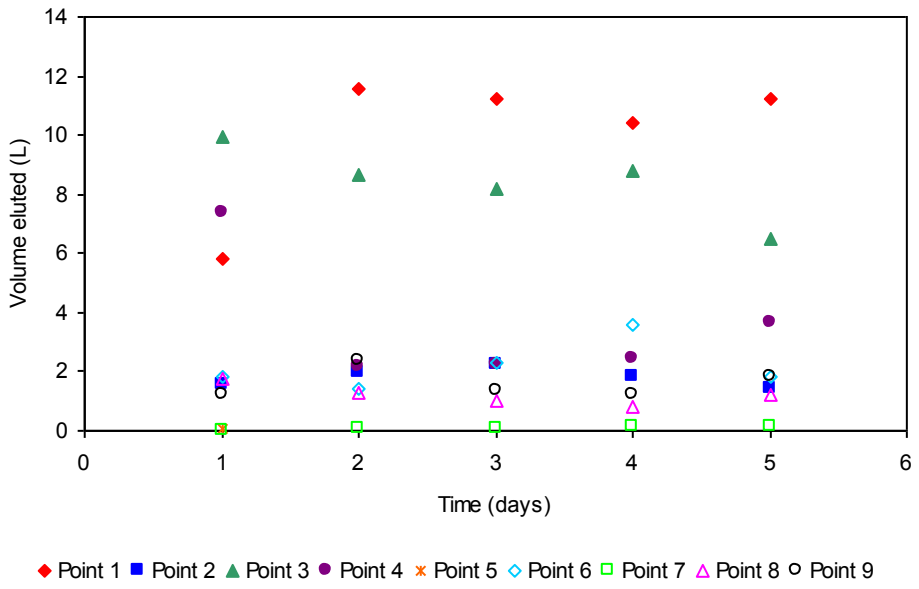

Figure 4.41: Daily volume elution from inner (point 1), middle (points 2-5) and outer (points 6-9) region

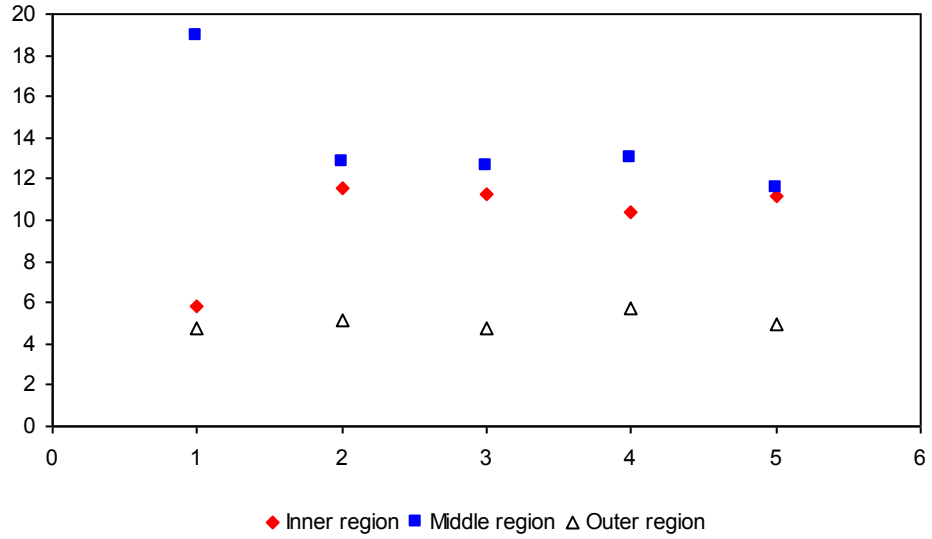

Figure 4.42: Total volume eluted for inner, middle and outer regions from Day 1 to 5

4.4.2 Residence time

The residence time data for reactor 2 is shown in Figures 4.43 and Figure 4.44 representing the low and high residence times associated with this leach. Figure 4.43 shows points 1, 3 and 4 having the lowest residence times which are in contrast to the residence times of reactor 3, where the lowest residence time was from the inner region.

However the unusual elution profile for reactor 2 resulted in exceedingly high residence times for points 5 and 7 (Figure 4.44) of 266 and 1589 hours on Day 1 respectively. These values well exceed the highest residence time of 109 hours for reactor 3 and indicate that preferential solution channelling is occurring away from these points. These are the highest residence times recorded for all four leach runs. It can be assumed that the increase in volume elution for points 1, 3, and 4, resulted in the loss of inter regional solution transfer for points 5 and 7 with their resultant high residence times.

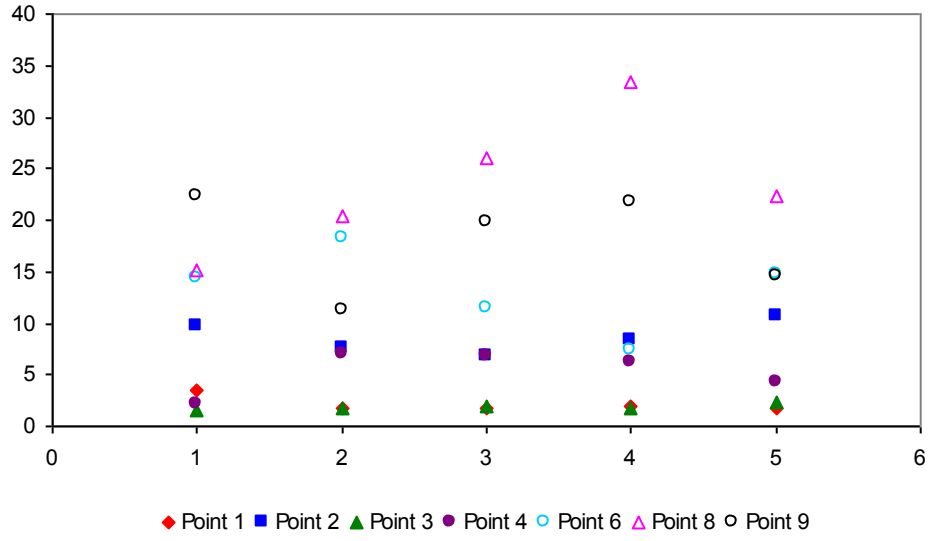

Figure 4.43: Low residence times associated with reactor 2

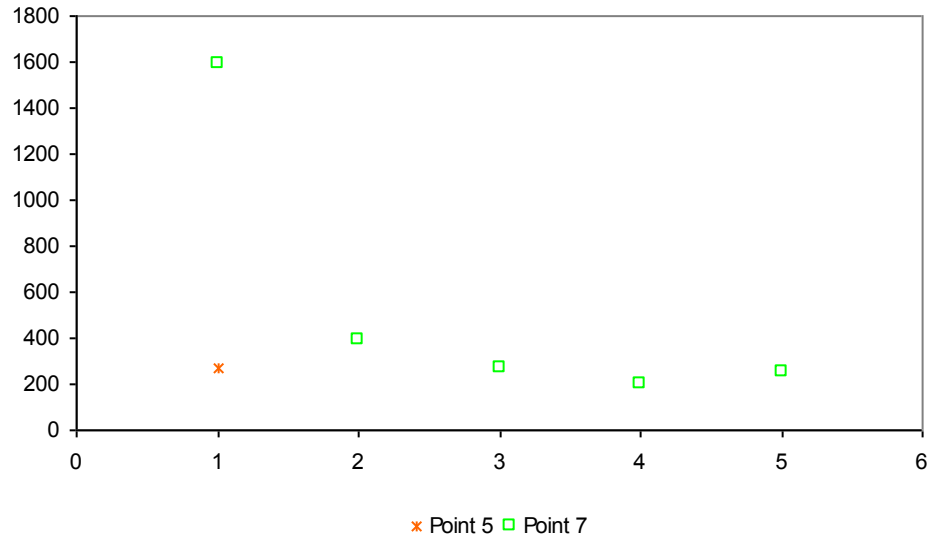

Figure 4.44: High residence times associated with reactor 2

4.4.3 pH analysis

The pH data from reactor 2 is presented in Figure 4.45. Two acid washes were conducted on reactor 2 after the agglomeration and packing of the ore into the reactor. This contributed to the initial low pH readings seen on Day 1.

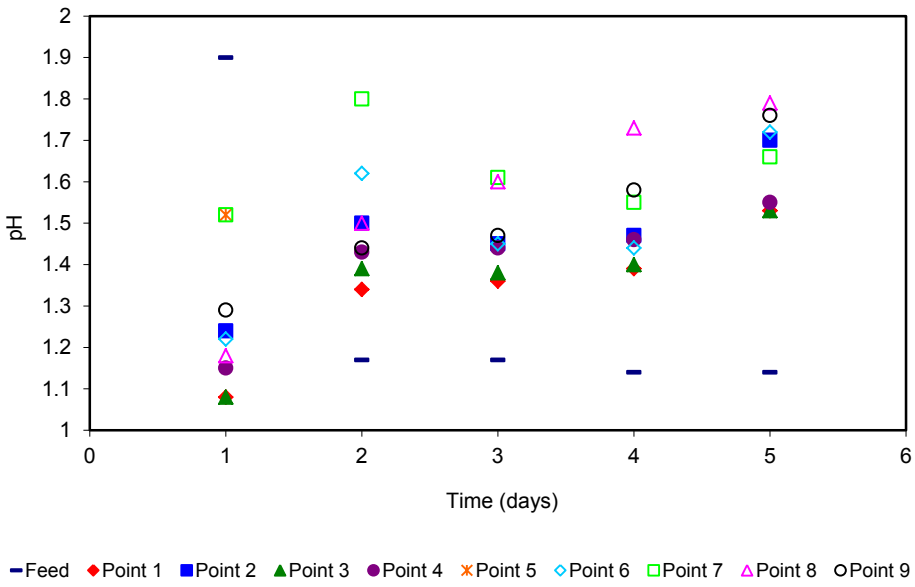

Figure 4.45: Daily eluted pH readings for elution points 1 to 9

In reactor 3, no region exceeds pH 1.6 until the start of the recycle period. However for reactor 2 (Figure 4.45), points 6 and 7 reach pH 1.62 and 1.80 on Day 2 respectively. These high pH readings may be related to the feed pH being incorrect on Day 1. However, the pH values for all the regions increase from Day 2 until the end of the leach, even when the feed pH is rectified on Day 2. The increase in pH for all regions for reactor 2 is uncertain.

4.4.4 Microbial attachment

The numbers of daily eluted cells from each region for reactor 2 are shown in Figure 4.46. Initial cell elutions from points 1, 2 and 3 on Day 1 are low, possibly due to rapid adhesion by microbes and a relatively low inoculating population of 3 x 10^{11} cells compared to reactor 3 (5.46 x 10^{11}). From Day 3 an increase in cell number is seen to occur for all these elution points.

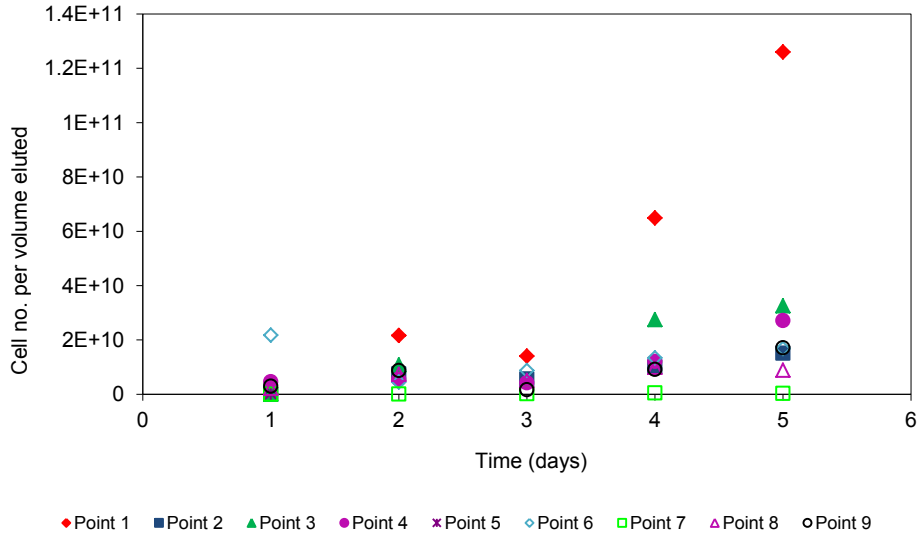

Figure 4.46: Daily elution profile for reactor 2

4.4.4 Redox potential

The redox potential was measured daily for the collected leachate and is shown in Figure 4.47. Initially the redox potential for eluting volumes is below that of the feed which may be indicative of low microbial activity, specifically a lower rate of microbial oxidation of ferrous iron than ferric leaching of sulphidic ore. This may be due to the adaptation of the micro-organisms to the new mineral environment. It may also be indicative of chemical leaching occurring due to the acid washes. However by Day 5, the redox readings for all collected volumes are above that of feed redox potential, indicating increasing microbial activity.

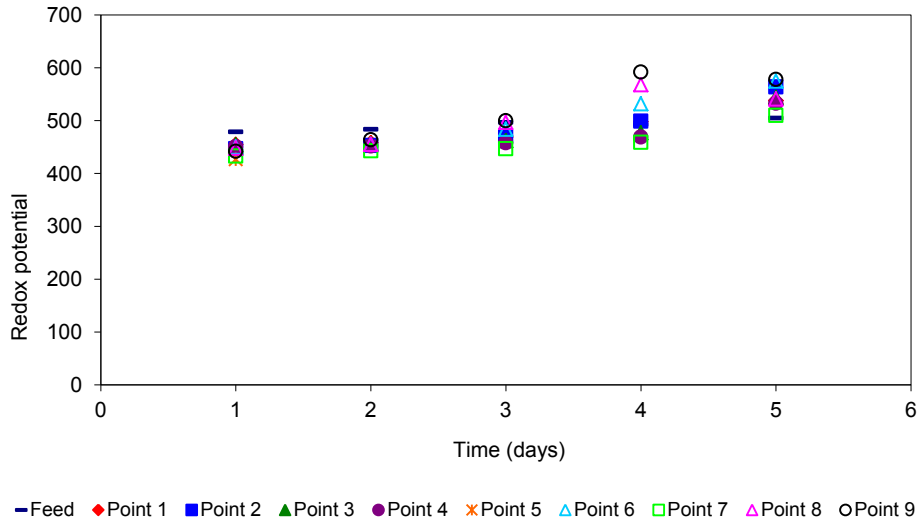

Figure 4.47: Redox potential readings for reactor 2

4.4.5 Iron elution

The iron concentration eluted from reactor 2 was measured on a daily basis and is shown in Figure 4.48. A greater proportion of iron is seen to have been eluted from points 3 and 4 than point 1 on Day 1. This may be attributed to the greater volume eluted through these points. However, the total iron released from reactor 2 (366 g) and reactor 3 (360 g) are similar, which may indicate that the influence of the 48 hour acid wash prior to the leach of reactor 2 had a negligible impact on the iron solubility of reactor 2.

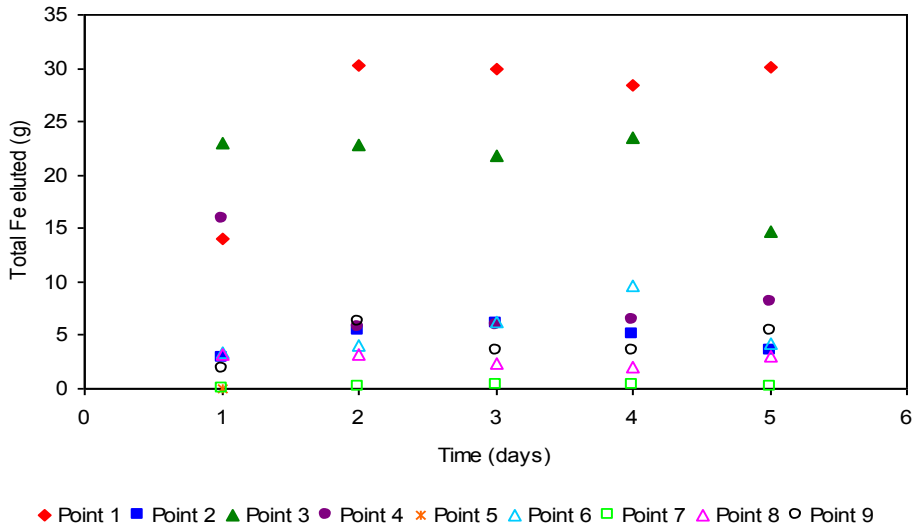

Figure 4.48: Daily iron collected from the eluted volumes of the inner, middle and outer regions

4.4.6 Copper elution

Copper concentrations in the collected eluent from reactor 2 were taken from each region as shown in Figure 4.49. Points 3 and 4 are seen to have the highest concentrations of copper eluted on Day 1. From Day 2, point 1 has the highest copper concentration eluted and remains so until the end of the 5 day leach period. The copper leached through region 3 remains similar to region 1 throughout this period. The combined copper elutions from points 1, 3 and 4 of 555 mg Cu, were similar to that of the copper eluted from point 1 in reactor 3 (633 mg). This might be due to the lower copper concentration remaining in the ore due to the 48 hour acid wash.

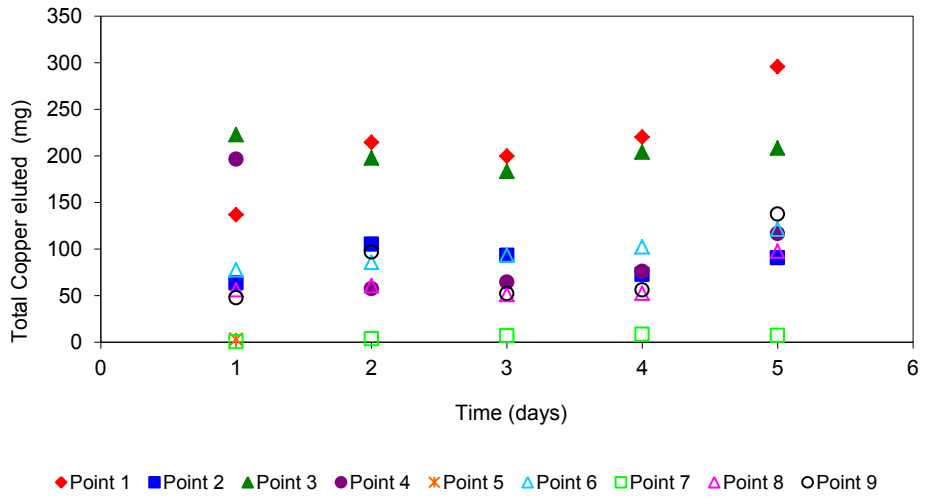

Figure 4.49: Daily copper collected for total eluted volumes

4.4.7 Post operational analysis

In the post operational analysis, the ore associated microbial population on a regional basis was estimated and is shown in Figure 4.50. The attached cell number per region ore was determined through a series of liquid vortexes and Tween washes as described in Chapter 3.7.8. The highest cell concentration is seen to occur from the inner region. Point 5 is seen to have the second highest cell concentration which could be attributed to the high residence time. However, point 7 has the highest residence time of 1589 hours with the fourth lowest cell concentration. This could be due to the excessively low % volume of liquid passing through point 7 of 0.3 %. As the reactor was not even, the use of point 5 volume eluted was excluded due to the biased results it would give.

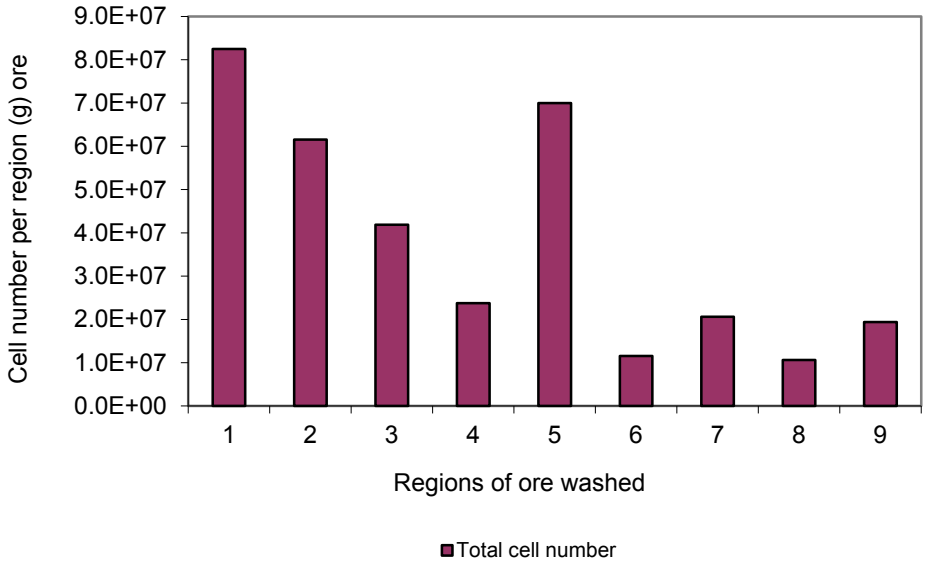

Figure 4.50: Adhered cell per region sample of ore collected

4.5 Analysis of simulated heap leach 1

The reactor set-up for heap leach 1 involved a 24 hour feed wash prior to the inoculation of a mixed mesophilic culture and start-up of the leach run. A flow rate of 1.5 ml/min or 90 ml/hr was used for reactor 1. When the surface area of the reactor was included and the area up scaled to 1 m^2 the flow rate corresponded to 1.12 L/hr/m^2. This falls below the industry standard of 5–6 L/hr/m^2 (Petersen & Dixon, 2003) and is considered a very low flow rate. The duration of reactor leach 1 was 15 days, during which time the collected leachate was analysed for volume, pH, redox potential and copper.

4.5.1 Volume elution

The volumes eluted for reactor 1 over the 15 day leach period are shown in Figure 4.51. Due to the low flow rate, intermittent volume elution is observed with point 1 being the only region to have eluted consistently during this period. The highest volume elution is seen to occur from point 1. Little lateral diffusion is seen to occur from point 1 as evidenced by the low and intermittent volume elutions from the middle and outer regional points.

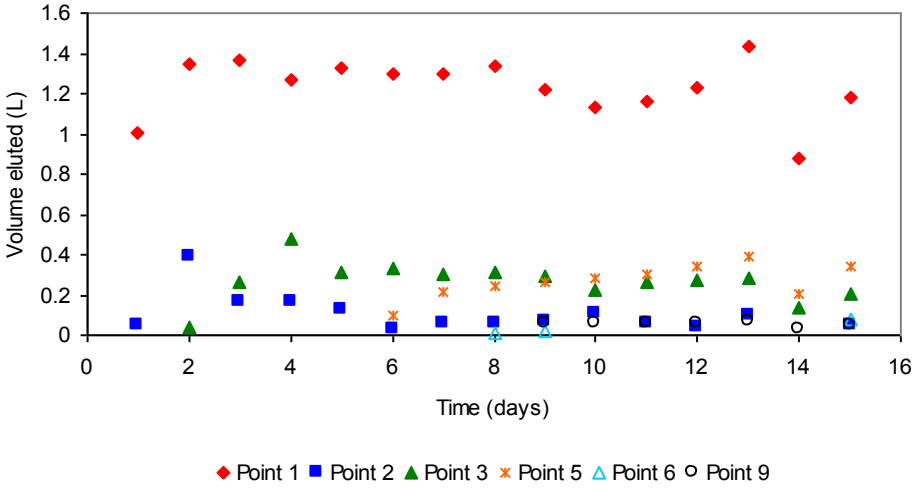

Figure 4.51: Daily volume elution from inner (point 1), middle (points 2, 3, 5) and outer (points 6, 9) region outlet points

The total volume eluted on a daily basis per region is shown in Figure 4.52. The volume elution profile tends to be region specific with the inner region eluting 68% and the outer region eluting 2 % of the total.

From Day 8 the outer region started to elute. This may be attributed to the low flow rate which may have reduced the lateral transference/diffusion of liquid from the inner region. It was also noted that from Day 14 a yellow sulphurous precipitate had formed around the exterior elution points of 2 and 6. This precipitate may have been the cause for the intermittent elution flow for these points. On Day 14, the precipitate covering these points was removed, whereupon immediate elution occurred suggesting a build of liquid around this point on the inside of the reactor.

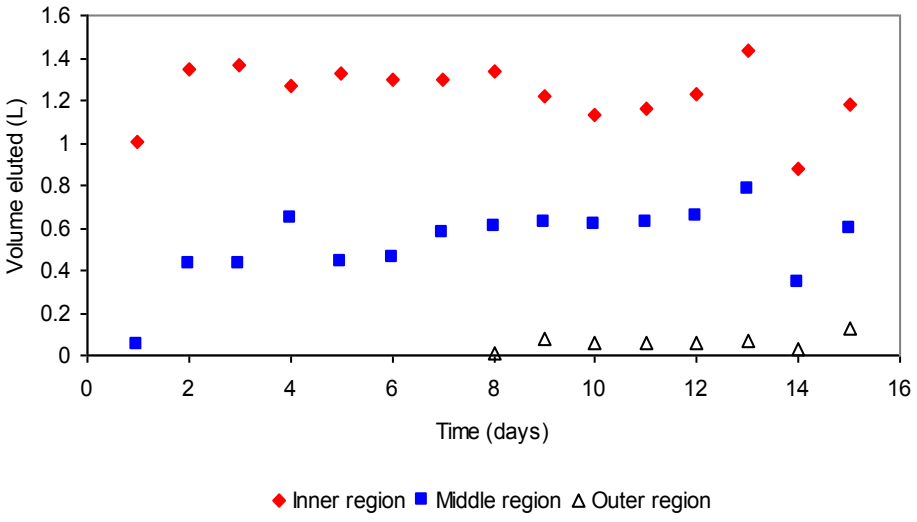

Figure 4.52: Total volume eluted for inner, middle and outer regions from Day 1 to 15

4.5.2 Residence time

The residence time data for reactor 1 is shown in Figure 4.53. The lowest and highest residence times are associated with the inner region and the outer region respectively. The highest residence time was recorded on Day 8 from point 6 with a residence time of 2413 hours. Average residence times for the four reactors are shown in Table 4.15.

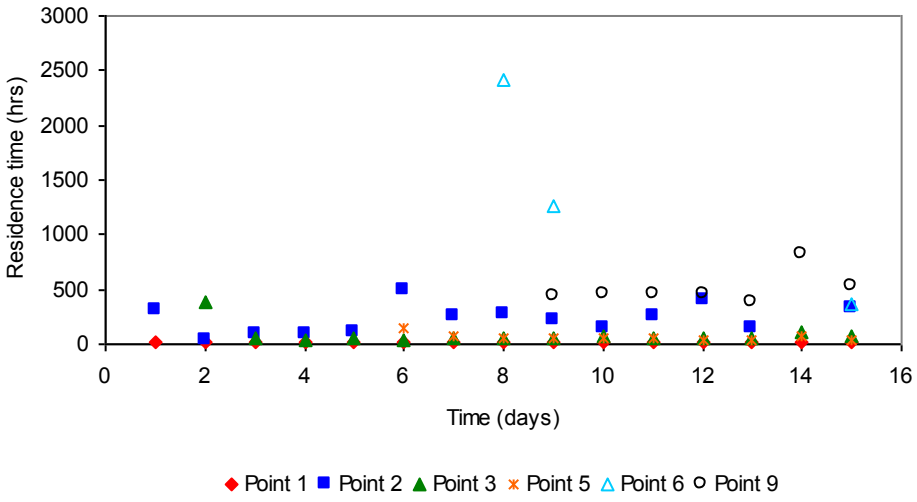

Figure 4.53: Residence times associated with elution points within the inner, middle and outer regions of reactor 1

Table 4.15: Average residence times for reactors 1 to 4

	Inner region	Middle region	Outer region
Reactor 4	5.5 hrs	83.3 hrs	139.8 hrs
Reactor 3	1.4 hrs	13.1 hrs	25.7 hrs
Reactor 2	2.2 hrs	21.6 hrs	148.5 hrs
Reactor 1	16.7 hrs	130.5 hrs	756.8 hrs

4.5.3 pH analysis

The pH elution profile data for reactor 1 is shown in Figure 4.54. A 24 hour wash of the acid agglomerated packed ore by feed solution commenced prior to the start of the leach run.

Figure 4.54 shows a relatively region specific pH profile with the inner region eluting the lowest pH and the outer region, towards the end of the leach, eluting the highest pH values. These data points follow a trend where a high residence time led to high

pH regardless of whether the ore was washed through with acid over a 48 hour period or with feed over a 24 hour period. These high pH regions may have contributed to the deposition of jarosite as was seen around points 2 and 6 towards the end of the leach.

The relatively high pH readings associated with reactor 1 can be attributed to the relatively low flow rate. This assumption is based on the data collected from reactors 2 to 4.

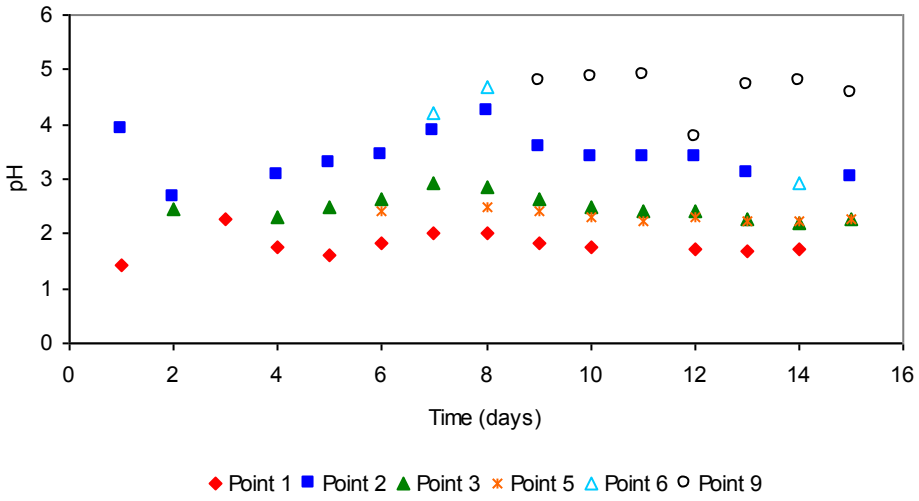

Figure 4.54: Daily eluted pH readings for inner, middle and outer region points

4.5.4 Microbial attachment

The cells eluted for reactor 1 daily are shown in Figure 4.55. Initial cell concentrations are the highest from points 1 and 2. The cell inoculum was the highest out of all four leaching runs with a total cell concentration of 1.52×10^{12}.

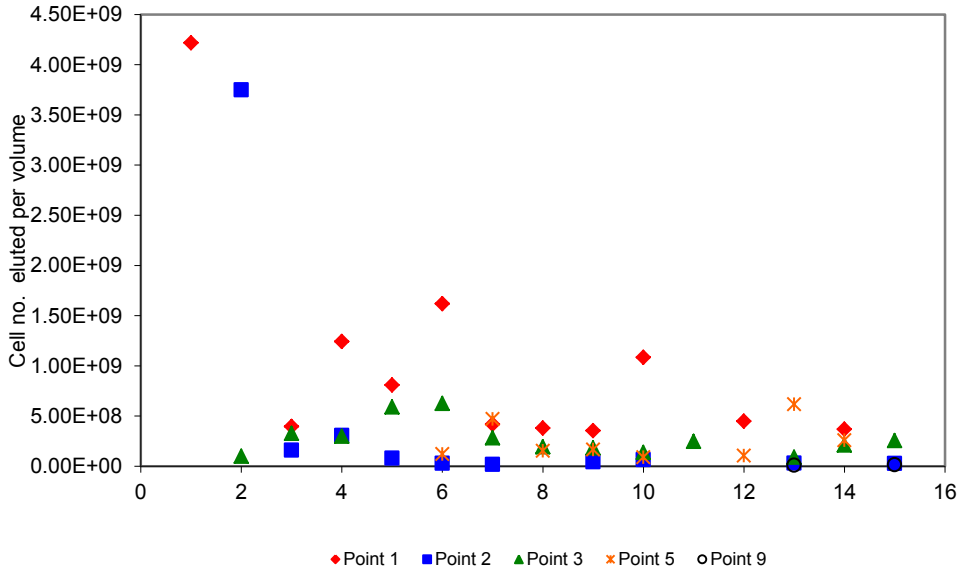

Figure 4.55: Daily cell elution profile for the leach run of reactor 1

4.5.5 Redox potential

The redox potential for reactor 1 was measured daily and is shown in Figure 4.56. The initial redox potential for all eluting points is seen to be below that of the feed. Reactor 1 has some of the initial lowest redox readings from points 1 and 2 of 259 mV and 176 mV respectively. These are the lowest redox potential readings recorded when compared to reactors 2, 3 and 4 over the first two days. These low readings may be attributed to the long initial residence times of liquid associated with points 1 and 2 and be a result of chemical leaching due to the extended interaction of ore with feed. The increase in redox potential is also rapid with most regions reaching 600 to 700 mV by Day 4, indicating good microbial activity. Unexpected low redox potential values for points 2, 6 and 9 were encountered, with regions 2 and 6 experiencing intermittent flow due to blocked points, from which anomalies in readings could be expected.

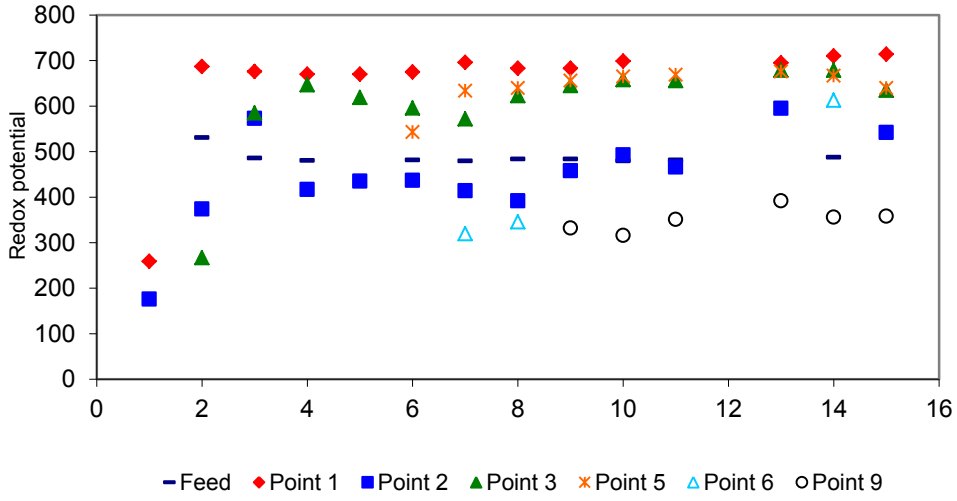

Figure 4.56: Daily redox readings for reactor 1

4.5.7 Copper elution

Daily copper readings were taken from the collected leachate and are shown in Figure 4.57. The highest copper values of copper are seen to be eluted from the inner region, with the outer region points, 6 and 9 eluting the least.

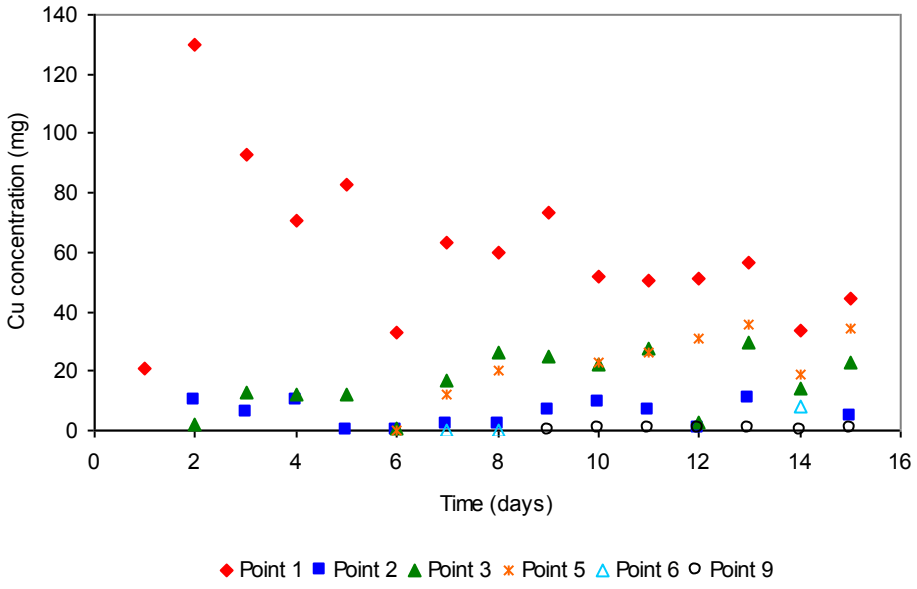

Figure 4.57: Daily copper concentrations eluted from the inner, middle and outer regions

A comparison between copper leached from reactors 1 to 4 is shown in table 4.16.

Table 4.16: Comparison of daily eluted Copper (mg) elutions per total volume for reactors 1 to 4

	Reactor 1			Reactor 2			Reactor 3			Reactor 4		
Day	I.R	M.R	O.R	I.R	M.R	O.R	I.R	M.R	O.R	I.R	M.R	O.R
1	20.6			136.8	485.9	181.8	633.3	277.2	214.4	393.5	80.5	30.3
2	150.8	12.1		214.6	360.3	246.6	116.8	109.4	136.5			
3	243.7	31.5		199.7	341.1	203.7	102.8	104.3	132.1	192.5	46.7	34.1
4	314.0	54.0		220.1	352.8	219.4	101.9	99.5	117.4	114.5	68.1	41.8
5	397.0	66.4		295.7	415.5	363.5	90.4	94.9	133.5	121.8	84.9	56.2

4.6 Analysis of scanning electron microscope

The morphology of the microbial cultures was determined using the SEM protocol as described in Section 3.7.7. Figure 4.58 and 4.59 show the morphology of a sample taken from the bioreactor of *At. ferrooxidans* and a magnification of complex biofilm found beneath the dripper in reactor 4. Further analysis is required to determine the extent of organic and mineral precipitate within this biofilm.

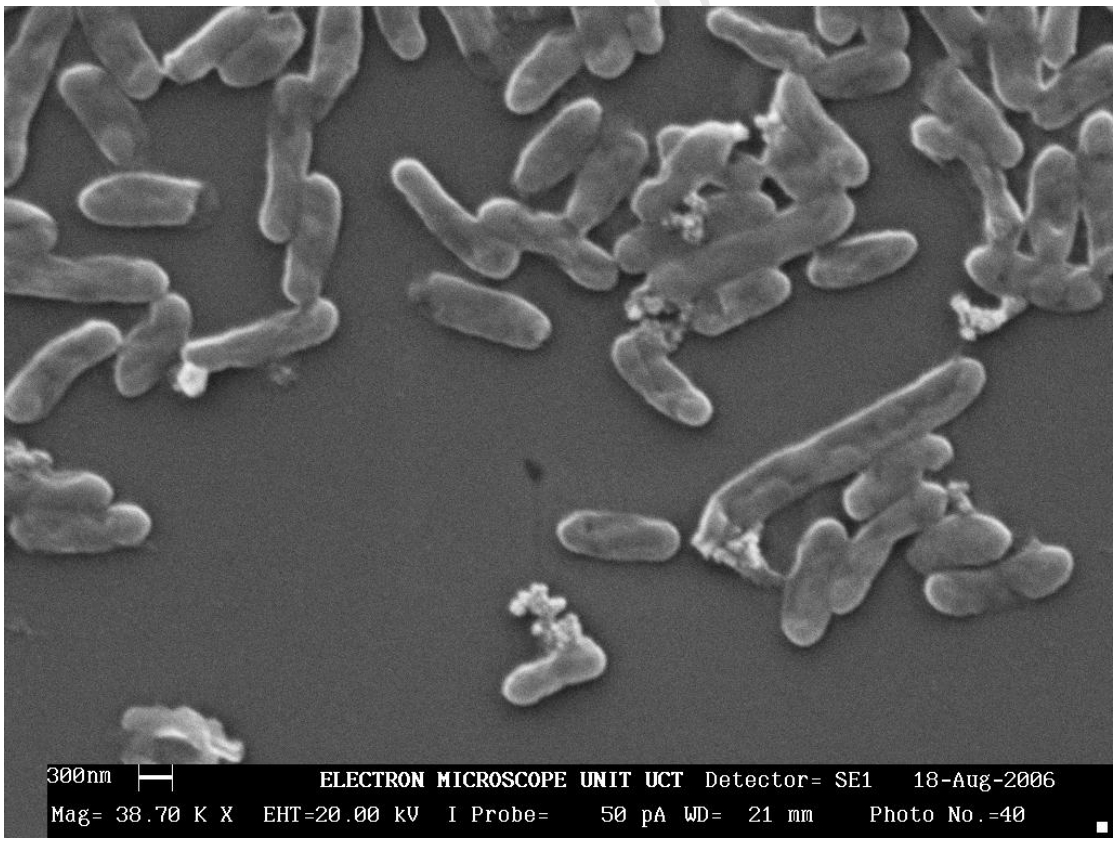

Figure 4.58: Sample of *At. ferrooxidans* taken from bio - reactor

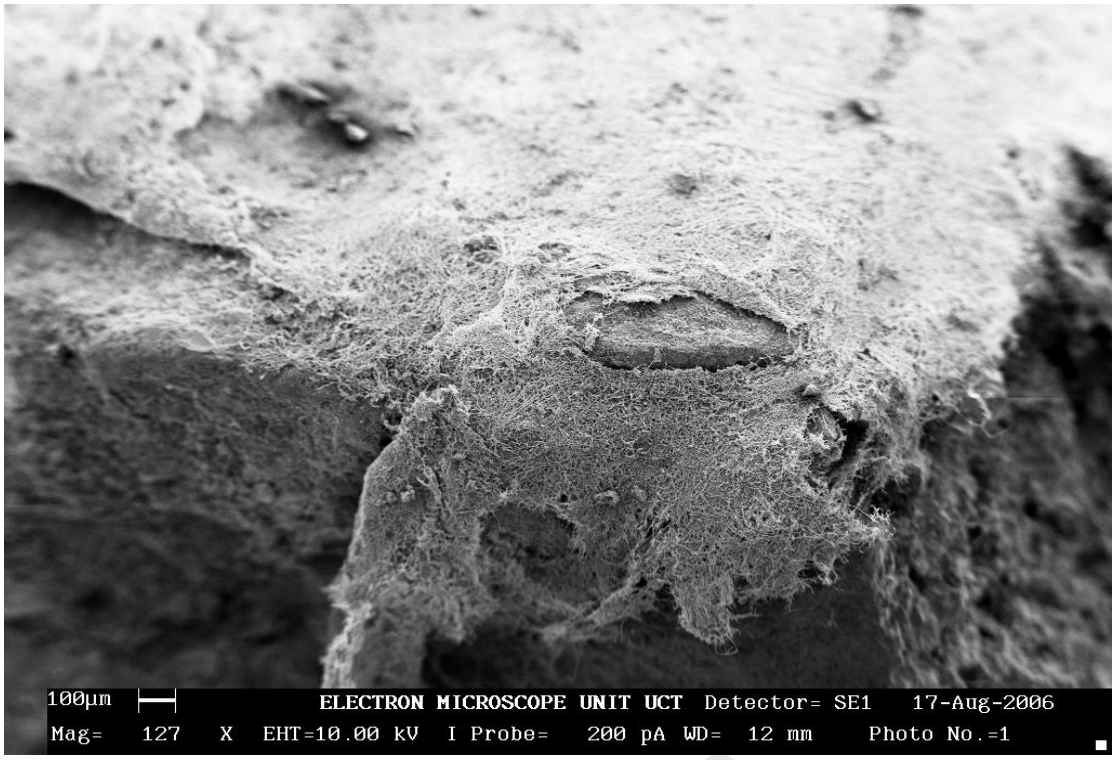

Figure 4.60: Magnification of bio-film from reactor 4.

5. Conclusion

The review of literature on the ability of bioleaching microorganisms to colonise an ore bed and the associated microbial ecology reveals that this has been little studied. It forms and important area for further research in optimising heap bioleaching.

Small scale studies of attachment to the mineral concentrate showed that the elution with a 10X basal salts concentration failed to remove a significant proportion of bacteria following their adsorption, with a cell detachment percentage of less than 13%. The results suggested a significant majority of the cells (up to 90 %) were retained in the columns and a significant portion of these are displaced by slurrying the mineral concentrate with the detergent Tween 20. However, in many cases good closure of the cell balance could not be achieved. Typically the number of cells counted exceeded the initial inoculum. The analysis of the chalcopyrite ore identified a small number of bacteria associated with the ore ($\pm 10^5$ cells/g) which could not account for the significant excess measured. The method of direct cell counting, particularly in the presence of small ore particles which often appear motile, was recognised to have introduced a large experimental error. In order to overcome inaccuracies, a new experimental approach was developed. Further study was carried out using a packed bed environment and refined experimental approach.

In the next phase of this work, a simulated heap leach was constructed using an ore bed to investigate microbial colonisation. A number of variables such as flow rate, recycle time and leach period were intorduced. These simulated heap leaches were repeated four times with changes in flow profiles investigated.

With irrigation from a single drip point, a conical flow pattern characterised the passage of liquid through the simulated heap leaches with differing flow rates influencing the lateral diffusion. At a high flow rate of 15.5 L/m^2/hr, the majority of liquid (53 %) passed through the inner region of the bed with comparatively little lateral diffusion seen to occur into the middle (14 %) and outer (30 %) regions. This lack of lateral diffusion can be related to the relatively short residence time of the liquid feed. At a lower flow rate of 5.5 L/m^2/hr, 49 % of liquid eluent passed through the inner region with a corresponding increase in the lateral diffusion of liquid to the middle and outer regional, with elution outflow percentages of 24 % and 27 % respectively. The higher percentages eluted from the middle and outer regions can be attributed to the higher residence times within the bed, with a greater mineral-

liquid contact occurring and lateral transfer. The increased lateral diffusion allowed for the ore to reach relative saturation by day 8 for the 5.5 L/m^2/hr flow rate compared to that of the higher flow rate of 15.5 L/m^2/hr which reached relative saturation by day 14. At the lowest flow rate of 1.12 L/m^2/hr, liquid flow eluted primarily via the inner region (69 %). The middle and outer regions experienced intermittent elution profiles which gradually decreased with a corresponding increase in the inner region's outflow. This was attributed to the build up of jarosite in the middle and outer regions which restricted flow.

The differences in flow rates through the bed associated with differing irrigation rates influenced the pH of the liquid eluents and by inference the pH within the bed. A relationship between residence time and liquid pH eluted was established where an increase in contact time between the slow weathering acid consuming mineral and liquid increased the pH of the eluent. At the relatively high flow rate of 15.5 L/m^2/hr, the eluent pH was relatively low (< 2.7) for all elution points while that of the low flow rate of 1.12 L/m^2/hr had a broad pH range extending from pH 2 to 5. This may have accounted for the formation of jarosite associated with this reactor as the rate of jarosite formation increases above pH 2.8.

An increase in redox potential is indicative of microbial activity oxidizing ferrous iron in solution at a greater rate than the reduction of ferric iron via mineral leaching. A high flow rate of 15.5 L/m^2/hr had a longer lag phase to reach the redox potential range of 600 to 700 mV. This could be attributed to the fact that at the higher flow rate the mass of ferrous iron entering the reactor was greater than the initial microbial population could oxidize completely within the reduced residence time. Only when significant microbial growth had occurred was complete oxidation of ferrous iron observed. The lower flow rate of 5 L/m^2/hr had a comparatively short redox potential lag phase with more consistent readings in the range of 600 mV for all regional elution points. The longer residence time allowed for a comparatively sized microbial population to oxidize more of the iron in the feed.

The amount of iron decreased during the recycle period where iron precipitation, in the form of ferric hydroxide or jarosite, was seen to have formed. This precipitate impeded solution flow and in some cases induced channel formation, which created some anomalous readings. The deposition of iron from solution can be related to the increase in the eluent pH and the consistently high ferric concentration. This is shown to be a valid explanation as at the end of each recycle period, which was characterised by the addition of non-recycled feed, a sharp increase in iron elution is seen which is due to the dissolution of some of the iron precipitate.

The initial elution of copper was relatively high for all reactors which could be attributed to the acid leaching. The rate of copper leaching was shown to be related to flow rate, residence time and cell population. At a high flow rate of 15.5 L/m^2/hr the total copper released was greater than at a flow rate of 5 L/m^2/hr. This relationship can be related to the duration of mineral-liquid contact. During the recycle phase, copper leaching continued, but at a decreased rate. The decrease in copper recovery was attributed to the reduction in iron concentration and the affinity copper had for adsorption to jarosite. Some copper was released upon the introduction of fresh feed which partially dissolved the ferric mineral precipitate. The balance between flow rate and residence time needs to be considered from a processing perspective, as to what would be the most beneficial for on-site operating needs

The pattern of microbial colonisation appeared to follow that of solution flow during the first 24 hours and was characterised by an initial weak attachment between the mineral and planktonic microbes as significant cell numbers were observed in the eluent for the first days after inoculation. This pattern of colonisation persisted for the duration of the experiments. The higher flow rate of 15.5 L/m^2/hr eluted the most cells initially while the low flow rate 1.12 L/m^2/hr eluted the least. The constant elution of cells over the varying leach periods is assumed to be due to microbial growth. The fate of attached cells needs to be investigated further.

The post operational analysis of the ore revealed microbial attachment following liquid flow patterns, with a greater number of cells associated with the inner region of the top layer, with the cell loading decreasing downwards and outwards. This was less evident at the higher flow rates, where distribution between the top and bottom halves was more evenly distributed.

The recycling of the high redox potential feed solution selected against the persistence of *At. ferrooxidans*. This was confirmed by the 16s gene restriction fragment analysis which indicated the dominance of *L. ferrooxidans* upon completion of the experimental runs.

In summary, it has been shown that the initial microbial attachment appears weak, with significant, but decreasing cell numbers in the eluent in the first days after inoculation. After this a relatively steady, low cell concentration is observed, most likely due to cell growth. The pattern of cell loading at the end of the experiments mimicked that of the inoculum flow, suggesting that weak initial attachment is important in determining colonisation patterns. Recycling of the feed solution led to

an increase in pH and a significant reduction in soluble iron concentration. Copper recovery was reduced during this period as a result of the reduced ferric concentration, passivation of the mineral surface by precipitate and adsorption of copper onto the precipitate.

Based on the findings of this research the following recommendations are made to further enhance the understanding of mineral microbe interaction. Given the apparent importance of initial attachment of the inoculum to long term colonisation a more robust protocol for quantifying attachment must be developed. The small column study presented here was hampered by inconsistent packing of the concentrate and associated inconsistencies with liquid flow patterns. Given the irregular particle shape it was not possible to quantify mineral surface area rigorously. In addition the occurrence of fine ore material in the eluent introduced inaccuracies in the cell counts, particularly when these were suspended in surfactant.

In terms of the simulated heap leaches the quantification of microbial attachment and distribution during the leach, rather than at the end only would provide additional information. A quantitative technique to differentiate between microbial species would allow the determination of shifts in dominance of *At. ferrooxidans* and *L. ferrooxidans*.

6. References

1. Acevedo F. (2000). The use of bioreactors in biomining processes. *EJB Electronic Journal of Biotechnology*, **3**, 1 – 11.
2. Acuńa J., Peirano I. and Jerez C.A. (1986). *In Vivo* and *In Vitro* methylation of proteins from chemolithotrophic microorganisms: A possible role in chemotaxis. *Biotechnology and Applied Biochemistry*, **8**, 309 – 317.
3. Acuńa J., Rojas J., Amaro A.M., Toledo H. and Jerez C.A. (1992). Chemotaxis of *Leptospirillum ferrooxidans* and other acidophilic chemolithotrophs. *FEMS Microbiology Letters*, **96**, 37 – 42 (cited in Gehrke *et al*., 1995).
4. Adler J. (1973). A method for measuring chemotaxis and use of the method to determine optimum conditions for chemotaxis by *Eschericia coli*. *Journal of General Microbiology*, **74**, 77 – 91 (cited in Acuńa *et al*., 1986).
5. Ahonen L. and Tuovinen O.H. (1995). Bacterial leaching of complex sulfide ore samples in bench-scale column reactors. *Hydrometallurgy*, **37**, 1 – 21.
6. Akbar T., Akhtar K., Ghauri M.A., Anwar M.A., Rehman M., Rehman M., Zafar Y. and Khalid A.M. (2005). Relationship among acidophilic bacteria from diverse environments as determined by randomly amplified polymorphic DNA analysis (RAPD). *World Journal of Microbiology and Biotechnology*, **21**, 645 - 648
7. Andrews G.F. (1987). The selective adsorption of *Thiobacilli* to dislocation sites on pyrite surfaces. *Biotechnology and Bioengineering*, **31**, 378 – 381.
8. Arredondo R., Garcia A. and Jerez C.A. (1994). Partial removal of lipopolysaccharide from *Thiobacillus ferrooxidans* affects its adhesion to solids. *Applied and Environmental Microbiology*, **60**, (8), 2846 – 2851.
9. Asai A.S., Konishi Y. and Yoshida K. (1992). Kinetic model for batch bacterial dissolution of pyrite particles by *Thiobacillus ferrooxidans*. *Chemical Engineering Science*, **47**, (1), 133 – 139 (cited in Moon, 1995).
10. Bagdigan R.M and Myerson A.S. (1986). The adsorption of *Thiobacillus ferrooxidans* on coal surfaces. *Biotechnology and Bioengineering*, **28**, 467 – 479.
11. Barrett J., Hughes M.N., Karavaiko G.I. and Spencer P.A. (1993). *Metal extraction by bacterial oxidation of minerals*. Ellis Horwood Limited, Chichester (cited in Karavaiko *et al*., 1995).
12. Battaglia-Brunet F., d'Hughes P., Cabral T., Cezac P., Garcia J.L. and Morin D. (1998). The mutual effect of mixed *Thiobacilli* and *Leptospirilli* populations on pyrite bioleaching. *Minerals Engineering*. **11**, (2), 195 – 205.
13. Bengrine A., Ohmura N. and Blake II R.C. (2001). *Acidithiobacillus ferrooxidans* and *Leptospirillum ferrooxidans* adhere to different sites on the surface of pyrite. In: Ciminelli V.S.T. and Garcia Jr O. (eds). *Biohydrometallurgy: Fundamentals, Technology and Sustainable Development*, *Part B*. Elsevier, Amsterdam, pp 573 – 581.

14. Bevilaqua D., Diéz-Perez I., Fugivara C.S., Sanz F., Benedetti A.V. and Garcia O. Jr. (2004). Oxidative dissolution of chalcopyrite by *Acidithiobacillus ferrooxidans* analyzed by electrochemical impedance spectroscopy and atomic force microscopy. *Bioelectrochemistry*, **64**, 79 – 84.
15. Blake II R.C., Lyles M.M and Simmons R.C. (1995). Morphological and physical aspects of attachment of *Thiobacillus ferrooxidans* to pyrite and sulphur. In: Vargas T., Jerez C.A., Wiertz J.V. and Toledo H. (eds). *Biohydrometallurgical Processing* Vol. 1, Elsevier, Amsterdam, pp. 13 – 22.
16. Blake II R.C. and Ohmura N. (1999). *Thiobacillus ferrooxidans* binds specifically to iron atoms at the exposed edge of the pyrite crystal lattice. In: Amils R. and Ballester A. (eds). *Proceedings of the International Biohydrometallurgy Symposium: Biohydrometallurgy and the environment toward the mining of the 21st Century* Vol. A, Elsevier, Amsterdam, pp. 663 – 672.
17. Blake II R.C, Sasaki K. and Ohmura N. (2001). Does aporusticyanin mediate the adhesion of *Thiobacillus ferrooxidans* to pyrite? *Hydrometallurgy*, **59**, 357 – 372.
18. Blake II R.C., Shute E.A. and White K.J. (1989). Enzymology of respiratory iron oxidation. In: Salley J., McCready G.L. and Wichlacz P.L. (eds). *Biohydrometallurgy CANMET*, Elsevier, Canada, pp. 391 – 401 (cited in Karavaiko *et al*., 1995).
19. Boon M. (2001). The mechanism of direct and indirect bacterial oxidation of sulphide mineral. *Hydrometallurgy*, **62** (1), 67 – 70.
20. Boon M. and Heijnen J.J. (1993) In: Torma A.E., Wey J.E. and Lakshmanan V.L. (eds). *Biohydrometallurgical Technologies* Vol. 1, Elsevier, Warendale, pp. 217 - 232 (cited in Stott *et al*., 2001).
21. Bouffard S.C. and Dixon D.G. (2001). Investigative study into the hydrodynamics of heap leaching processes. *Metallurgical and Materials Transactions B*, **32** (5), 763 – 776.
22. Brandel H. (2001). In: Rehm, H - J. (ed.). *Biotechnology* 2nd Edition, Wiley – VCH, Germany, Vol. **10**, 191 – 224.
23. Brierley J.A. and Brierley C.L. (2001). Present and future applications of biohydrometallurgy. *Hydrometallurgy,* **59,** 233 – 239.
24. Brierley C.L. (1997). Mining Biotechnology: Research to Commercial Development and Beyond. In: Rawlings D.E. (ed.). *Biomining: Theory, Microbes and Industrial Processes*, RG Landes/Springer–Verlag, Berlin, pp 3 – 17.
25. Brunet-Battaglia F., Hugues P., Cabral T., Cezac P., Garcia J.L. and Morin D. (1998). The mutual effect of mixed *Thiobacilli* and *Leptospirilli* populations on pyrite bioleaching. *Minerals Engineering,* **11** (2), 195 – 205.
26. Bruynesteyn A. and Duncan D.W. (1974). Effect of particle size on the microbiological leaching chalcopyrite bearing ore. *Solution Mining Symposium* 1974 (cited in Schnell 1997).
27. Busenberg E. and Clemency C. (1976). The dissolution kinetics of feldspars at 25°C and 1 atmosphere CO_2 partial pressure. *Geochim et Cosochim Acta,* **40**, 41 – 49.

28. Chang Y.C. and Myserson A.S. (1982). Growth models for the continuous bacterial leaching of iron pyrite by *Thiobacillus ferrooxidans*. *Biotechnology and Bioengineering*, **24**, 889 – 902 (cited in Moon, 1997)
29. Clark D.A. and Norris P. (1996a). *Acidomicrobium ferrooxidans* gen. nov., sp. nov.: mixed-culture ferrous iron oxidation with *Sulfobacillus* species. *Microbiology*, **142**, 785 – 790 (cited in Escobar *et al*., 2003).
30. Clark D.A. and Norris P. (1996b). Oxidation of mineral sulphides by thermophilic microorganisms. *Minerals Engineering,* **9**, (11), 1119 – 1125.
31. Coram N.J. and Rawlings D.E. (2002). Molecular relationship between two groups of the genus *Leptospirillum* and the finding that *Leptospirillum ferriphilum* sp. nov. dominates South African commercial biooxidation tanks that operate at 40^{o}C. *Applied and Environmental Microbiology*, **68**, (2), 838 – 845.
32. Cox J.C. and Brand M.D. (1982). Iron oxidation and energy conservation in the chemoautotrophic *Thiobacillus ferrooxidans.* In: Strohl W.R and Tuovinen O.H. (eds). *Microbial Chemoautotrophy*. Ohio State University Press, Columbia, pp 31 – 46 (cited in Karavaiko *et al*., 1995).
33. Crundwell F.K. (2001). How do bacteria interact with minerals? In: Ciminelli V.S.T. and Garcia Jr O. (eds). *Biohydrometallurgy: Fundamentals, Technology and Sustainable Development*, *Part A*. Elsevier, Amsterdam, pp. 149 – 158.
34. Crundwell F.K. (1997). Physical Chemistry of Bacterial Leaching. In: Rawlings D.E. (ed.). *Biomining: Theory, Microbes and Industrial Processes*, RG Landes/Springer–Verlag, Berlin, Ch. 9, pp. 177 – 199.
35. Curutchet G. and Donati E. (2000). Iron-oxidising and leaching activities of sulphur-grown *Thiobacillus ferrooxidans* cells on other substrates: Effect of culture pH. *Journal of Bioscience and Bioengineering,* **90**, (1), 57 – 61.
36. Das T., Ghosh M.K. and Chaudhury G.R. (2005). Assessment of the significant parameters influencing the bio-oxidation and bio-precipitation of iron from industrial leach liquor. *Mineral Processing and Extractive Metallurgy*, **114**, 57 – 64.
37. Devasia P., Natarajan K.A. and Rao G.R. (1996). Role of bacterial growth conditions and adhesion in the bioleaching of chalcopyrite by *Thiobacillus ferrooxidans*. *Minerals & Metallurgical Processing*, **13**, 82 – 86.
38. Devasia P., Natarajan K.A., Sathyanarayana D.N. and Ramananda Rao G. (1993). Surface chemistry of *Thiobacillus ferrooxidans* relevant to adhesion on mineral surfaces. *Applied and Environmental Microbiology*, **59**, (12), 4051 – 4055.
39. DiSpirito A.A., Dugan P.R. and Tuovinen O.H. (1983). Sorption of *Thiobacillus ferrooxidans* to particulate material. *Biotechnology and Bioengineering*, **25**, 1163 – 1168 (cited in Moon 1995).
40. Dutrizac J.E. (1989). Elemental sulphur formation during the ferric sulphate leaching of chalcopyrite. *Canadian Metallurgical Quarterly*, **28**, 337 – 344 (cited in Stott *et al*., 2003).

41. Edwards K.J., Gihring T.M and Banfield J.F. (1999). Seasonal variations in microbial populations and environmental conditions in an extreme acid mine drainage environment. *Applied Environmental Microbiology*, **65**, 3627 – 3632.
42. Edwards K.J., Schrenk M.O., Hamers R. and Banfield J.F. (1998). Microbial oxidation of pyrite: Experiments using microorganisms from an extreme acidic environment. *American Mineralogist*, **83**, 1444 – 1453.
43. Ehrlich H.L. (2002). How microbes mobilize metals in ores: A review of current understandings and proposals for further research. *Minerals & Metallurgical Processing*, **19** (4), 220 – 224.
44. Escobar B., Hevia M.J. and Vargas T. (2003). Evaluating the growth of free and attached cells during the bioleaching of chalcopyrite with *Sulfolobus metallicus*. In: Tzesos M. (ed.). Proceedings of the 15th International Biohydrometallurgy Symposium, IBS 2003, Greece, CD Volume, paper 120.
45. Escobar B. and Lazo D. (2003). Activation of bacteria in agglomerated ores by changing the composition of the leaching solution. *Hydrometallurgy*, **71**, 173 – 178.
46. Fowler T.A., Holmes P.R. and Crundwell F.K. (1999). Mechanism of pyrite dissolution in the presence of *Thiobacillus ferrooxidans. Applied and Environmental Microbiology*, **65**, (7), 2978 – 2993.
47. Gates J.E. and Pham K.D. (1979). An indirect fluorescent antibody staining technique for determining population levels of *Thiobacillus ferrooxidans* in acid mine drainage waters. *Microbial Ecology*, **5**, 121 – 127 (cited in Moon 1995).
48. Geesey G.G and Lang L. (1989). Interactions between metalions and capsular polymers, 325 – 357. In: Beveridge T.J. and Doyle R.J. (eds). *Metal ions and bacteria*, John Wiley & Sons, New York, N.Y. (cited in Gehrke et., 1998).
49. Gehrke T., Hallmann R. and Sand W. (1995). Importance of exopolymers from *Thiobacillus ferrooxidans* and *Leptospirillum ferrooxidans* for bioleaching, In: Vargas T., Jerez C.A., Wiertz J.V. and Toledo H. (eds), *Biohydrometallurgical Processing* Vol. 1, Universidad de Chile, Santiago, 1 – 11.
50. Gehrke T., Telegdi J., Thierry D. and Sand W. (1998). Importance of extracellular polymeric substances from *Thiobacillus ferrooxidans* for bioleaching. *Applied and Environmental Microbiology*, **64**, (7), 2743 – 2747.
51. Gericke M., Muller H.H., Neale J.W., Norton A.E. and Crundwell F.K. (2005). Inoculation of heap-leaching operations. In: Harrison S.T.L., Rawlings D.E. and Petersen, J. (eds). *Proceedings of the 16th International Biohydrometallurgy Symposium*, IBS 2005, Cape Town, South Africa, pp. 255 – 264.
52. Gericke M., Pinches A. and van Rooyen J.V. (2001). Bioleaching of a chalcopyrite concentrate using an extremely thermophilic culture. *International Journal of Mineral Processing*, **62**, 243 – 255.
53. Goebel, B.M. and Stackebrandt E. (1994). Cultural and phylogenetic analysis of mixed microbial populations found in natural and commercial bioleaching environments.

Applied and Environmental Microbiology, **60**, 614 – 1621 (cited in Rawlings *et al*., 2003).

54. Gonzalez R., Gentina J.C. and Acevedo F. (1999). Attachment behaviour of *Thiobacillus ferrooxidans* cells to refractory gold concentrate particles. *Biotechnology Letters*, **21**, 715 – 718.
55. Gromova L.A., Karavaiko G.I., Sevsov A.V. and Pereverzev N.A. (1983). Identification and distribution of sulphur in the cells of *Thiobacillus ferrooxidans*. *Mikrobiologya*, **52**, 455 – 460 (cited in Karavaiko *et al*., 1995).
56. Hackl, R.P., Dreisinger, D.B., Peters, E. and King, J.A. (1995). Passivation of chalcopyrite during oxidative leaching in sulphate media. *Hydrometallurgy*, **39**: 25 – 48 (cited in Petersen and Dixon, 2002).
57. Hallberg K.B. and Johnson D.B. (2001). Biodiversity of acidophilic prokaryotes. *Advances in Applied Microbiology*, **49**, 37 – 84 (cited in Rawlings *et al*., 2003).
58. Hallberg K.B. and Lindstrom E.B. (1994). Characterization of *Thiobacillus caldus* sp. nov., a moderately thermophilic acidophile. *Microbiology*, **140**, 3451 – 3456.
59. Hallmann R., Friedrich A., Koops H.P., Pommerening-Röser A., Rohde K., Zenneck C. and Sand W. (1993). Physiological characteristics of *Thiobacillus ferrooxidans* and *Leptospirillum ferrooxidans* and physicochemical factors influence microbial metal leaching. *Geomicrobiology Journal*, **10**, 193 – 206 (cited in Battaglia-Brunet *et al*., 1998).
60. Hansford G.S and Vargas T. (2001). Chemical and electrochemical basis of bioleaching processes. *Hydrometallurgy*, **59**, 135 – 145.
61. Harniet K., Goksel A. Kock D., Klock J.H., Gehrke T. and Sand W. (2005). Adhesion to metal sulphide surfaces by cells of *Acidithiobacillus ferrooxidans*, *Acidithiobacillus thiooxidans* and *Leptospirillum ferrooxidans*. In: Harrison S.T.L., Rawlings D.E. and Petersen, J. (eds). *Proceedings of the 16th International Biohydrometallurgy Symposium*, IBS 2005, Cape Town, South Africa, pp. 635 – 645.
62. Ingledew W.J., Cox J.C. & Halling P.J. (1977). A proposed mechanism for energy conservation during Fe^{2+} oxidation by *Thiobacillus ferrooxidans*: chemiosmotic coupling to net H^+ influx. *FEMS Microbiology Letters*, **2**, 193 – 197 (cited in Karavaiko *et al*., 1995).
63. Jaffer M.A. (2001). *An investigation of the bioleaching of copper from a chalcopyrite concentrate by a mesophilic bacterial culture*. MSc Thesis, Department of Chemical Engineering, University of Cape Town, South Africa.
64. Johnson D.B. (1998). Biodiversity and ecology of acidophilic microorganisms. *FEMS Microbiology Ecology*, **27**, 308 – 317.
65. Kai T., Nagano T., Fukumoto T., Nakajima M. and Takahashi T. (2007). Autotrophic growth of *Acidithiobacillus ferrooxidans* by oxidation of molecular hydrogen using a gas – liquid contactor. *Bioresource Technology* **98**: 460 – 464.

66. Karavaiko G.I. and Pivovarova T.A. (1973). Oxidation of elementary sulphur by *Thiobacillus ferrooxidans. Mikrobiologya*, **42**, 389 – 395 (cited in Karavaiko *et al*., 1995).
67. Karavaiko G.I., Sakhno T.V., Emelyanov V.M., Philinova N.I and Pivovarova T.A. (1995). Electrophoretic mobility of Thiobacillus ferrooxidans oxidizing Fe^{2+}, S^{o}, and Sulfide Minerals. In: Vargas T., Jerez C.A., Wiertz J.V. and Toledo H. (eds), *Biohydrometallurgical Processing* Vol. 1, Universidad de Chile, Santiago, 23 – 31.
68. Kelly D.P. and Harrison A.P. (1989). Genus *Thiobacillus,* Beijernick, In: Statéy J.T., Bryant M.P., Pfennig N. and Holt J.G. (eds). *Bergey's Manual of Systematic Bacteriology* Vol. 3. The Williams & Wilkins Co, Baltimore, pp 1842 – 1858 (cited in Rawlings 1998).
69. Kelly D.P. and Wood A.P. (2000). Reclassification of some species of *Thiobacillus* to the newly designated genera *Acidithiobacillus* gen. nov., *Halothiobacillus* gen. nov. and *Thermithiobacillus* gen. nov. *International Journal of Systematic and Evolutionary Microbiology*, **50**, 511 – 516 (cited in Rawlings *et al*., 2003).
70. Klauber C. (2003). Fracture induced reconstruction of a chalcopyrite $CuFeS_2$ surface. *Surface and Interface Analysis*. **35**, 415 – 428 (cited in Watling 2006).
71. Klauber C., Parker A., van Bronswijk W. and Watling H. (2001). Sulphur speciation of leached chalcopyrite surfaces as determined by X-ray photoelectron spectroscopy. *International Journal of Mineral Processing*. **62**, 65 – 94 (cited in Watling 2006).
72. Kleene S.J., Hobson A.C. and Adler J. (1979). Attractants and repellents influence methylation and demethylation of methyl-accepting chemotaxis proteins in an extract of *Escherichia coli*. *Proceedings of the National Academy of Sciences USA*. **76**, 6309 – 6313 (cited in Acuńa *et al*., 1986).
73. König R. (1989). C. Plinii secundi – Naturalis historiae, Libri XXXVII, Volume Liber XXXIII. München: Artemis (cited in Brandel 2001)
74. Kort E.N., Goy M.F., Larsen S.H. and Adler J. (1975). Methylation of a membrane protein involved in bacterial chemotaxis. *Proceedings of the National Academy of Sciences USA*, **72**, 3939 – 3943 (cited in Acuńa *et al*., 1986).
75. Koshland D.E., Jr. (1981). Biochemistry of sensing and adaptation in a simple bacterial system, *Annual Review of Biochemistry*. **50**, 765 – 782 (cited in Acuńa *et al*., 1986).
76. Kwong, Y.T.J. (1993a). Minesite Acid Rock Drainage Assessment and Prevention – A New Challenge for a Mining Geologist. *Proceedings of the International Mining Geology Conference*, Kalgoorlie, WA, 213 – 217.
77. Kwong, Y.T.J. (1993b). *Prediction and Prevention of Acid Rock Drainage from a Geological and Mineralogical Perspective*, MEND Report 1.32.1, Ottawa, ON (NHRI Contribution CS-92054)
78. Linge H.G. (1976). A study of chalcopyrite dissolution in acidic ferric nitrate by ptentiometric titration. *Hydrometallurgy*. **2**, 51 – 64 (cited in Stott *et al*., 2001).
79. Lizama H.M., Fairweather M.J., Dai Z. and Allegretto T.D. (2003). How does bioleaching start? *Hydrometallurgy*, **69**, 109 – 116.

80. Lusty J.R., Hughes M.N. and Kelly D.P. (2006). Inhibitory effects of sulfamic acid on three thiosulfate-oxidizing chemolithtrophs. *FEMS Microbiology Letters*, **264**, 70 – 73.
81. Madigan M.T., Martinko J.M. and Parker J. (1997). *Biology of Microorganisms* (8th Edition), Prentice-Hall, New Jersey, pp 1 – 835.
82. Moon J.H. (1995). *Quantification of Biomass in a Biooxidation System*. MSc Thesis, Department of Chemical Engineering, University of Cape Town, South Africa.
83. Murthy K.S.N. and Natarajan K.A. (1992). The role of surface attachment of *Thiobacillus ferrooxidans* on the biooxidation of pyrite. *Minerals and Metallurgical Processing*. **9**, 20 – 24.
84. Myerson S. and Kline P. (1983). The Adsorption of *Thiobacillus ferrooxidans* on solid particles. *Biotechnology and Bioengineering*. **25**, 1669 – 1676 (cited in Moon 1995).
85. Nemati M. and Harrison S.T.L. (2000). A comparative study on thermophilic and mesophilic biooxidation of ferrous iron. *Minerals Engineering*. **13**, (1), 19 – 24.
86. Nemugumoni L.J. (2008). *The effect of silver on inducing microbial stress responses in thermophilic bioleaching using Sulfolobus*. MSc Thesis, Department of Chemical Engineering, University of Cape Town, South Africa.
87. Nordstrom D.K. and Southoam G. (1997). Geomicrobiology of sulfide mineral oxidation. In: Banfield J.F. and Nealson K.H. (eds), *Geomicrobiology: Interaction Between Microbes and Minerals. Reviews in Microbiology* **35**, 361 – 390 (cited in Boon 2001).
88. Norris P.R., Barr D.W. and Hinson U.K. (1987). Iron and mineral oxidation by acidophilic bacteria: affinities for iron and attachment to Pyrite. In: Norris P.R. and Kelly D.P. (eds). *Proceedings of the International Biohydrometallurgy Symposium*, IBS 1987, Warwick, pp. 43 – 59.
89. Norris P.R., Burton N.P. and Foulis N.A.M. (2000). Acidophiles in bioreactor mineral processing. *Extremophiles*. **4**, 71 - 76 (cited in Rawlings *et al*. 2001).
90. Norris P.R. and Johnson D.B. (1998). Acidophilic microorganisms. In: Horikoshi, K. and Grant, W.D. (eds), *Extremeophiles: Microbial Life in Extreme Environments*. Wiley, New York, NY, 133 – 154 (cited in Johnson, 1998).
91. O'Kane Consultants Inc. (2000). Demonstrations of the application of unsaturated zone hydrology for heap leach optimisation. IRAP. Report No. 628-1, pp 1-38. Available from URL:http://www.okane-consultants.com/acrobat/Heapleaching.pdf, Last accessed on 20/09/2006.
92. Ohmura N., Kitamura K. and Saiki H. (1993). Selective adhesion of *Thiobacillus ferrooxidans* to pyrite. *Applied and Environmental Microbiology*. **59**, (12), 4044 – 4050.
93. Ohmura N., Tsugita K., Koizumi J-I and Saiki H. (1996). Sulphur - binding protein of flagella of *Thiobacillus ferrooxidans*. *Journal of Bacteriology*. **178**, (19), 5776 – 5780.
94. Okibe N., Gericke M., Hallberg K.B and Johnson D.B. (2003). Enumeration and characterization of acidophilic microorganisms isolated from a pilot plant stirred-tank bioleaching operation. *Applied and Environmental Microbiology*. **69** (4), 1936 – 1943.

95. Olubambi P.A., Ndlovu S., Potgieter J.H. and Borode J.O. (2007). Effects of ore mineralogy on the microbial leaching of low grade complex sulphide ores. *Hydrometallurgy*. **86**, 96 – 104.
96. Parker A., Klauber C., Stott M., Watling H. and van Bronswijk W. (2004). An x-ray photoelectron spectroscopy study of the mechanism of microbially assisted dissolution of chalcopyrite, In: Tzesos M., Hatzikioseyan A., Remoundaki E. (eds), *Biohydrometallurgy: A Sustainable Technology in Evolution* (Athens, 2003). National Technical University of Athens, Athens, pp. 1011 – 1022 (cited in Watling 2006).
97. Petersen J., Dixon D.G., Timmins M. and Ruitenberg R. (2001). Batch reactor studies of the leaching of a pyrite/chalcopyrite concentrate using thermophilic bacteria, In: Ciminelli V.S.T. and Garcia Jr O. (eds). *Biohydrometallurgy: Fundamentals, Technology and Sustainable Development*, *Part A*. Elsevier, Amsterdam, pp. 525 – 533 (cited in Watling 2006).
98. Petersen J. and Dixon D.G. (2002). Thermophilic heap leaching of a chalcopyrite concentrate. *Minerals Engineering*, **15**, 777 – 785.
99. Petersen J. and Dixon D.G. (2003). The dynamics of chalcocite heap bioleaching. In: Young C.A., Alfantazi A.M., Anderson C.G., Dreisinger D.B., Harris B. and James A. (eds). *Proceedings Hydrometallurgy,* Volume 1, pp 351 – 364.
100. Petersen J. and Dixon D.G. (2005). Comparative Leaching of Chalcopyrite by Selected Acidophilic Bacteria and Archaea. *Geomicrobiology Journal*, **20**, 215 - 230.
101. Petersen J., Harrison S.T.L., Watling H.R., Franzmann P. and Dixon D. (2004). Understanding and Optimisation of Heap Bioleach Processes. In: *Innovations in Leaching Technologies Colloquium*, SAIMM, Johannesburg, ISBN 1-919-783-62-8, 16 pp.
102. Pivovarova T.A., Miller Yu.M., Krasheninnikova S.A., Kapustin O.A. and Karavaiko G.I. (1982). The role of phospholipids in the fractionation of stable sulphur isotopes in the course of oxidation by *Thiobacillus ferrooxidans. Mikrobiologya*, **51**, 552 – 556 (cited in Karavaiko *et al*., 1995).
103. Plumb J.J., Gibbs B., Stott M.B., Robertson W.J., Gibson J.A.E., Nicholas P.D., Watling H.R. and Franzmann P.D. (2002). Enrichment and characterisation of thermophilic acidophiles for the bioleaching of mineral sulphides. *Minerals Engineering*. **15**, (11), 787 – 794.
104. Plumb J.J., McSweeney N.J. and Franzmann P.D. (2008). Growth and activity of pure and mixed bioleaching strains on low grade chalcopyrite. *Minerals Engineering*, **21**, 93 – 99.
105. Pogliani C. and Donati E. (1999). The role of exopolymers in the bioleaching of non-ferrous metal sulphide. *Journal of Industrial Microbiology and Biotechnology*. **22**, 88 – 92.
106. Qiu M., Xiong S., Zhang W. and Wang G. (2005). A comparison of bioleaching of chalcopyrite using pure culture or a mixed culture. *Minerals Engineering*. **18**, 987 – 990.

107. Rawlings D.E. (1997). Mesophilic, Autotrophic Bioleaching Bacteria: Description, Physiology and Role. In: Rawlings D.E. (ed.). *Biomining: Theory, Microbes and Industrial Processes*, RG Landes/Springer–Verlag, Berlin, Ch. 11 pp. 229 – 246
108. Rawlings D. E. (1998). Industrial Practice and the Biology of Leaching of metals from ores. The 1997 Pan Labs Lecture. *Journal of Industrial Microbiology and Biotechnology.* **20**, 268-274.
109. Rawlings D.E. (2002). Heavy Metal Mining Using Microbes. *Annual Review of Microbiol*ogy. **56**, 65 – 91.
110. Rawlings D.E., Dew D. and du Plessis C. (2003). Biomineralization of metal-containing ores and concentrates. *Trends in Biotechnology*. **21**, (1), 38 – 44.
111. Rawlings D.E., Tributsch H. and Hansford G.S. (1999). Reasons why '*Leptospirillum*'-like species rather than *Thiobacillus ferrooxidans* are the dominant iron-oxidizing bacteria in many commercial processes for the biooxidation of pyrite and related ores. *Microbiology*. **145**, 5 – 13.
112. Ritchie A.I.M. (1994). The waste rock environment. In: Jambor J.L. and Blowes D.W. (eds). *Environmental Geochemistry of Sulfide Mine-wastes*, *Mineralolgical Association of Canada Shortcourse Handbook*, Vol. 22, 133 – 161.
113. Ritchie A. I. M. (1997). Mining Biotechnology: Research to Commercial Development and Beyond. In: Rawlings D.E. (ed.). *Biomining: Theory, Microbes and Industrial Processes*, RG Landes/Springer–Verlag, Berlin, Ch. 10.
114. Rodriguez Y., Ballester A., Blazquez M.L., Gonzalez F. and Munoz J.A. (2003a). New information on the chalcopyrite bioleaching mechanism at low and high temperature. *Hydrometallurgy*. **71**, 47 – 56.
115. Rodriguez Y., Ballester A., Blazquez M.L., Gonzalez F. and Munoz J.A. (2003b). Study of bacterial attachment during the bioleaching of pyrite, chalcopyrite and sphalerite. *Geomicrobiology Journal*. **20**, 131 – 141.
116. Rohwerder T., Gehrke T., Kinzler K. and Sand W. (2003). Bioleaching review part A: Progress in bioleaching: fundamentals and mechanisms of bacterial metal sulphide oxidation. *Applied Microbiology and Biotechnology*. **63**, 239 – 248.
117. Rojas-Chapana J.A., Bartels C.C., Pohlmann L. and Tributsch, H. (1998). Co-Operative leaching and chemotaxis of *Thiobacilli* studied with spherical sulphur/sulphide substrates. *Process Biochemistry*. **33** (3), 239 – 248.
118. Romero J., Yaȟez C., Vásquez Moore E.R.B., Espejo R.T. (2003). Characterization and identification of an iron-oxidizing, *Leptospirillum* – like bacterium, present in the high sulphate leaching solution of a commercial bioleaching plant. *Research in Microbiology*. **154** (5): 353 – 359.
119. Salkfield L.U. (1987). *A technical history of the Rio-Tinto mines: some notes on exploitation from pre - Phoenician times to the 1950s*. Institution of Mining and Metallurgy, London (cited in Brandel 2001).

120. Sampson M.I., Phillips C.V. and Blake R.C. (2000). Influence of the attachment of acidophilic bacteria during the oxidation of mineral sulphide. *Minerals Engineering*. **13**, (4), 373 – 389.
121. Sand W., Gerke T., Hallman R. and Schippers A. (1995). Sulfur chemistry, biofilm and the (in) direct attack mechanism - a critical evaluation of bacterial leaching. *Applied Micriobiology and Biotechnology*, **43**, 961 – 966.
122. Sanhueza A., Ferrer I.J., Vargas T., Amils R and Sanchez C. (1999). Attachment of *Thiobacillus ferrooxidans* on synthetic pyrite of varying structural and electronic properties. *Hydrometallurgy*. **51**, 115 – 129.
123. Schiffner C. (1977). *Georg. Agricola. Vom Bergund Hüttenwessen*. München: Deutscher Taschenbuch Verlag.
124. Schippers A., Rohwerder T., Sand W. (1999). Intermediary sulphur compounds in pyrite oxidation: implications for bioleaching and biodepyritization of coal. *Applied Microbiology and Biotechnology*. **52**, 104 – 110 (cited in Harniet *et al*., 2005).
125. Schippers A., Jozsa P-G. and Sand W. (1996). Sulfur chemistry in bacterial leaching of pyrite. *Applied and Environmental Microbiology*. **62**, (9), 3424 – 3431.
126. Schippers A. and Sand W. (1999). Bacterial Leaching of Metal Sulfides Proceeds by two Indirect Mechanisms via Thiosulphate or via Polysulphides and Sulfur. *Applied and Environmental Microbiology*. **65**, (1); 319 – 321.
127. Schnell H.A. (1996). *The Quebrada Blanca operation*. SME, March 1996 (cited in Rawlings D.E. 1997).
128. Schnell H.A. (1997). Bioleaching of Copper. In: Rawlings D.E. (ed.). *Biomining: Theory, Microbes and Industrial Processes*, RG Landes/Springer–Verlag, Berlin, Ch. 2 pp. 21 – 43.
129. Shrihari Kumar R., Gandhi K.S. and Natarajan K.A. (1991). Role of cell attachment in leaching of chalcopyrite mineral by *Thiobacillus ferrooxidans*. *Applied Microbiology and Biotechnology*. **36**, 278 – 282.
130. Sissing A. and Harrison S.T.L (2003). Thermophilic mineral bioleaching performance: A compromise between maximizing mineral loading and maximizing microbial growth and activity. *Journal of South African Institute of Mining and Metallurgy*. March: 1 – 4.
131. Solari J.A., Huerta G., Escobar B., Vargas T., Badilla-Ohlbaum R. and Rubio J. (1992). Interfacial phenomena affecting the adhesion of *Thiobacillus ferrooxidans* to sulphide mineral surfaces. *Colloids and Surfaces*. **69**, 159 – 166.
132. Stott M.B., Sutton D.C., Watling H.R. and Franzmnn P.D. (2003). Comparative leaching of chalcopyrite by selected acidophilic Bacteria and Archaea*. Geomicrobiology Journal*. **20**, 215 – 230.
133. Stott M.B., Watling H.R., Franzmann P.D. and Sutton D. (2000). The role of ion-hydroxy precipitates in the passivation of chalcopyrite during bioleaching. *Minerals Engineering*. **13**, 1117 – 1127 (cited in Stott *et al*. 2001)

134. Stott M.B., Watling H.R., Franzmann P.D. and Sutton D.C. (2001). The effect of solution chemistry on jarosite deposition during the leaching of chalcopyrite by the thermophilic archaeon, *Sulfolobus metallicus*. In: Ciminelli V.S.T. and Garcia Jr O. (eds). *Biohydrometallurgy: Fundamentals, Technology and Sustainable Development*, *Part B*. Elsevier, Amsterdam, pp. 207 - 216.
135. Sverdrup H.U. (1990). *The Kinetics of Base Cation Release due to Chemical Weathering*. Lund University Press, Lund, pp. 1 – 246.
136. Third K.A., Cord-Ruwisch R. and Watling H.R. (2000). The role of iron-oxidizing bacteria in stimulation or inhibition of chalcopyrite bioleaching. *Hydrometallurgy*. **57**, 225 – 233.
137. Toro L., Paponetti B. and Cantallini C. (1988). Precipitate formation in the oxidation of ferrous ions in the presence of Thiobacillus ferrooxidans. *Hydrometallurgy*. **20**, 1 – 9 (cited in Das et al. 2005).
138. Tributsch H. (2001). Direct vs. indirect bioleaching. *Hydrometallurgy*. **59**, 177-185.
139. Tshilombo A.F., Petersen J. and Dixon D.G. (2002). The influence of applied potentials and temperature on the electrochemical response of chalcopyrite during bacterial leaching. *Minerals Engineering*. **15**, 809-813.
140. Tupikina O.V., Kondrat'eva T.F., Samorukova V.D., Rassulov V.A and Karavaiko G.I. (2005). Dependence of the Phenotypic Characteristics of Acidithiobacillus ferrooxidans on the Physical, Chemical and Electrophysical Properties of Pyrite. *Microbiology.* **74** (5): 596 – 603.
141. Tyson G.W., Chapman J., Hugenholtz P., Allen E.E., Ram R.J., Richardson P.M., Solovyev V.V., Rubin E.M., Rokhsar E.S. and Banfield J.F. (2004). Community structure and metabolism through reconstruction of microbial genomes from the environment. *Nature*. **428**, 37 – 43.
142. Van Loosdrecht M.C.M., Lyklema J., Norde W. and Zehnder A.J.B. (1990). Influence of interfaces on microbial activity. *Microbiological Reviews*, **54**, 75 – 87.
143. Vogel, A.I. (1989). *A Textbook of Quantitative Chemical Analysis*, 5th ed., Longman Group, London.
144. Watling H.R. (2006). The bioleaching of sulphide minerals with emphasis on copper sulphide – A review. *Hydrometallurgy*. **84**, 81 – 108.
145. Watling H.R., Johnson J.A., Whittington B.I., Cashmore B.C., Shiers D.W., Hockridge R.J., O'Connor G. And Maley M. (2005). Leaching chemistry and kinetics for sulphide and gangue minerals. In: *Amira Progress Report P768A: Improving Heap Bioleaching*, Amira International. Pp. 30 – 34.
146. Watling H.R., Franzmann P.D., Readett D.J., Petersen J. and Dixon D.G. (2004). Progress towards the heap bioleaching of chalcopyrite. In: *Green Processing 2004 - 2nd International Conference on the Sustainable Processing of Minerals*. Western Australia, Fremantle,. Australasian Institute of Mining and Metallurgy, pp. 133–140.

147. Whitlock J.L. (1997). Biooxidation of Refractory Gold Ores (The Geobiotics Process). In: Rawlings D.E. (ed.). *Biomining: Theory, Microbes and Industrial Processes*, RG Landes/Springer–Verlag, Berlin, Ch. 6, pp. 117 – 126, ,

148. Yeh, T.Y., Godshalk J.R., Olson G.J. and Kelly R.M. (1986). Use of epifluorescence microscopy for characterising the activity of *Thiobacillus ferrooxidans* on iron pyrite. *Biotechnology and Bioengineering*. **30**, 138 –146.

Appendix A: Spectrophotomeric determination of ferrous iron

Calibration curve of Dilution Series

Fe2+ (ppm)	1	2	3	Average	Regression
0	0	0	0	0	
10	0.422	0.421	0.416	0.420	0.424
20	0.858	0.860	0.857	0.858	0.848
30			1.283	1.283	1.273
40	1.726	1.699	1.696	1.707	1.697
50			2.104	2.104	2.121

Statistical Summary Output

Regression Statistics	
Multiple R	0.999901
R Square	0.999802
Adjusted R Square	0.799802
Standard Error	0.011138
Observations	6

ANOVA

	df	*SS*	*MS*	*F*	*Significance F*
Regression	1	3.131926	3.131926	25244.306	9.4126E-09
Residual	5	0.00062	0.000124		
Total	6	3.132546			

	Coefficients	Standard Error	t Stat	P-value	Lower 95%	Upper 95%	Lower 95.0%	Upper 95.0%
Intercept	0	N/A	N/A	N/A	N/A	N/A	N/A	N/A
X Variable 1	0.0424242	0.0001501	282.46	1.055E-11	0.0420381	0.0428103	0.042038	0.042810

Calibration Curve

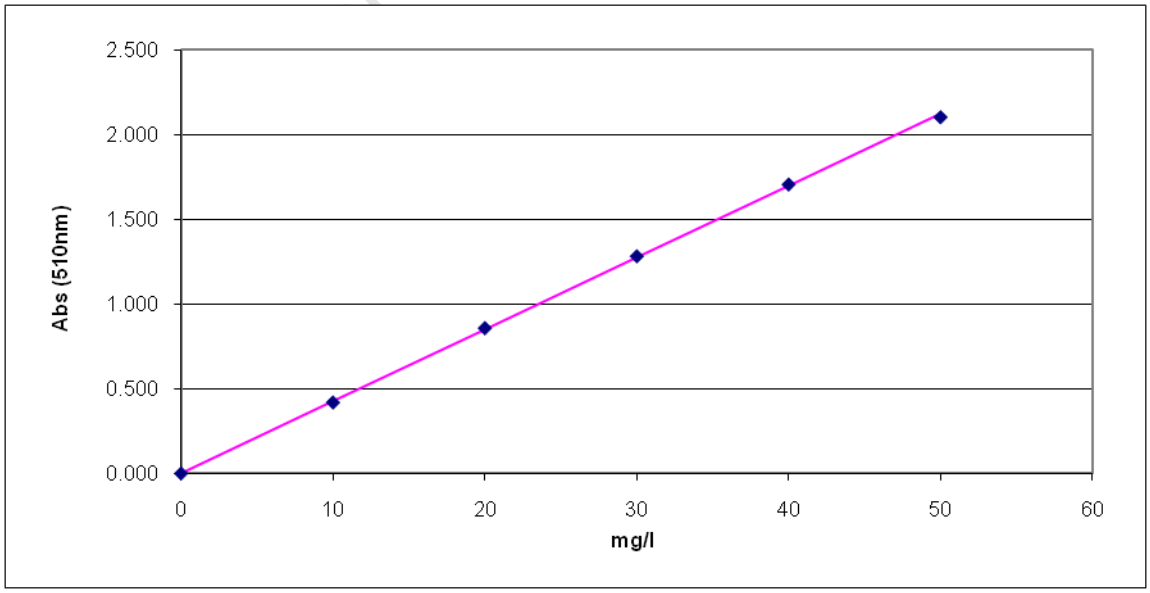

Detection Limit

Appendix B: Heap Leach 4 Data

Initial Cell Concentration:

	Cells / ml	Inoculated per volume
At. ferrooxidans	3.52E+08	1.05E+11
L. ferrooxidans	5.20E+08	1.56E+11

	Volume (L)								
Day	1	2	3	4	5	6	7	8	9
1	8.091	1.997	1.487	1.240	1.099	1.327	1.290	1.219	1.427
2									
3	7.196	1.615	1.613	1.280	1.126	1.319	1.310	1.460	1.300
4	6.505	1.651	1.482	1.863	1.194	1.318	1.315	1.535	1.303
5	6.678	1.795	1.529	1.786	1.117	1.374	1.288	1.491	1.296
6	6.901	1.828	1.537	1.763	1.097	1.507	1.263	1.501	1.342
7	6.566	1.801	1.514	1.661	1.234	1.501	1.243	1.500	1.567
8	6.141	1.731	1.515	1.655	1.292	1.489	1.245	1.598	1.646
9	6.303	1.679	1.726		1.235	1.542	1.294	1.633	1.394
10	6.054	1.624	1.848	1.871	1.243	1.570	1.368	1.604	1.323
11	6.066	1.578	1.925	1.953	1.287	1.578	1.427	1.733	1.339
12	5.957	1.522	1.918	1.846	1.330	1.541	1.334	1.695	1.387
13	6.162	1.576	1.918	1.730	1.371	1.545	1.288	1.598	1.474
14	5.626	1.435	2.200	1.786	1.376	1.639	1.477	1.594	1.335
15	4.750	1.149	2.759	1.727	1.534	1.825	1.950	1.432	1.260
16	4.884	1.137	2.468	1.670	1.808	1.832	1.782	1.475	1.315
17	4.856	1.132	2.489	1.610	1.842	1.890	1.724	1.466	1.345
18	4.594	1.127	2.384	1.540	1.836	1.895	1.652	1.457	1.355
19	4.679	1.125	2.027	1.612	2.093	1.748	1.635	1.643	1.358
20	4.494	1.121	2.159	1.692	1.833	1.716	1.725	1.610	1.316
21	4.284	1.119	2.457	1.688	1.561	1.723	1.925	1.511	1.276
22	3.802	1.120	2.531	1.631	1.486	1.741	2.076	1.499	1.274
23	4.328	1.133	2.255	1.588	1.820	1.595	1.810	1.556	1.313
24	3.726	1.120	2.530	1.643	1.525	1.506	2.043	1.557	1.276
25	3.778	1.123	2.464	1.612	1.583	1.419	1.956	1.595	1.294
26	4.109	1.124	1.841	1.770	1.801	1.360	1.732	1.712	1.284
27	3.963	1.121	1.876	1.830	1.724	1.331	1.709	1.667	1.276
28	4.848	1.136	2.097	2.071	1.866	1.346	1.827	1.786	1.308
29	5.035	1.141	2.000	2.002	2.029	1.169	1.788	1.820	1.320
30	4.057	1.141	2.110	2.086	1.857	1.324	1.754	1.765	1.305
31	5.045	1.155	2.260	2.072	2.019	1.344	1.763	1.823	1.322
32									
33									
34	4.876	1.133	2.052	1.883	1.775	1.253	2.013	2.164	1.227
35	4.607	1.115	1.983	2.102	1.593	1.240	2.107	2.026	1.204
36	4.288	1.121	1.836	1.990	1.597	1.171	2.049	2.207	1.222
37	4.609	1.131	1.928	2.080	1.676	1.169	2.124	2.354	1.231
38	4.416	1.142	1.794	1.638	1.781	1.167	1.728	2.120	1.238
39									
40									
41	4.889	1.152	1.923	1.650	1.868	1.166	1.720	2.290	1.228
42	4.276	1.130	2.046	1.665	1.582	1.166	1.889	2.029	1.190
43	4.048	1.121	2.239	1.753	1.490	1.171	2.239	1.920	1.206
44	4.460	1.128	2.033	1.663	1.600	1.167	1.906	2.075	1.191
45	4.409	1.125	1.974	1.801	1.575	1.187	1.917	2.096	1.200
46	4.476	1.127	1.907	1.775	1.580	1.145	1.704	2.166	1.199
47									
48	4.595	1.120	1.899	1.726	1.584	1.212	1.649	2.147	1.195
49	4.590	1.096	2.142	1.724	1.761	1.186	1.736	2.182	1.199
50	5.120	1.110	2.239	1.847	1.755	1.177	1.849	2.266	1.199
51	5.165	1.098	2.243	1.751	1.772	1.178	1.792	2.295	1.205
52	4.651	1.111	2.086	1.665	1.681	1.169	1.675	2.084	1.193
53	4.359	1.123	1.954	1.879	1.560		1.900	2.182	1.209
54	4.933	1.132	2.342	1.786	1.732		1.896	2.314	1.216
55	4.753	1.142	2.357	1.683	1.876	1.185	1.786	2.478	1.222
56	4.554	1.13	2.267	1.689	2.335	1.177	1.995	2.057	1.211
57	4.573	1.13	2.232	1.923	1.929	1.174	1.92	2.561	1.207
58	4.465	1.134	2.137	1.889	1.83	1.171	1.948	2.387	1.218

	pH									
Day	Feed	1	2	3	4	5	6	7	8	9
1	1.16	1.44	1.50	1.59	1.87		1.68	2.68	1.98	1.79
2										
3	1.11	1.42	1.49	1.52	1.75	2.18	1.90	1.90	1.75	2.15
4	1.17	1.38	1.52	1.51	1.57	1.85	1.95	1.77	1.68	1.97
5	1.19	1.36	1.54	1.50	1.54	1.80	1.83	1.88	1.80	1.79
6	1.18	1.40	1.49	1.51	1.57		1.76	1.93	1.81	1.81
7	1.16	1.36	1.48	1.52	1.59	1.70	1.78	2.02	1.80	1.64
8	1.07	1.39	1.41	1.47	1.57	1.61	1.72	1.94	1.73	1.61
9	1.15	1.38	1.51	1.50		1.76	1.77	1.87	1.78	1.76
10	1.02	1.32	1.44	1.45	1.49	1.76	1.70	1.74	1.72	1.77
11	1.07	1.37	1.48	1.44	1.48	1.75	1.72	1.71	1.70	1.77
12	1.15	1.34	1.43	1.42	1.46	1.64	1.70	1.72	1.70	1.67
13	1.00	1.35	1.39	1.42	1.51	1.59	1.72	1.74	1.76	1.62
14	1.13	1.36	1.43	1.38	1.48	1.59	1.61	1.55	1.73	1.65
15	1.14	1.36	1.42	1.35	1.47	1.57	1.52	1.47	1.76	1.73
16	1.11	1.29	1.48	1.41	1.52	1.51	1.60	1.57	1.75	1.55
17	0.94	1.36	1.30	1.39	1.49	1.43	1.58	1.61	1.65	1.43
18	1.37	1.46	1.39	1.50	1.59	1.53	1.64	1.68	1.68	1.56
19	1.44	1.49	1.39	1.54	1.62	1.55	1.62	1.76	1.68	1.56
20	1.48	1.62	1.58	1.69	1.72	1.69	1.80	1.85	1.81	1.70
21	1.57	1.65	1.63	1.68	1.72	1.75	1.81	1.78	1.86	1.79
22	1.62	1.63	1.59	1.65	1.67	1.73	1.73	1.72	1.83	1.80
23	1.57	1.79	1.76	1.82	1.85	1.86	1.94	1.90	1.94	1.90
24	1.75	1.76	1.77	1.81	1.83	1.82	1.88	1.87	1.99	1.92
25	1.87	1.83	1.79	1.85	1.87	1.92	1.91	1.90	2.01	1.93
26	1.74	1.83	1.81	1.87	1.85	1.89	1.98	1.94	1.97	1.91
27	1.86	1.80	1.79	1.87	1.87	1.90	1.95	1.94	1.96	1.93
28	1.49	1.73	1.72	1.73	1.72	1.81	1.90	1.81	1.86	1.91
29	1.61	1.63	1.69	1.71	1.69	1.76		1.84	1.83	1.83
30	1.65	1.7	1.74	1.73	1.72	1.8	1.87	1.83	1.84	1.93
31	1.75	1.7	1.73	1.73	1.74	1.81	1.85	1.82	1.85	1.93
32										
33										
34	1.75	1.82	1.79	1.81	1.81	1.87	1.96	1.93	1.96	1.89
35	1.75	1.78	1.76	1.8	1.8	1.89	1.99	1.88	1.95	1.92
36	1.84	1.85	1.76	1.85	1.84	1.9		1.92	1.96	1.93
37	1.87	1.86	1.84	1.9	1.89	1.93		1.95	1.98	1.98
38	1.92	1.92	1.89	1.94	1.93	1.95		2.01	2.02	1.98
39										
40										
41	1.95	1.92	1.91	1.92	1.89	1.92		2	2	1.96
42	1.93	2.01	1.96	2.03	2.05	2.05		2.12	2.15	1.96
43	2.07	1.97	1.94	1.98	1.98	2.02		2.03	2.14	2.03
44	2.01	2	1.91	2	1.99	2.02		2.06	2.11	2.01
45	2.03	2.05	1.99	2.07	2.07	2.1	2.12	2.14	2.18	2.08
46	2.08	2.06	1.95	2.08	2.08	2.09		2.15	2.19	2.12
47										
48	1.17	1.44	1.54	1.56	1.65	1.59	2.02	1.82	1.83	1.65
49	1.47	1.37	1.39	1.44	1.48	1.48	1.82	1.65	1.67	1.52
50	1.16	1.62	1.6	1.65	1.66	1.67	1.7	1.68	1.69	1.58
51	1.24	1.32	1.33	1.42	1.45	1.46	1.54	1.61	1.63	1.56
52	1.16	1.38	1.34	1.37	1.37	1.38		1.49	1.51	1.43
53	1.09	1.36	1.36	1.42	1.51	1.43		1.58	1.6	1.51
54	1.15	1.38	1.4	1.45	1.49	1.49		1.57	1.66	1.57
55	1.19	1.38	1.45	1.44	1.5	1.47	1.44	1.58	1.63	1.53
56	1.2	1.41	1.36	1.4	1.41	1.41	1.4	1.52	1.58	1.47
57	1.14	1.33	1.32	1.37	1.36	1.41		1.53	1.54	1.42
58	1.13	1.36	1.38	1.42	1.39	1.49		1.52	1.58	1.52

	Cell Elution per Volume								
Day	1	2	3	4	5	6	7	8	9
1	4.33E+10	1.01E+10	2.41E+09	1.37E+09		5.15E+08	3.51E+08	2.00E+08	1.73E+08
2									
3	2.07E+10	5.09E+08	1.54E+09	6.78E+08	1.63E+08	4.95E+08	3.23E+08	2.93E+08	3.28E+08
4	1.00E+11	1.50E+10	2.15E+09	4.38E+09	1.21E+08	6.77E+08	3.98E+08	7.26E+08	3.35E+08
5	5.51E+10	1.29E+10	5.37E+09	1.07E+10	3.75E+07	2.29E+09	1.73E+09	4.82E+09	1.05E+09
6	8.78E+10	1.23E+10	7.95E+09	9.97E+09		3.26E+09	1.75E+09	2.98E+09	2.40E+09
7									
8									
9	4.33E+10	8.73E+09	6.06E+09		2.24E+09	3.68E+09	2.57E+09	4.40E+09	4.04E+09
10									
11									
12	4.94E+10	4.36E+09	5.24E+09	1.15E+10	2.91E+09	6.30E+09	4.76E+09	9.23E+09	2.96E+09
13									
14									
15	1.79E+10	1.52E+09	1.33E+10	6.58E+09	4.23E+09	4.84E+09	8.21E+09	3.11E+09	1.93E+09
16									
17									
18	2.03E+10	7.22E+08	1.74E+10	4.28E+09	5.08E+09	5.08E+09	6.18E+09	3.28E+09	2.18E+09
19									
20									
21	2.92E+10	7.05E+08	1.00E+10	6.86E+09	6.67E+09	5.64E+09	1.05E+10	2.72E+09	1.69E+09
22									
23									
24	4.07E+10	4.35E+08	1.41E+10	6.64E+09	4.28E+09	5.29E+09	6.76E+09	4.09E+09	1.26E+09
25									
26									
27	3.14E+10	7.66E+08	7.09E+09	1.01E+10	6.86E+09	3.68E+09	7.20E+09	7.62E+09	1.30E+09
28									
29									
30	2.35E+10	8.41E+08	1.30E+10	1.14E+10	9.74E+09	3.87E+09	5.29E+09	7.52E+09	2.08E+09
31									
32									
33									
34									
35									
36	1.75E+10	3.37E+08	4.70E+09	5.68E+09	4.69E+09		7.10E+09	9.93E+09	7.65E+08
37									
38	3.14E+10	1.01E+09	9.48E+09	4.65E+09	7.91E+09		4.10E+09	8.20E+09	9.63E+08
39									
40									
41	2.91E+10	9.50E+08	1.00E+10	5.09E+09	9.40E+09		7.71E+09	1.32E+10	8.29E+08
42									
43									
44	3.08E+10	1.05E+09	9.70E+09	6.05E+09	7.07E+09		1.08E+10	1.10E+10	7.82E+08
45									
46	3.20E+10	8.08E+08	1.03E+10	6.30E+09	5.28E+09		6.95E+09	1.34E+10	5.21E+08
47									
48									
49	4.60E+10	3.60E+08	1.69E+10	9.92E+09	1.04E+10	2.54E+09	1.40E+10	1.62E+10	1.18E+09
50									
51									
52	3.26E+10	1.24E+09	1.69E+10	7.76E+09	8.21E+09		1.07E+10	1.67E+10	7.53E+08
53									
54									
55	3.36E+10	8.31E+08	4.64E+09	4.01E+09	5.11E+09	2.46E+09	9.18E+09	1.37E+10	8.78E+08
56									
57									
58	3.81E+10	5.62E+08	9.85E+09	7.40E+09	9.85E+09		8.71E+09	1.55E+10	4.46E+08

	Redox potential									
Day	Feed	1	2	3	4	5	6	7	8	9
1	500	451	449	447	429		440	336	440	403
2										
3	503	491	493	484	460	449	463	449	460	451
4	502	532	594	512	487	457	490	472	471	473
5	487	599	607	616	613	483	580	588	597	587
6	534	588	595	603	598		595	593	602	593
7	493	590	592	599	596	596	594	586	596	601
8	518	583	587	587	587	553	591	578	592	515
9	468	588	588	600		592	590	588	594	599
10	473	577	607	570	595	598	600	591	598	602
11	496	617	595	599	596	600	597	592	595	595
12	511	614	618	609	603	609	597	600	599	604
13	484	560	528	589	588	593	581	583	583	586
14	503	597	613	597	602	601	597	598	594	599
15	496	549	609	501	576	603	520	501	597	606
16	477	544	599	529	595	591	591	588	585	587
17	495	546	585	520	590	588	586	587	581	589
18	558	592	599	596	592	591	587	586	585	595
19	592	584	594	591	589	592	589	585	589	593
20	595	589	588	589	591	585	584	581	581	589
21	583	571	589	587	584	584	584	585	578	584
22	581	587	582	588	590	587	593	595	586	591
23	584	581	586	585	582	579	578	582	574	583
24	566	602	601	601	606	605	598	598	592	593
25	619	611	623	617	607	611	618	610	608	614
26	608	611	615	613	623	616	611	615	609	610
27	607	595	605	584	582	579	574	575	571	573
28	522	597	615	605	572	585	582	587	590	578
29	546	580	579	580	579	579		576	578	577
30	583	588	618	580	584	583	583	582	581	576
31	589	588	592	592	584	585	586	584	588	586
32										
33										
34	593	571	596	592	591	588	588	590	582	583
35	591	615	617	616	620	616	607	617	614	615
36	625	612	612	617	620	610		620	609	623
37	619	624	629	629	628	630		632	630	629
38	632	623	627	628	630	631		626	626	626
39										
40										
41	598	611	620	621	608	624		623	621	628
42	596	602	605	609	609	610		610	608	623
43	610	611	623	625	626	624		628	617	618
44	589	605	618	618	617	619		621	616	624
45	583	607	612	613	616	612	611	612	604	615
46	585	603	617	614	621	619		618	618	619
47										
48	479	512	510	553	633	546	600	627	633	558
49	511	645	610	635	638	647	629	643	644	653
50	468	617	643	646	650	650	642	648	650	662
51	472	643	668	651	653	653	657	660	660	667
52	467	635	648	648	650	653		648	648	656
53	469	642	651	647	643	633		644	644	650
54	445	652	642	648	658	652		642	648	657
55	448	642	644	598	645	652	646	631	653	663
56	458	638	644	658	654	656	661	659	662	670
57	459	636	628	656	578	648		653	651	663
58	482	637	645	648	655	652		652	653	661

	Total Iron (mg / L)									
Day	Feed	1	2	3	4	5	6	7	8	9
1	2964	2112	1765	1664	1044		1094	1064	673	1050
2										
3	1726	2560	2127	2279	1806	744	872	1020	1338	624
4	1695	2514	2292	2738	2469	1691	1141	1918	1787	1693
5	1814	2629	2516	2690	2723	2040	1656	1790	1763	2307
6	1365	2457	2499	2426	2437		2026	1806	1886	2324
7	1592	2363	2395	2394	2214	2575	1726	1503	1772	2261
8	1562	2551	2784	2525	2468	3049	2121	1806	2280	2841
9	1894	2656	2672	2544		2752	2015	1968	2235	2549
10	1860	2472	2452	2652	2580	2507	2036	2153	2232	2302
11	1473	2481	2550	2571	2552	2495	2063	2200	2240	2299
12	1329	2555	2559	2533	2630	2665	2088	2055	2350	2435
13	1509	2273	2299	2247	2151	2142	1731	1602	1894	1994
14	1532	2835	3157	2798	2885	2845	2568	2368	2426	2870
15	1659	2721	3271	2805	2740	2602	2508	2400	2196	2365
16	1896	2709	3219	3049	2743	2416	2468	2529	2040	2282
17	1572	2711	3377	2940	3041	2484	2521	2752	2119	2349
18	2714	2604	3099	2567	2477	2602	2315	2292	1958	2534
19	2556	2694	3107	2671	2446	2610	2337	2119	2177	2626
20	2347	2290	2794	2246	2128	2208	1933	1851	1951	2267
21	2419	2399	2836	2628	2297	2148	2069	2062	1683	2108
22	2096	2198	2657	2107	2030	1887	2015	1982	1411	1719
23	2192	2216	2567	2177	1940	1957	1740	1836	1305	1907
24	1962	2355	1977	1906	1806	1676	1815	1746	1139	1717
25	1935	1925	2204	1866	1691	1416	1785	1758	1029	1741
26	1773	1806	2112	1679	1607	1483	1176	1314	1213	1382
27	1678	1640	1813	1582	1466	1314	1023	1213	1185	1158
28	1714	1786	1884	1608	1701	1388	1121	1356	1235	1066
29	1695	1740	1810	1607	1636	1562		1355	1431	1349
30	1697	1833	1860	1677	1747	1546	1376	1493	1517	1221
31	1794	1824	1866	1706	1756	1506	1418	1529	1464	1159
32										
33										
34	1629	1520	1663	1405	1373	1260	877	1088	946	1252
35	1629	1620	1789	1501	1535	1225		1205	1022	1081
36	1383	1372	1610	1329	1360	1224		1179	1010	1121
37	1184	1140	1340	1076	1089	962		926	846	851
38	1054	1137	1208	1031	1021	985		810	789	1023
39										
40										
41	896	1029	1174	948	927	939		693	324	992
42	911	788	983	712	619	644		482	389	854
43	883	863	987	780	726	603		622	365	586
44	679	556	874	528	524	482		430	691	518
45	443	561	690	523	470	429	956	382	284	461
46	422	456	625	420	401	365		302	256	377
47										
48	2006	2053	1978	1830	1544	1788	487	1075	1082	2010
49	2548	2647	3421	2621	2633	2630	1578	2598	2044	2976
50	2165	2784	3617	2647	2680	2824	3187	2245	2067	3363
51	2370	2888	4357	2837	2799	2774	3894	2412	2256	3244
52	2523	2674	3540	2622	2659	2650		2254	2144	3081
53	2576	2759	3303	2670	2683	2740		2277	2260	3134
54	2550	2805	3405	5161	2630	2731		2372	2175	3115
55	2364	2616	3113	2534	2632	2582	6015	2382	2180	2961
56	2402	2629	3145	2530	2567	2143	5692	2370	2577	3083
57	2381	2681	3201	2590	2562	2605	6497	2481	2187	3092
58	1728	2738	3527	2732	2734	2652		2592	2258	3027

	Fe^{2+} (mg / L)								
Day	1	2	3	4	5	6	7	8	9
1									
2									
3									
4									
5									
6									
7									
8	13.34	13.95	12.92	12.40	14.52	11.13	9.66	11.31	73.78
9	14.71	13.44	13.01		13.39	10.61	10.32	11.41	12.92
10	13.34	12.73	13.62	13.48	12.78	11.03	12.02	11.55	11.97
11	18.15	16.38	16.62	16.50	16.03	15.20	14.38	14.73	29.70
12	19.09	16.26	16.50	16.62	17.09	14.26	14.03	15.68	15.91
13	12.73	32.81	12.07	11.60	11.46	9.85	9.52	10.84	11.17
14	14.47	15.56	26.40	14.19	14.05	12.82	12.26	12.30	14.28
15	11.64	13.67	202.48	14.10	12.73	12.68	36.11	11.36	11.83
16	17.02	22.44	60.11	14.33		12.49	10.37	14.05	10.23
17	13.34	15.27	38.61	15.23	12.21	12.21	13.01	11.17	12.54
18	13.11	14.43	12.96	12.30	12.45	11.64	11.17	10.51	12.87
19	12.82	14.43	12.82	11.88	12.40	11.22	10.32	10.51	12.92
20	11.55	13.58	11.31	10.94	11.50	10.14	10.04	10.18	11.64
21	12.63	16.08	12.21	12.87	11.74	11.22	11.08	9.52	11.46
22	11.13	13.62	11.03	10.56	9.76	10.32	10.14	8.06	9.10
23	11.17	12.68	10.80	10.04	9.95	9.19	9.62	7.54	9.76
24	9.95	8.77	10.42	9.76	9.43	9.81	7.26	9.57	
25	10.23	11.36	10.14	9.33	8.39	9.66	9.48	6.93	9.38
26	9.66	10.42	9.19	8.82	8.49	7.31	7.83	7.35	8.06
27	14.61	9.99	8.44	8.53	8.01	6.79	7.35	7.26	7.35
28	9.57	9.99	8.96	9.19	8.06	6.98	7.97	7.45	6.46
29	9.81	9.95	9.38	9.38	8.91		8.20	8.58	8.01
30	9.76	10.04	9.33	9.43	8.77	8.11	8.53	8.67	7.17
31	9.90	9.95	9.52	12.12	8.72	9.24	9.19	8.53	7.07
32									
33									
34	9.15	9.57	8.58	8.39	8.01	6.46	7.35	6.79	7.97
35	9.00	9.52	8.44	8.53	7.54		7.35	6.41	6.88
36	8.06	9.05	7.68	7.78	7.17		7.02	6.60	6.84
37	6.93	7.73	6.65	6.69	6.08		6.46	5.94	5.89
38	7.59	7.87	7.54	7.17	6.18		6.08	5.28	6.18
39									
40									
41	7.21	7.64	6.84	6.60	6.88		5.70	6.08	7.17
42	6.88	5.52	5.09	5.37	4.53		3.77	6.13	5.00
43	7.07	6.27	6.03	5.47	5.52		4.10	5.28	5.19
44	4.53	5.89	4.29	4.29	4.01		3.91	3.11	4.38
45	4.43	5.14	4.15	3.96	3.68	6.27	3.35	2.73	3.96
46	3.77	4.71	3.58	3.49	3.35		2.92	2.69	3.54
47									
48	229.12	209.08	49.26	12.96	56.81	5.42	9.19	9.19	41.25
49	14.85	16.97	14.73	14.03	14.50	8.72	10.84	10.73	16.15
50	13.06	16.36	12.63	12.54	12.82	13.11	10.89	9.95	14.85
51	12.59	17.40	12.35	12.16	12.35	15.09	10.84	10.09	13.95
52	13.11	15.13	12.26	12.21	12.26		10.84	10.18	13.39
53	12.96	14.66	12.59	13.01	12.78		11.08	10.47	13.91
54	13.62	15.32	13.11	12.92	13.39		11.93	10.94	14.19
55	13.34	14.99	12.87	12.87	13.01	23.67	12.45	11.64	14.10
56	13.06	14.76	13.06	12.96	11.17	22.35	11.64	12.68	14.38
57	13.58	14.52	12.78	18.24	13.20	24.75	12.26	11.64	14.24
58	13.53	15.75	13.48	13.34	13.06		12.68	11.97	14.61

	Copper (mg / L)									
Day	Feed	1	2	3	4	5	6	7	8	9
1	0.12	56.9	51.7	61.6	87.5		32.2	33.3	47.5	50.7
2										
3	0.06	32.0	31.5	39.4	56.1	49.8	31.8	45.2	39.1	41.9
4	0.21	21.5	35.5	35.8	40.5	48.6	44.3	46.1	37.7	57.3
5	0.22	22.1	47.4	40.3	49.8	62.5	57.2	64.2	57.7	68.8
6	0.26	19.6	45.1	39.0	50.2		59.6	71.2	62.3	75.1
7	0.17	19.0	36.7	38.7	52.8	66.4	54.9	72.6	68.0	54.9
8	0.18	20.8	35.1	46	63	59.2	63.1	83.6	75.3	50.3
9	0.2	18.3	37.4	37.6		73.7	59.1	73.4	75.5	65.9
10	0.22	16.4	35.3	30.4	40.6	81.4	57	65.1	76.1	76.2
11	0.15	16.2	33.2	26.8	36.2	74.8	62.7	65.8	71.7	78.8
12	0.25	15.8	33.9	26.4	39.9	67.4	73.8	79.4	77.5	74.6
13	0.09	14.2	25.8	24.6	42.6	56.7	76.7	88.3	82.9	62.5
14	0.03	13.9	27.7	21.5	41.3	54.4	68.1	63.4	85.5	71.8
15	0.16	15.4	36.2	14.9	37.7	52.2	59.2	53.8	98	88.8
16	0.13	16.3	42.5	17.3	41.2	42.4	63.1	59.3	92.4	61.8
17	0.04	14.6	31.8	21.1	48	34	63.7	70.2	86.9	44.4
18	32.2	37	45.2	43.2	59.1	45.5	71.4	84	95.2	61.6
19	29	42.6	55.7	55.2	73.5	52.1	77.3	105.3	88.5	59
20	48.1	52.5	70.3	63.1	75.5	61.5	93.6	107.2	91.2	69.7
21	57.9	66.1	88.9	71.29	81.1	83.3	103.2	99.5	109.3	101.7
22	60.2	71.7	103	77.8	87.3	98.7	101.3	96.1	136.2	142.9
23	79.2	85.2	108.9	84.8	91	94.8	122.3	106.7	131.9	124.1
24	76.8	115.7	83.9	86.8	97.7	109.1	114.1	105.2	133.7	121.43
25	84.9	93	139.9	92.8	99.6	124.4	125.4	114.2	143	128.2
26	95.7	100.6	139.7	108.9	119.8	130.4	155.6	144.6	143.7	138.1
27	104.6	110.1	144.7	120.2	112.6	120.6	146.5	144.4	133.8	139.7
28	78.4	94.6	152.4	115.3	110.6	128.9	160.8	141.2	144.5	157.2
29	93.2	88.8	126.5	102.9	103.7	110.4		130.3	123.5	139
30	94.8	97.5	131.3	107.8	110.9	117	150.3	128.3	128.3	143.4
31	89.7	98.8	147.3	111.3	104.6	123.5	159.5	132.6	130.5	148.2
32										
33										
34	107.5	106.3	136.9	115.3	113.7	124.8	198.5	138.5	141	172.6
35	105.3	119.8	164	128.9	124.3	142.3		154.2	158.3	210.3
36	129.4	130.4	169.4	137	129.5	143		149.8	151.1	182.5
37	122.2	121.7	165	131.1	122.8	137.4		138.8	138.5	177.8
38	123	131.8	158.9	137.3	132.8	137.1		149.8	143.1	169.8
39										
40										
41	114.6	137.6	169.6	143.9	144.1	140.5		164.5	157.5	171.4
42	135.8	136.1	161.3	142.1	153.6	151.7		166.9	160.67	266
43	128.2	147.2	192.5	155.7	152.4	154		170.6	174.3	236
44	139.4	134.6	185.7	134.9	144.5	145.5		157.3	150.1	215.1
45	129.3	139.8	179	141	142.4	146.3	506	163.1	161.5	203.7
46	130.4	135.9	183.6	142.1	139.1	150.4		157.7	152.2	200.9
47										
48	0.09	57.4	142.1	96.2	117.6	107.3	382	160.3	154.6	194.3
49	0.12	15.4	86.3	54.1	60.6	57.9	412.4	128.3	131.7	160.4
50	0.18	11.8	79.4	36.3	38.9	42	435.9	107.6	124.1	140.1
51	0.52	10.2	71.3	32.3	32.7	35.1	471.7	92.8	104.5	125.2
52	0.07	11	60	32.3	33.6	35.4		94.6	101.9	95.2
53	0.51	11.5	47.3	33.9	35.8	30.6		92.1	91.5	98.5
54	0.32	12.9	48.7	35.3	36.6	34.1		82.2	100.9	102.2
55	0.2	12.4	44.3	31.1	32.8	28.6	576	75.4	83.4	82.9
56	0.43	35	44.4	32	30.4	80.5	460	68.4	27.9	81.2
57	0.55	11	42.2	24	22.5	28.9	409	62.1	79.7	85.1
58	0.14	11.1	50.4	27.8	20.9	40.9		61.5	83.7	98

Appendix C: Residence Time Calculation

Residence time calculations

Residence time was calculated assuming that perfect plug flow occurred and that immediate radial distribution happened when the feed solution entered into the ore matrix.
This is shown in Equation 1 where:

$$T = Vp / Q$$

Equation 1

Where: T = Mean Residence time (L / Hrs)
Vp = Void volume
Q = Volumetric flow rate

The void volume was calculate by dividing the porosity of the bed by the volume of that region. We know that porosity (Ø) is the non - solid volume of a region divided by the total volume of that region and is shown in Equation 2.

$$Ø = Vp / Vm$$

Equation 2

Where Ø = porosity of the ore
Vm = total volume of that region

To determine the porosity a 1 Kg basis was used with a visually estimated 10 % moisture content of the ore, with the result that 0.1 Kg of water and 0.9 Kg was solid ore. The volume of water (Vw) and the volume of ore (Vo) was calculated per region.

$$Vw = 0.1 / \rho H_2O$$
$$= 0.1 / 998 \text{ Kg.m}^3$$
$$= 0.0001 \text{ m}^{-3}$$

$$Vore = 0.9 / \rho ORE$$
$$= 0.9 / 2700 \text{ kg.m}^3$$
$$= 0.0003 \text{ m}^{-3}$$

$$Ø = Vw / (Vw + Vore)$$
$$= 0.0001 / (0.0001 + 0.0003)$$
$$= 0.25$$

This is the fractional voidage of the entire reactor. To calculate the void volume in a particular region, the volume of that region is multiplied by the fractional voidage to give you the interstitial volume of that region (Vr).
For example:

$$Vr = \pi.r^2.h$$
$$= \pi. (5)^2.43$$
$$= 3377 \text{ cm}^3$$

$$Vp = 3377 \text{ cm}^3 \text{ x } 0.25$$
$$= 844.25 \text{ cm}^3$$
$$= 844.25 / 1000$$
$$= 0.844 \text{ L}$$

The volumetric flow rate (Q) was calculated:

$$(Q) = (\text{Vol. collected from inner segment} / 24 \text{ Hr})$$
$$= 6.921 \text{ L} / 24 \text{ Hr}$$
$$= 0.288 \text{ L per Hr}$$

Therefore a mean residence time (T) for the inner region for 1 day is:

$$T = H / Q$$
$$T = 0.844 / 0.288$$
$$T = 2.93 \text{ Hr}$$

Appendix D:

Tween washed ore

L. ferrooxidans inoculation number : 8.72×10^8 (cells/2ml)

Steps	Cells released (cells/2ml)	% Released
1 – Inoculation	1.06×10^7	1.2
2 – Basal salt	1.09×10^8	12.5
3 – Iron and ammonium sulphate	2.19×10^7	2.5
4 – Distilled water	3.75×10^7	4.3
5 – Distilled water	5.00×10^6	0.6
6 – Tween wash	8.50×10^8	97.5
Total cell dislodgment	1.03×10^9	118.6

Cell balance incomplete as total number of cells eluted and dislodged exceed that of the cell inoculum.

Tween washed ore

L. ferrooxidans inoculation number : 8.72×10^8 (cells/2ml)

Steps	Cells released (cells/2ml)	% Released
1 – Inoculation	6.88×10^6	0.8
2 – Basal salt	1.00×10^8	11.5
3 – Iron and ammonium sulphate	2.19×10^7	2.5
4 – Distilled water	4.00×10^7	4.6
5 – Distilled water	4.44×10^7	5.1
6 – Tween wash	6.50×10^8	74.5
Total cell dislodgment	8.63×10^8	99.0